THE ROLE OF MUTANT *PIK3CA* AND *TP53* IN HUMAN BREAST CARCINOGENESIS

by
Sarah Elizabeth Croessmann

A dissertation submitted to Johns Hopkins University in conformity with the requirements for the degree of Doctor of Philosophy

Baltimore, Maryland
March, 2015

Abstract

Breast cancer is the second leading cause of cancer-associated deaths among women in the United States, with greater than 40,000 women dying each year from this disease. While specific DNA mutations have been shown to be involved in the development of breast cancer, it is the cooperation and collaborative effects of multiple mutations and genetic alterations that leads to carcinogenesis. The accumulation of mutations suggests that accurate models cannot focus on a single mutation but rather the interplay of several mutations. Thus, it has becoming increasingly apparent that the successful treatment of breast cancer will rely upon understanding how multiple pathogenic mutations and pathways interact. Each year, approximately 11,000 new cases of breast cancer will harbor both a *TP53* and *PIK3CA* mutation, the two most common somatic mutations in nonhereditary breast cancer. The implementation of gene targeting to develop a panel of somatic knock-in isogenic cell lines harboring both a *PIK3CA* and a *TP53* mutation in human breast epithelial cells provides a model with multiple pathogenic mutations. The model more accurately demonstrates the progressive genetic events leading to breast carcinogenesis. The development of a closely related panel of isogenic cell lines will all phenotypic transformations to be attributed to dysregulation of an entire pathway, a specific mutation, or a clonal variation. Furthermore it allows for the identification of potential therapeutic biomarkers, targets, and provides new mechanistic insight between the two most somatically mutated pathways in breast cancer.

Thesis Advisor: Ben Ho Park, M.D., Ph.D.

Thesis Readers: Ben Ho Park, M.D., Ph.D.
Samuel R Denmeade, M.D.

ACKNOWLEDGEMENTS

When I think of the path I have traveled down to earn my PhD, I often think of the proverb "It takes a village…" My dissertation is just as much a product of my hard work as it is the product of the love, advice, and overall support from countless individuals in my life. Without this amazing network of family, friends, and mentors, I am certain I would not have accomplished the things I have thus far in my life.

First, I would like to thank my amazing mentor and thesis advisor, Dr. Ben Ho Park. It has truly been a privilege to be accepted into the Park family. It is hard to express in a short paragraph all the knowledge, both in laboratory and in life, which you have provided me. To me, it seems that your knowledge, selflessness, care, understanding and guidance know no bounds and I am beyond grateful to have you as my graduate mentor. You are a scientist and mentor that I aspire to be one day.

The Park and Lauring Lab members, past and present, I cannot imagine ever finding a better community of scientists. Not only was each day in lab filled with jokes, pranks, laughs, and interesting conversations, but I have learned more about science from each of you than I could ever learn from papers and books. I am continually humbled by the bright minds that enter the lab and feel privileged to be exposed to them daily.

To my Baltimore and Hopkins friends, thank you for your support, for keeping me sane, happy, and always in good spirits. The love and support from everyone here in my life is invaluable and I am so lucky to have all of you in my life.

To my very large extended family, thank you for your love and support. I specifically want to thank my Uncle Tom and Aunt Patti. Thank you for being my home away from home. I am so grateful to have such an amazing family in my life and even more grateful to have you all so close. Thank you for all your love and support (and countless home cooked meals). Your family helped me through some of the hardest points in my PhD and I am forever grateful.

Rachel, love you sthister.

To my parents: unlike most people, I was fortunate to have four amazing, loving parents in my life. Without their endless love, unwavering support, and immeasurable patience, I would not be the person I am today. There are not enough pages in this book to express my gratitude to each of you. You have supported me through every stage in my life and have been my constant cheerleaders through both the highs and lows. I am so lucky to have such amazing and supportive role models who have provided me with love, advice, and who I look up to each day. Mom, thank you for being there for every phone call, regardless if it was to celebrate or to breakdown and for providing a strong woman role model. You're amazing. Dad, thank you for always being there and continuing to remind me that I can aspire to be whatever I put my mind towards. Bill, thank you for always making me smile, whether if it's mailing me a random book or framed photo, or sending me a funny text. I love you all so much and I am so lucky to have you all as parents.

TABLE OF CONTENTS

LIST OF TABLES

LIST OF FIGURES

1 Introduction

Breast Cancer and Genetics Overview

Breast cancer is the second most common cause of cancer-associated death among women in the United States. Approximately 1 in 8 women will be diagnosed with breast cancer in the span of their lifetime. In 2013, the American Cancer Society estimated 232,340 new cases of invasive breast cancer and 64,640 new cases of non-invasive (in situ) breast cancer were diagnosed in women in the US. Approximately 39,620 of these cases resulted in death (1), Human cancer develops due to the accumulation and selection of rare subvariant mutations in oncogenes and tumor suppressor genes. The acquisition and clonal expansion of these subvariants promotes increasingly aggressive phenotypes, which lead to the development of cancer (2). Statistical analyses suggest that, on average, an individual tumor contains approximately 80 mutations with less than 15 of these being responsible for driving the initiation, progression, or maintenance of the tumor. Recently, *PIK3CA* and *TP53* were identified as the most mutated oncogene and tumor suppressor gene, respectively, in human breast cancer (3, 4).

In 1991, it was suggested that underlying genetic instability was absolutely required for the accumulation of multiple mutations in cancer (5). The link between genetic instability and the development of cancer was repeatedly established until in 2011, genomic instability and increased mutational rates were officially recognized as new

enabling hallmarks of carcinogenesis (6). It is important to distinguish here the difference between the genomic instability of a cell line versus the mutational state of a cell line. By definition, genomic instability refers to the rate of mutational accumulation, and does not imply that a cell line is genetically unstable. The existence of mutations in a cell line represents the static state and does not provide information on the occurrence of acquired mutations (7). It has been previously shown that many aneuploid breast cancers have cell-to-cell variability in copy number, suggesting a carcinogenic component of genomic instability (8).

Often, the accumulation of mutations is accelerated by compromising checkpoints in the cell cycle that normally monitor damage within the cell. *TP53*, known as the "guardian of the genome", plays an essential role in maintaining the genome integrity. The loss of *TP53* leads to increased genomic insult and a higher rate of mutational accumulation. These "driver" mutations thus lend themselves as potential markers for prognosis, and are also ideal targets for therapy, given their importance for the growth and viability of cancer cells. Recently, the gene *PIK3CA*, was found to be frequently mutated in many cancer types, with a high frequency of about 25-30% in breast (3) and colorectal (9) cancers. Hotspot mutations in *TP53* and *PIK3CA* may lead to chromosomal loss of other tumor suppressor genes and/or important regulatory genes due to genomic instability. The instability and potential allelic loss of these genes significantly increases the potential for carcinogenesis and the development of cancer.

TP53

p53 was the first identified in 1979 as a cellular protein tightly associated with the simian virus 40 large T protein (SV40LT). SV40LT, a nonstructural product of the viral

genome, played an important role in the oncogenic capacity of SV40 (10). The strong association with p53 led to several studies identifying it as a tumor antigen and postulating that p53 might be a cellular oncogene product linked to the viral transformation process (11, 12). In the early 1980s, several isolates of p53 cDNA clones were studied and found to transform cells in combination with the Ras oncogene (13, 14). Therefore, p53 was initially and incorrectly established as an oncogene. However, in the late 1980s several studies demonstrated mutations in both alleles were required for tumor formation and p53 was re-identified as the first tumor-suppressor protein (15-18).

TP53 encodes p53, a 53 kDa nuclear phosphoprotein expressed at a biologically latent state in all cells. In 1992, three groups of scientists showed that the p53 protein acts as a transcription factor and binds to specific DNA sequences or response elements (REs). As a transcription factor, p53 initiates three different processes that define it as a tumor suppressor; First, p53 initiates cell cycle arrest through the regulation of p21 and cdc25c (19). Secondly, p53 regulates the apoptotic genes bax, puma, noxa, and apaf-1(20). Lastly, p53 can initiate cell senescence leading to a terminal state of replication (20). Through the transcriptional regulation of these three pathways, p53 has been shown to play a central role in protecting against DNA damage and maintaining genomic integrity. As part of its central role, p53 monitors and governs the G1/S phase checkpoint of the cell cycle. Upon DNA damage, ATM kinase activates and upregulates p53, which acts as a transcription factor and activates the cyclin-dependent kinase inhibitor, p21 (21). p21, in turn, stalls the cell cycle and allows the cell time for DNA repair, thus preventing the replication of damaged chromosomes. Alternatively, if DNA is beyond repair, p53 activates members of the Bcl-2 family to carry out programmed cell death, also known as

apoptosis (22). In the absence of stress, wild-type p53 is strongly regulated to allow normal cellular functions to process. MDM2, a key negative regulator, binds to the transactivation domain of p53 and ubiquitylates the protein, targeting it for degradation (23). When functioning properly, p53 acts as a critical brake on tumor development. Therefore, it is not surprising that 50% of all cancers harbor a *TP53* mutation (24). In the absence of p53, both cell cycle arrest and apoptosis are compromised, presumably allowing cancer cells to progress.

TP53 is the most commonly mutated tumor suppressor gene in breast cancer and is most often associated with the triple negative subtype (25, 26). Approximately 70% of *TP53* mutations found in breast cancer are attributed to inactivating point mutations with >90% of these occurring in the DNA binding domain, termed contact mutations. Contact mutations disrupt p53's ability to bind to DNA and function as DNA modulator (27, 28). The majority of contact mutations occur at codon 248 with the R248W mutant being associated with the highest rate of mortality (29, 30). While mutation of p53 generally results in the inactivation of tumor suppressor function, missense mutants also confer a dominant-negative and/or gain-of-function phenotype, which is highly tissue specific (31, 32). While most tumor suppressor genes require biallelic inactivation, *TP53* hotspot mutations impart a dominant-negative and/or gain-of-function effect. p53 functions as a tetramer, however in the presence of a dominant-negative mutant, it and the wild-type protein form functionally inactive hetero-oligomers (33, 34). Although the concept of mutant p53 gaining oncogenic properties, commonly referred to as gain-of-function (GOF), was first suggested in 1984, it still remains a controversial and poorly understood mechanism (25, 35). In 1995 Dittmer *et al*. was the first to distinguish a gain of function

phenotype in the absence of the dominant negative effect. By introducing a mutant p53 allele into a mouse model devoid of all endogenous p53 protein, new acquired phenotypes were attributed to the presence of the mutant protein (36). Dittmer *et al* concluded that mutant p53 expression conferred a growth advantage in the absence of endogenous wild-type p53 protein. For the next two decades, it was shown that mutant p53 exhibited a variety of transformative phenotypes in a variety of models; increased DNA synthesis and proliferation (37, 38), cell survival (39), chemoresistance (40), abnormal centrosome checkpoints (41), gene amplification (42), stem cell characteristics, migration, invasion, and metastatic abilities (43).

PIK3CA

Phosphatidylinositol 3-kinases (PI3Ks) were discovered in the 1980s and are comprised of a family of heterodimeric lipid kinases consisting of a regulatory subunit (p85) and a catayitic component (p110), which participate in a diverse set of cellular signaling pathways. There are several isoforms and classes of known PI3Ks. The majority of PI3Kinases are organized under three main classes (I, II, and III) based on their structure, substrate, specificity, and regulation. Briefly, Class I PI3Ks are divided into two subfamilies, A and B depending on the receptors to which they couple (44). Class 1A consists of a p85 regulatory subunit and a p110 catalytic subunit (45). The p85 subunit is crucial in mediating the activation of class 1As by receptor tyrosine kinases (RTKs). Alternatively, class 1Bs consist of a p101 regulatory subunit and a p110γ catalytic subunit. Although the catalytic subunits share extensive homology, the p101 is distinct from p85 proteins and is activated by G-protein-coupled receptors (GPCRs).

Under normal cellular conditions, Class I PI3Ks are responsible for the phosphorylation of phosphatidylinositol 4,5-bisphosophate (PIP_2) to phosphatidylinositol 3,4,5-bisphosophate (PIP_3) at the cell membrane (46). Class II PI3Ks consist of only a p110-like catalytic subunit and preferentially phosphorylates phosphatidylinositol and to a lesser extent, phosphatidylinositol-4-P (PI-4-P) (47). Lastly, class III PI3Ks consist of a single member known as Vacuolar Protein-sorting Defective 34 (Vps34). Relatively little is known about the specific functions of Vps34, however, it was recently implicated that the Vps34 is involved in the regulation of mTOR and may be crucial for controlling cell growth (44, 48, 49). The majority of our understanding of PI3K signal transduction is based on studies of class I PI3Ks, which are involved in many important physiological processes.

As mentioned previously, Class I PI3Ks are responsible for the phosphorylation of PIP_2 to PIP_3. Upon growth factor stimulation, the regulatory protein p85 binds to phospho-motifs of RTKs, relieving its inhibitory effect over p110. There are three different isoforms of the p110 subunit, p110α, p110β, and p110δ which are encoded by *PIK3CA*, PIK3CB, and PIK3CD, respectively. Activated p110 catalyzes the conversion of PIP_2 to PIP_3, which acts as a lipid second messenger and binds to the pleckstrin-homology (PH) domain of many downstream molecules (50). The principle target of PIP_3 is the protein serine/threonine kinase AKT (or PKB), which leads to the subsequent intracellular cascade of phosphorylation and regulation of a range of cellular functions. Activation of the AKT pathway leads to the control of 4 main cellular processes: (1) cell metabolism, (2) cell cycle and cell survival, (3) protein synthesis, and (4) cell polarity and motility.

The p110α catalytic subunit of the Class IA PI3Ks is encoded by the gene *PIK3CA* and is one of the most highly mutated oncogenes in human cancers. In 2004, *PIK3CA* was identified as the most mutated oncogene in human breast cancer (3). High mutational frequencies of *PIK3CA* have been reported in colorectal (9), breast (51), and liver cancers (52) while lower rates of mutation have been described in many other human malignancies including ovarian (53), lung (9, 52), gastric (9, 52, 54, 55), and brain cancers (56-58). In breast cancer, *PIK3CA* has a reported overall mutational rate of 25%, with more than 80% being attributed to "hot spot" regions within exon 9 of the helical domain and exon 20 of the catalytic domain (3). These three mutations, E542K and E545K in exon 9 and H1047R in exon 20 lead to increased PI3K catalytic activity through the activation of the PI3K/AKT/mTOR pathway. This increased activity results in cellular transformation through growth factor- and anchorage-independent cellular proliferation (59, 60). Studying the effects of these mutations in colorectal cells (61-63), breast epithelial cells (60, 64), and chicken embryo fibroblasts (65, 66) have illustrated a direct connection between these mutations and carcinogenesis.

Through crystallographic and biochemical methods, it has been determined that the probable oncogenic mechanism of the E545K mutation is the disruption of an inhibitory charge-charge interaction between p110α and the N-terminal SH2 domain of the p85 regulatory subunit (67). It has been previously proposed that the oncogenic mechanism of the E542K mutation is similar to E545K, exhibiting a change in the interaction of p110α with the p85 regulatory subunit. The proposed oncogenic mechanism of the H1047R mutation differs from the exon 9 mutations. The H1047R mutation increases the binding affinity of p110α for the negatively charged

phosphatidylinositol substrate leading to increased activity and transforming potential (68).

Along with the above transformative changes in cells with increased PI3K signaling, aberrant PI3K signaling has also been linked to resistance of cells in preclinical models to a number of targeted and cytotoxic cancer therapies, including trastuzumab and paclitaxel resistance in human breast epithelial cells harboring *PIK3CA* mutations (60, 69). Clinically, the presence of *PIK3CA* mutations has been linked to both favorable (70, 71) and unfavorable (72, 73) patient prognosis, and it has also been reported that exon 9 mutations have a less favorable prognosis than exon 20 mutations in breast cancer (74). The reasons for these conflicting data are not clear, but likely reflect limited sample sizes and difference in treatment regimens between the various studies. Changes in activity have been associated with increased resistance to chemotherapeutics in breast malignancies.

Clinical Occurrence of Mutant *PIK3CA* and *TP53*

In 2011, a clinical study genotyped 120 primary breast tumors and determined the combined frequency of mutations in both *TP53* and *PIK3CA* to be approximately 5.3% which accounts for approximately 11,000 cases of breast cancer per year (75). As mentioned earlier, approximately 50-60% of breast cancers contain either a *TP53* or *PIK3CA* mutation, while only 5.3% of these contain both. The low frequency compared to the individual mutation rates can be attributed to hormone receptor expression. *TP53* is commonly associated with ER-/PR- breast cancers, while *PIK3CA* is often associated ER+/PR+. However, the combined frequency of *TP53* and *PIK3CA* was relatively high

when compared to other combined frequencies in the study, which exhibited numbers closer to 1.3% (75). It is also important to note that *TP53* can often be mutated in late stage disease, for which mutational data on metastatic samples is limited.

In general, when using systemic therapies to treat cancer, combining therapies is a more effective strategy for eliminating potential drug resistance rather than the use of single agents. The importance of studying mutations in the context of one another was demonstrated by Di Nicolantanio and colleagues in 2010, where they showed that *PIK3CA* mutations, while sensitive to rapamycin individually, became resistant in the presence KRAS or BRAF mutations (76). Di Nicolantonio *et al.* demonstrated the importance of studying molecular markers in the context of one another and the vastly different phenotypes that can arise in the presence of additional mutations. While specific oncogenic DNA mutations help to provide insight to the development and treatment of breast cancer, it is the cooperation and collaborative effect of these mutations that leads to carcinogenesis. The accumulation of mutations suggests that accurate models cannot focus on a single mutation but rather the interplay of several mutations. It is becoming increasingly apparent that the successful understanding and treatment of breast cancer will rely on targeting several oncogenic DNA mutations. Therefore, the rationale for targeting both *PIK3CA* and *TP53* hotspot mutations becomes immediately obvious.

This study provides new insight into how targeting separate but cooperating pathways increases the hallmarks of cancer. The generation of a panel of different mutations in a relatively isogenic system allows for the examination of these mutations singly and in combination. The investigation of two different mutations within each of

the genes within a relatively normal background provides a controlled model for investigating these mutations. Furthermore, the development of completely independent clones harboring the same mutations allows for the direct comparison of phenotypic similarities and differences. This allows us to attribute whether a transformative property is due to the combination of a two mutated genes, the dysregulation of a specific gene regardless of mutation type, a specific mutation type, a clonal variant, or any permutation of these characteristics. This panel provides a stronger understanding of the hallmarks of cancer and the role two of the most frequently mutated genes in cancer can potentially lead to new therapeutic methods for treating cancer.

2 MCF10As harboring an isogenic *TP53* R248W hotspot mutation

Introduction

TP53 encodes p53 and is one of the most well-studied tumor suppressor genes. Among its many functions, p53 plays a central role in apoptosis, cell cycle arrest and maintaining genomic integrity (15, 16). Normally, p53 acts as a critical cellular checkpoint monitor in response to stress such as DNA damage. This function prevents cells with aberrant or damaged DNA from proceeding through the cell cycle, allowing time to correct damaged DNA, or induce apoptosis if DNA cannot be repaired. This critical role thus prevents cells with altered DNA from inappropriate cell division.

Although *TP53* is one of the most well described tumor suppressor genes, the mechanisms of many of its functions have not been fully elucidated. In particular, p53's role in maintaining genomic stability remains incompletely understood. It is well known that in the absence of normal p53 function, downstream effectors such as p21 are crippled and can no longer prevent aberrant cell cycling in response to DNA damage(19). However, this suggests that lack of p53 function is not directly responsible for genome instability, but instead that damaged DNA is allowed to inappropriately propagate through cell division if p53 function is absent(77). This would also suggest that increased cell cycling would produce more opportunities for DNA errors, and thus the absence of p53 function in this instance would allow cells with DNA errors to propagate rapidly and lead to an increased potential for producing oncogenic changes. However,

many human cancers have low proliferation rates, yet still display genomic instability and aneuploidy(78). In addition, seminal studies have demonstrated that loss of *TP53* has distinct functional consequences compared to *TP53* missense mutations (30, 79), yet both types of alterations are found in human cancers. Thus, mechanisms of how genomic instability and aneuploidy arise may differ in cancer cells with homozygous loss of *TP53* versus those with heterozygous missense mutations.

In this study, we sought to elucidate the mechanism of genomic instability specifically associated with *TP53* loss. We approached this via genome editing using the non-cancerous human breast epithelial cell line, MCF10A, and comparing p53 null cells to isogenic cells harboring a common *TP53* missense mutation, R248W. Relative to control and *TP53* missense cell lines, we determined that p53 loss leads to increased genomic instability which is associated with the presence of supernumerary centrosomes, a described mechanism of instability resulting in aneuploidy (80). Using an unbiased proteomic screen, we identified NDRG1 as differentially upregulated in control and *TP53* missense cell lines compared to *TP53* null cells, but only under physiological low proliferation conditions. We show that forced expression of NDRG1 reduced abnormal centrosome numbers in MCF10A and HCT116 p53 null cells, while knock down of *NDRG1* by RNA interference (RNAi) in *TP53* wild type parental cells led to supernumerary centrosomes. Using proximity ligation assays, we found that NDRG1 associates with γ-tubulin, a key component of centrosomes, thus providing a mechanistic link between p53, NDRG1 and centrosome homeostasis. Strikingly, *in silico* analysis of multiple human tumor samples revealed that homozygous loss of *TP53* is nearly mutually exclusive with *NDRG1* overexpression, strongly corroborating our in vitro data to actual

human cancers (81, 82). Taken together, our results provide a new model suggesting that under conditions of physiological low proliferation conditions, p53 upregulates *NDRG1* expression, altering its interaction with γ –tubulin, thereby regulating centrosome homeostasis in a precise fashion. In cells with loss of p53, *NDRG1* expression is not increased during cellular arrest and/or low proliferative states, allowing for supernumerary centrosome numbers that results in genomic instability and aneuploidy.

Results

Distinct phenotypes of p53 null versus p53 R248W heterozygous missense gene targeted cell lines. We have previously described the generation of *TP53* null clones in the MCF10A cell line using genome editing with recombinant adeno-associated virus (rAAV) (83). MCF10A is a spontaneously immortalized non-tumorigenic human breast epithelial cell line (84) that is ideal for genome editing studies given its relatively normal karyotype, genome stability and lack of oncogenic mutations (85). For these studies, we utilized two independent p53 null clones: 3b and 4b, hereafter designated KO1 and KO2. To characterize phenotypes unique to p53 loss versus common missense mutations, we used rAAV genome editing to "knock in" a common *TP53* heterozygous missense mutation, R248W, using a previously described vector (86) (Fig. 2.1A). Two independently derived clones were isolated and confirmed as having a single site of integration and equivalent allelic expression of mutant and wild type alleles (Fig. 2.1B). These were designated KI1 and KI2, and used for further studies.

MCF10A cells require exogenous growth factors, including epidermal growth factor (EGF), for continued proliferation, and indeed, growth factor independence is a

hallmark of a transformed phenotype. Prior work in our lab demonstrated that introduction of oncogenic mutations in MCF10A by gene targeting leads to EGF independent growth (59). In addition, our past studies demonstrated that p53 null cells could propagate without EGF in 2% charcoal dextran treated serum (83). However, for the current studies, we employed physiological concentrations of EGF (0.2 ng/ml), as we have previously shown that this dose of EGF allows for comparison with parental MCF10A cells, which are EGF dependent, but can proliferate slowly at this concentration (59). Using physiological doses of EGF also allows for pathway signaling and drug sensitivity studies that can be masked by high proliferation rates due to hyperactivation of PI3 Kinase and MAP Kinase pathways when using the historic media formulation for tissue culture maintenance of 20 ng/ml EGF (59).

Under physiological doses of EGF, p53 KO cells proliferated more slowly when compared to the MCF10A cells and p53 KI cells (Fig. 2.2A). Since these cells are aneuploid (83), this is consistent with observations that in non-cancerous cells aneuploidy can lead to reduced cell proliferation(87). However, in elevated levels of EGF, p53 KO cells demonstrated similar proliferation rates to parental MCF10A cells, consistent with our prior report (83) (Fig. 2.2B). Interestingly, p53 KI cells demonstrated increased proliferation in high EGF culture conditions, consistent with studies demonstrating gain of function with *TP53* missense mutations (30). In accord with these results, colony formation assays also demonstrated no appreciable difference between p53 KO clones and parental cells, but p53 KI clones had a significantly increased number of colonies in limiting dilution assays (Fig. 2.3).

TP53 is also thought to play a role in preventing genomic instability. Although knock out of *TP53* by genome editing was not shown to influence chromosomal instability (CIN) or lead to aneuploidy in the HCT116 colorectal cancer cell line, p53 null HCT116 do have an increased rate of tetraploidy (88), suggesting possible effects of genome instability due to p53 loss. In contrast, our past work demonstrated that gene targeting of MCF10A cells did lead to aneuploidy, though formal CIN analysis was not performed in those studies (83). We therefore performed fluorescent in situ hybridization (FISH) with multiple probes and carried out a CIN analysis with our cell line panel. As shown in Figure 2.4, one of two p53 KO cells demonstrated a statistically significant elevated rate of CIN compared to parental MCF10A cells and p53 KI cells. It should be noted that KO2 has an increase in chromosomal alterations/aneuploidy relative to KO1 (83). Thus it is likely that additional alterations in KO2 account for a high degree of CIN, possibly in mitotic spindle check point genes as previously described (89). In agreement with this, using Matrigel and soft agar assays, only p53 KO2 demonstrated aberrant acini and colony formation, suggesting this effect was mediated by other genomic changes present in this clone (Fig. 2.5).

TP53 loss leads to abnormal centrosome homeostasis and failure to upregulate NDRG1 under physiological low proliferation conditions. Another known mechanism of genomic instability is supernumerary centrosomes leading to abnormal chromosomal segregation and aneuploidy (80, 90). To determine whether altered centrosome homeostasis was present in p53 null cells, we stained for γ-tubulin as previously described(91). As seen in Figure 2.6, increased centrosomes were seen only in p53 KO

cells and not in parental or p53 KI cell lines. This difference was statistically significant for both p53 KO clones and suggests a direct effect of p53 loss. Interestingly, supernumerary centrosomes in p53 KO cells were seen predominantly in physiological EGF conditions (Fig. 2.6A, B). However, under high proliferative conditions with 20 ng/ml EGF, cells displayed increased cytoplasmic fluorescence, which was marked in *TP53* KO cells (Fig. 2.6C). Although there did not appear to be an appreciable difference in centrosome numbers between parental, *TP53* KI and *TP53* KO cells in 20 ng/ml EGF, accurate quantification could not be determined due to the increased fluorescence intensity in *TP53* KO cells.

In order to gain insight into the mechanism of how p53 loss leads to centrosome amplification, we performed reverse phase protein array on protein lysates from our cell line panel under physiological EGF conditions. As seen in Figure 2.7A, one of the most notable differences between p53 KO cells and parental and p53 KI cells was the decreased expression of phosphorylated NDRG1 and total NDRG1. *NDRG1*, also known as Drg1, Cap43, Rit42, RTP, and PROXY-1, was first described as differentiation-related gene 1 (92, 93). *NDRG1* encodes the 46 kD protein, NDRG1, which is highly conserved among multicellular organisms and is ubiquitously expressed in tissues in response to cellular stress (94). Prior studies demonstrated that NDRG1 is necessary but not sufficient for p53-mediated apoptosis (95), and may play a role in spindle organization, as NDRG1 has been shown to co-localize with centrosomes (96). However, NDRG1 as a direct mediator of p53 regulated centrosome homeostasis has not been demonstrated. To correlate and confirm expression of NDRG1 related to abnormal centrosome numbers, cells were cultured in physiological and maintenance dosages of EGF, harvested for cell

lysates, and used for western blot. As shown in Figure 2.7B, under conditions of high EGF, phosphorylated and total amounts of NDRG1 were not significantly different among our panel of cell lines. However, under physiological doses of EGF and lower proliferation rates, parental MCF10A cells and p53 KI cell lines displayed a dramatic increase in NDRG1 expression by western blot (Fig. 2.7B). In contrast, p53 KO cell lines demonstrated minimal to no increase in NDRG1 protein. These data suggest that p53 directly regulates expression of *NDRG1* that is governed by the proliferative state of the cell. Of note, phosphorylated NDRG1 and total NDRG1 levels were consistently similar for all experiments, suggesting that differential phosphorylation of NDRG1 was not involved with any functional role between p53 KO and parental cell lines, and that p53 may be directly regulating gene expression of *NDRG1*.

p53 increases under physiological low proliferative conditions and binds the promoter region of NDRG1. We initially tested whether lowering cell proliferation to physiological levels would have the expected result of increasing p53 protein levels in MCF10A cells. As shown in Figure 2.8A, both MCF10A and p53 KI cells demonstrated relative increases in p53 when placed in physiological EGF conditions, though was absent as expected in p53 KO cells. It should be noted that the p53 KI cells showed elevated levels of p53, consistent with this missense mutation's ability to stabilize the p53 protein (43). Using the same antibody, we next performed ChIP to determine if p53 was bound to a consensus p53 binding site within the *NDRG1* promoter and whether this binding increased in physiological EGF conditions. Quantitative real time PCR demonstrated that parental cells had significantly increased binding of p53 at the *NDRG1*

promoter under physiological EGF conditions relative to high EGF conditions. As expected, no binding of p53 was observed in the p53 KO cells regardless of EGF conditions (Fig. 2.8B). Interestingly, p53 KI cells had a relatively low increase in p53 binding, perhaps indicating that expression of wild type p53 from the unmodified allele could still mediate some binding at the *NDRG1* promoter despite the presence of the dominant negative R248W allele. Together, these data strongly support that *NDRG1* is a p53 inducible gene.

Homozygous deletion of TP53 is mutually exclusive with NDRG1 overexpression in human cancers. To further substantiate the link between p53 and NDRG1, we reasoned that human cancers with homozygous deletion of *TP53* would be unable to upregulate *NDRG1* gene expression. The cBioPortal database provides gene expression, mutational status, and protein expression from a number of clinical studies including from The Cancer Genome Atlas (TCGA)(81). Using this database, we analyzed a potential inverse relationship between homozygous loss of *TP53* and *NDRG1* overexpression across a variety of cancers. To distinguish any differences between *TP53* homozygous deletion and *TP53* missense mutations, only cancer sets containing both *TP53* homozygous deletion and mutations were investigated. Within cBioPortal, twenty-four datasets contained genomic information on cancers with *TP53* homozygous deletions, *TP53* missense mutations, and *NDRG1* overexpression, representing thousands of patients. When analyzing tumors with *TP53* alterations (n=3132), (Fig. 2.9, SI Fig. 1), homozygous deletion of *TP53* was found in 153 cases with only 6 demonstrating *NDRG1* overexpression (3.9%). In contrast, 2979 cases were found to have *TP53* missense

mutations, of which 387 demonstrated *NDRG1* overexpression (14.0%). This result was highly statistically significant by *Chi* square test ($p < 0.000957$) (SI Fig. 1C). These data strongly suggest that homozygous loss of *TP53* prevents overexpression of *NDRG1*, but this is not seen with common *TP53* missense mutations. These results support that our in vitro studies are directly relevant to a large and diverse population of human cancers.

NDRG1 affects centrosome homeostasis. Having established that *NDRG1* is a p53 inducible gene, and the applicability of this relationship to human cancers, we next sought to determine if NDRG1 directly affected centrosome homeostasis. We first generated *NDRG1* knock down clones with short hairpin RNAi (shRNA) vectors in the parental MCF10A cell line. As seen in Figure 2.10, shRNA against *NDRG1* led to a significant decrease in protein levels in both physiological and high EGF conditions. In addition, we established *NDRG1* overexpressing cell lines in p53 KO cells via transfection of a full length cDNA. As shown in Figure 2.10B, NDRG1 p53 KO overexpressing cells had high levels of NDRG1 in physiological EGF conditions. These cell lines were then subjected to centrosome analyses. As shown in Figure 2.11, knock down of *NDRG1* in parental p53 wild type cells demonstrated an increase in centrosomes, while *NDRG1* overexpression in p53 KO cells resulted in a statistically significant decrease in centrosome numbers. To determine if these results were generally applicable, we repeated these studies using a very different cell line, HCT116. This is a human colorectal cancer cell line with a microsatellite instability phenotype, and p53 KO cells have been previously described (97). We generated *NDRG1* knock down cells with shRNA in parental p53 wild type HCT116 cells, as well as *NDRG1* overexpressing cells

in HCT116 p53 KO cells akin to our MCF10A cell line panel and verified protein expression by western blot (Fig. 2.12A). As demonstrated in Figure 2.12B and C, knock down of *NDRG1* in HCT116 parental cells led to a modest but significant increase in centrosome number, while overexpression of NDRG1 in HCT116 p53 KO cells led to a dramatic decrease in centrosome amplification compared to p53 KO cells. These data confirm our results in MCF10A cells, and demonstrate that the level of NDRG1 directly regulates centrosome homeostasis.

NDRG1 interacts with γ –tubulin, a major component of the centrosome. A potential interaction between NDRG1 and γ-tubulin has been previously reported as both proteins are present within the same fraction in co-sedimentation assays (98). In order to confirm that NDRG1 directly interacts with centrosome assembly and mitotic division in vitro, a proximity ligation assay (PLA) was carried out with antibodies against NDRG1 and γ-tubulin. PLA relies upon antibody detection of proteins and if the antibodies are within 40 nm of one another, then ligation of PLA probes occurs followed by amplification and fluorescence probe detection in situ. As shown in Figure 2.13, MCF10A, p53 KI and p53 KO demonstrated positive signals relative to the provided negative controls in physiological EGF conditions. However, signals were reduced in intensity and number in p53 KO cells. Interestingly, numerous positive fluorescence signals were identified throughout the cells, suggesting that NDRG1 and γ-tubulin are continuously associated throughout the cell cycle and are not limited to the centrosomes. These results suggests that NDRG1 and γ-tubulin physically interact throughout the cell cycle, and therefore NDRG1 levels could directly mediate normal versus abnormal centrosome numbers.

Discussion

TP53 is the most altered tumor suppressor gene in all human cancers. It is clear after decades of research that p53 has many roles in both normal and cancer cells, and that common missense mutations have distinct functional consequences compared to complete loss of p53, though both are found in human cancers. Despite numerous studies, there remain areas of uncertainty as to p53's role as the "guardian of the genome" in maintaining genomic stability. Using a panel of isogenic cell lines, our study provides new mechanistic insights into how p53 regulates the centrosome via *NDRG1* depending on the proliferative status of the cell, and helps reconcile past conflicting studies regarding p53, centrosome homeostasis and aneuploidy.

Conflicting studies on whether loss of p53 function leads to aneuploidy and/or CIN likely are due to differences in cell lines and models used to study these phenotypes (83, 88). Furthermore, as demonstrated here, p53 missense mutations have a profoundly different effect than homozygous deletion on a variety of cellular functions and past studies have varied in the methods used to inactivate p53. In addition, prior work using p53 null mouse embryonic fibroblasts suggested that p53 does indeed directly regulate centrosome homeostasis and subsequently aneuploidy(99), while other reports refute this notion(100). We propose that p53 does not directly alter CIN, as missense mutations did not have appreciable increase in CIN. Further, we speculate that loss of p53 does not directly affect CIN as only one of two p53 KO clones, KO2, demonstrated significantly elevated CIN and an increased aneuploid karyotype (83), suggesting that CIN in this clone resulted from secondary genetic events. Consistent with this notion, HCT116 p53

KO cells also do not display CIN, though they do tend to become tetraploid(88). However, our data provide a model whereby loss of p53, but not mutation, leads to abnormal centrosome amplification with resultant aneuploidy, specifically during low, yet physiologically relevant levels of proliferation. As most cell lines in culture are in a highly proliferative state, including HCT116, centrosome amplification and aneuploidy may or may not be seen depending on the proliferative index and status of NDRG1 protein levels, as demonstrated in this study. The ability to precisely control MCF10A proliferation using varying doses of EGF allowed us to identify this property in p53 null cells. Moreover, the striking inverse correlation between homozygous loss of *TP53* and overexpression of *NDRG1* using the cBioPortal database, strongly supports that our model is applicable to human cancers. Although it is arguable that cancers are hallmarked by a high proliferation index, perhaps questioning our model's relevance, many human cancers are in fact known to have a low proliferation rate, particularly in early stage disease. For example, the majority of oestrogen receptor positive breast cancers display very low rates of proliferation as measured by Ki-67 staining. In addition, since loss of p53 is an early event in some tissue types with low proliferation rates, our model provides an explanation as to how loss of p53 under conditions of low cell proliferation could provide the necessary genomic instability that results in subsequent alterations and ultimately leads toward a more aggressive cancer phenotype.

This work also provides a new mechanistic link between p53, NDRG1, centrosome homeostasis and maintaining genome stability (Fig. 2.14). We propose that loss of p53 is more than a "permissive" event that allows cells with damaged DNA to continue through the cell cycle leading to mutations and aneuploidy. Instead our data

suggests that loss of p53 in cells that are undergoing low proliferation fail to upregulate *NDRG1*, a p53 inducible gene. In turn, this inability to increase *NDRG1* expression dysregulates normal centrosome homeostasis, resulting in supernumerary centrosomes with resultant aneuploidy. Although we show that NDRG1 interacts with γ-tubulin, a principal component of the centrosome, we do not yet know how lower levels of NDRG1 during low proliferative states affects centrosome homeostasis. However, it is tempting to speculate that NDRG1 normally sequesters γ-tubulin under low proliferative states such that only the proper amount is available for a normal number of centrosomes to be synthesized. In the absence of p53, NDRG1 is not appropriately increased, leading to excess γ-tubulin and increased numbers of centrosomes with resultant aneuploidy. This model is supported by our PLA results examining the association of NDRG1 and γ-tubulin in p53 KO versus parental and p53 KI cell lines.

In conclusion, we have identified that loss of p53 leads to a distinct form of genomic instability mediated by abnormal centrosome numbers, specifically under conditions of low cell proliferation. These results have potential translational implications as cancers with complete loss of p53 may have a form of genomic instability that may be "turned off" by paradoxically administering mitogens that induce a higher rate of proliferation. As genomic instability is thought to be the driver of clonal evolution and drug resistance, this provocative strategy could potentially allow for use of cytotoxic therapies that are currently thought to be less effective for cancers with a low proliferative index, yet may provide improved outcomes due to prevention of drug resistant clones.

Table 2.1: *TP53* R248W Cloning and Screening Primers

Screen	Homology Arm	Forward/Reverse
Homology Arm Cloning Primers	5’	5’-TCTTCCTCTTCCTACAGTAC
		5’-ATGAGGCCAGTGCGCCTTGG
	3’	5’-CTTGGGCCTGTGTTATCTCCTA
		5’-TGTCTTTGAGGCATCACTGC
Pre-Cre	5’	5’-TGAGGTGTAGACGCCAACTCT
		5’-GTTGTGCCCAGTCATAGCCGT
	3’	5’-CGCATCGCCTTCTATCGCCT
		5’-AGTTAGCTACAACCAGGAGC
Post-Cre	-	5’-CTGCCGTCTTCCAGTTGCC
		5’-GCACAGTGGTACCTTAAAATTTGG

Table 2.2: *TP53* R248W Sequencing Primers

Screen	Primer Direction	Sequence
Targeted Allele Sequencing Primers	FWD	5’-CTGCCGTCTTCCAGTTGC
	REV	5’-AGATTCTCTTCCTCTGTGCG
	SEQ	5’-ACGCACCTCAAAGCTGTTC
Bi-Allelic Sequencing	FWD	5’-CTGCCGTCTTCCAGTTGC
	REV	5’-ACGCACCTCAAAGCTGTTC
	SEQ	5’-AGAAATCGGTAAGAGGTGGGC
cDNA Sequencing	FWD	5’-CCAAGTCTGTGACTTGCACG
	REV	5’-AGATTCTCTTCCTCTGTGCG
	SEQ	5’-AGAAATCGGTAAGAGGTGGGC

Table 2.3 Chromatin Immunoprecipitation primers

Screen	Primer Direction	Sequence
Putative p53 binding site	FWD	5’-AAGTGAAGGGAGTCGCTCAG
	REV	5’-GTTGCGCAAGCAGTCGTAG
Negative control: Upstream	FWD	5’-TTCAGCAGGAAGTGTTGTGC
	REV	5’-CTGGGCATTGGGGTTTTTAC

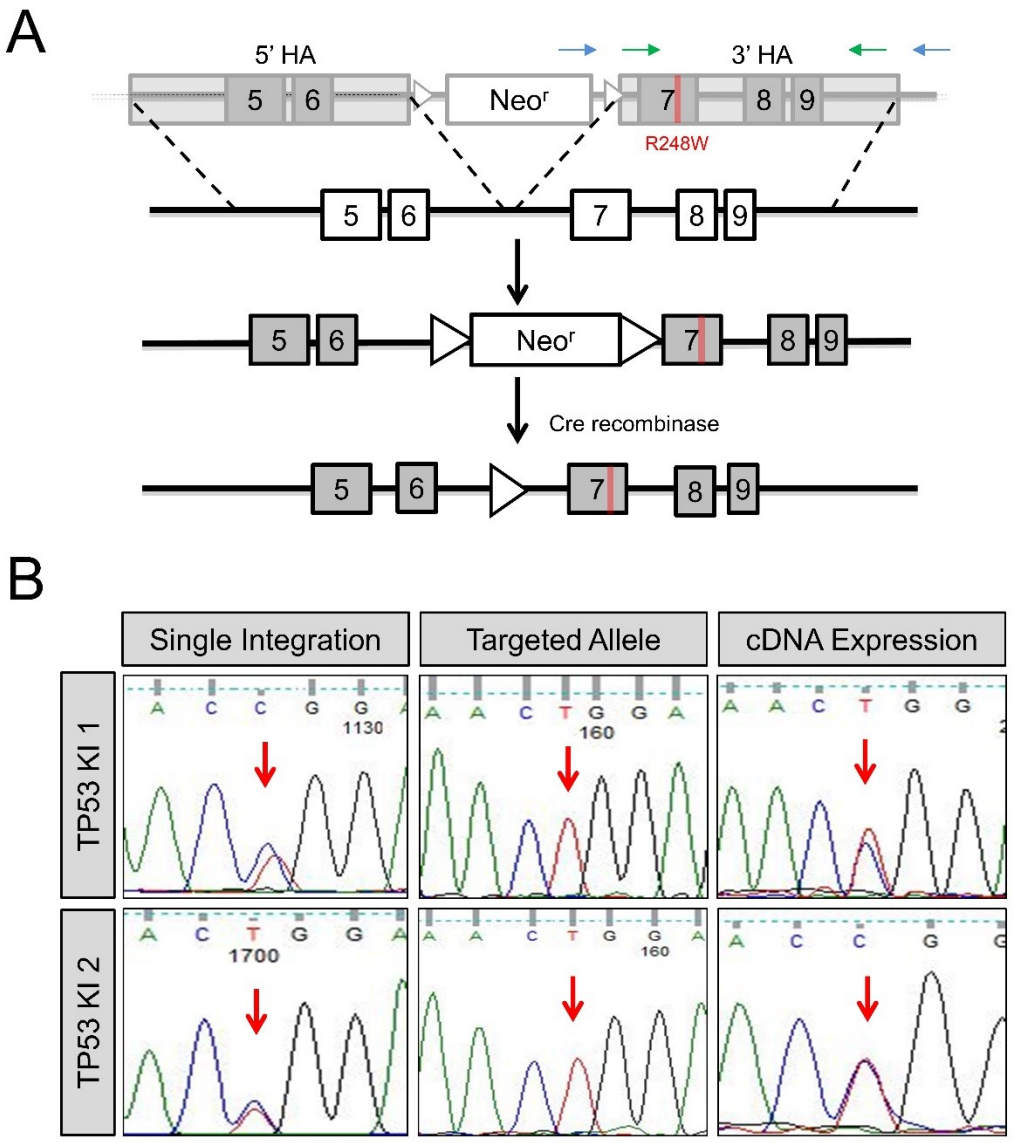

Figure 2.1: Gene targeting overview for TP53 R248W mutation. A) Representative rAAV-mediated gene targeting schematic for a targeting vector with an exonic TP53 mutation (R248W) within the 3' homology arm (HA). rAAV transduction facilitates integration of the targeting vector into the genome via homologous recombination between the 5' and 3' HA. Following neomycin selection and clone isolation, the *LoxP* flanked (white triangle) SEPT cassette is excised using Cre Recombinase, leaving a small intronic *loxP* scar. B) Sanger sequencing confirmation of proper integration of the R248W hotspot mutation within the TP53 gene: Single integration (green arrows) and targeted allele (blue arrows).

A

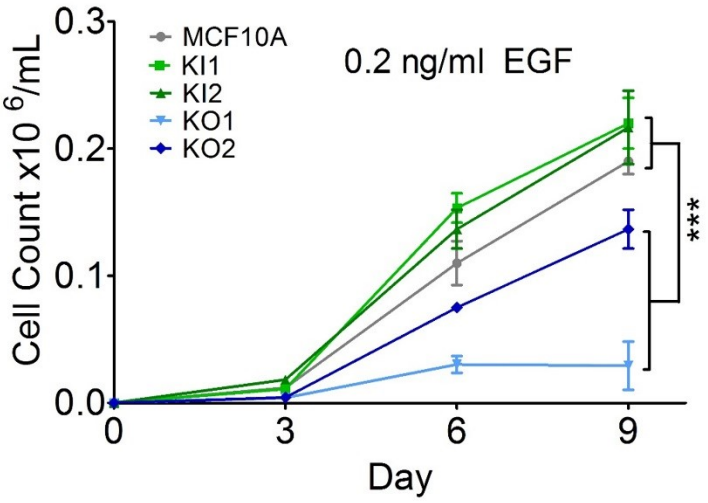

B

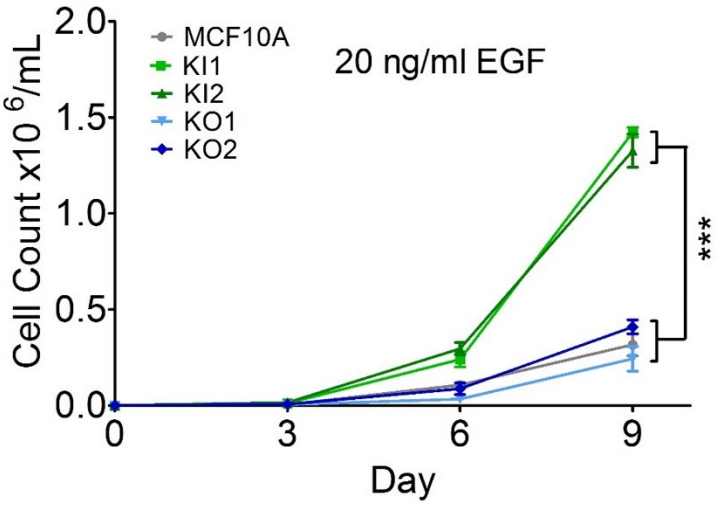

Figure 2.2: Proliferation assay of the TP53 isogenic mutants. A) An increase in proliferation due to the TP53 R248W mutation was verified by a standard growth curve using a Beckman Coulter Vi-Cell XR counter to count viable cells on day 9 of propagation. In physiological (0.2 ng/ml) doses of EGF, both TP53 missense mutations showed a slight growth advantage compared to the MCF10A parental and a significant growth advantage to the TP53 KO mutations (***p value <.001). B) In propagating (20 ng/ml) doses of EGF, the TP53 missense mutations had a significant growth advantage when compared to both the parental MCF10As, as well as the TP53 KO cell lines (***p value <.001). Assays were performed in triplicate within each proliferation assay and each assay was performed at least 4 times.

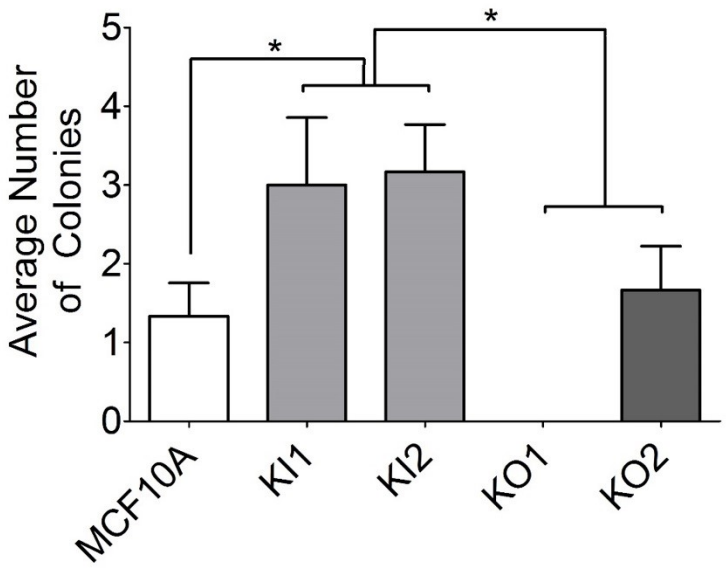

Figure 2.3: Clonogenic potential of the R248W mutation. MCF10A and TP53 mutant cell lines were seeded into 96 wells at cell densities of .5, 1, and 2 cells/well in both physiological and full doses of EGF. The above graph is representative for the .5 and 1 cell/well densities. KO1 was only capable of forming colonies at 2 cells/well regardless of incubation time. Colonies were monitored weekly for 4 weeks. Both TP53 KI cell lines showed a higher rate of clonogenic development when compared to parental MCF10As and the TP53 KOs (*p value <.05). This suggests that the TP53 KI growth is not impaired by loss of cell-cell contact as seen with the KO counterparts and parental MCF10As. Average counts per row were taken for each cell line. Assays were run in triplicate and repeated twice.

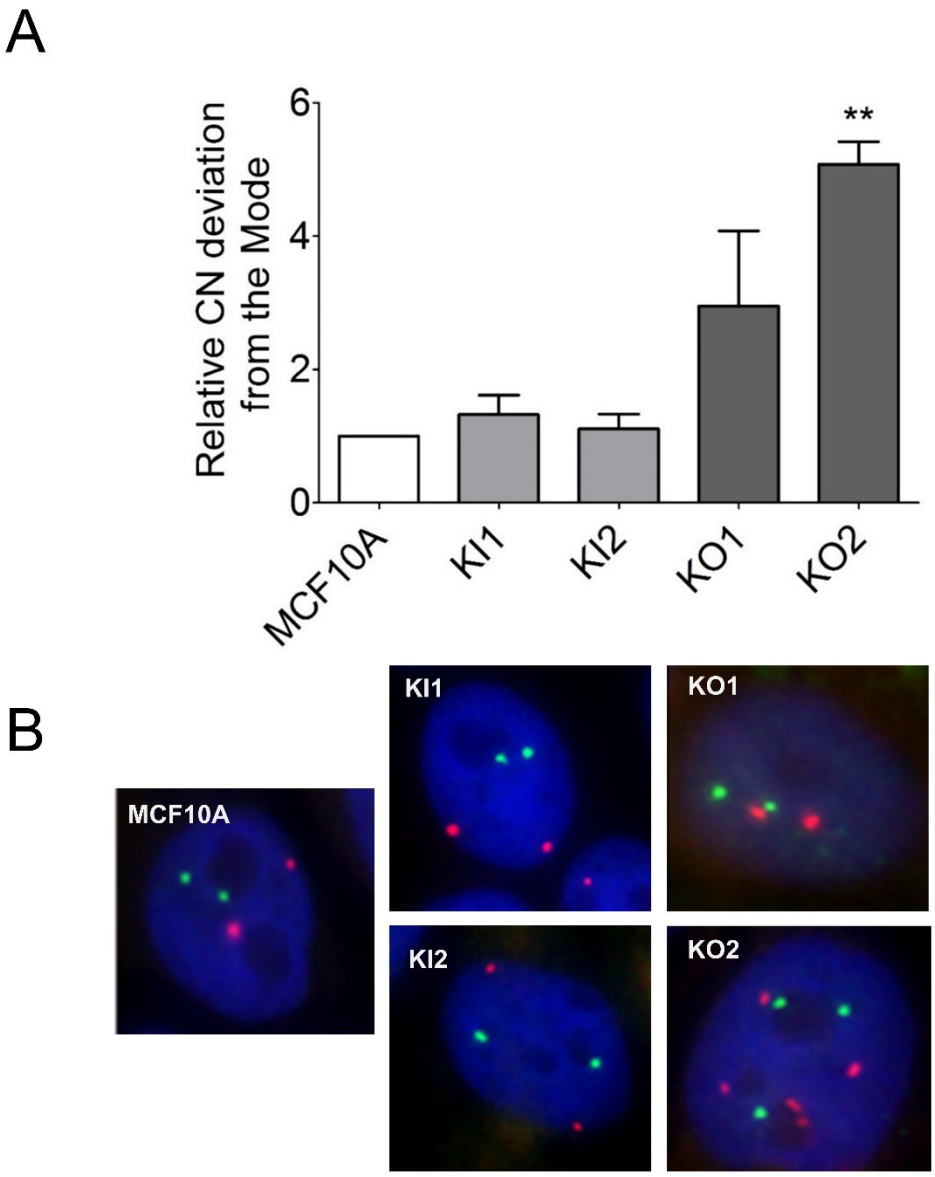

Figure 2.4: Chromosomal instability in the TP53 mutant isogenic cell lines. A) Relative copy number (CN) deviation from the modal population was determined using Fluorescent *In Situ* Hybridization (FISH). The relative change from the modal population is equivalent to the amount of chromosomal instability experienced by the cell. Three genes were objectively selected and probed (c-MYC, EGFR, BCR). KO2 showed a significant increase in chromosomal instability (**p<.01). B) Representative FISH Images for each cell line. EGFR probe (red) and BCR probe (green) with DAPI staining for nucleic acids shown in blue.

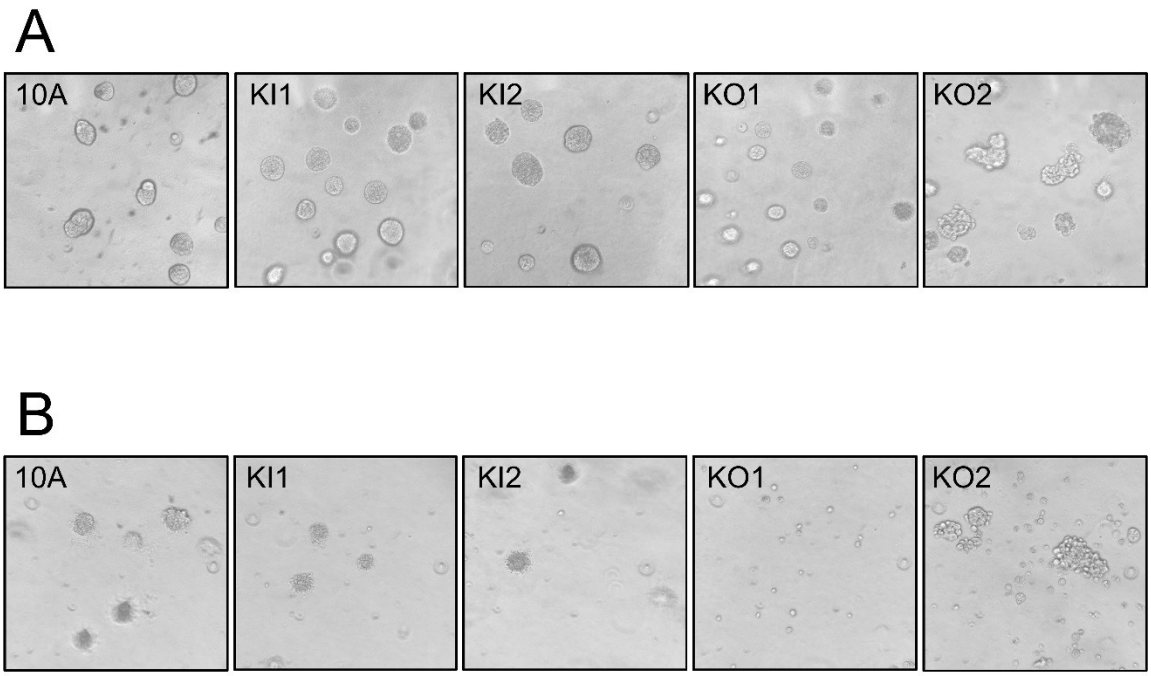

Figure 2.5: TP53 R248W missense mutation and TP53 KO in 3D culture. A) Matrigrel Acini Formation Assay. Cells were seeded at equal densities in Matrigel, which provides a three-dimensional basement membrane culture that allows for acini formation of mammary epithelial cells. Cells were supplemented with low EGF containing assay media. Abnormal acini formation was not observed for either the TP53 KI or TP53 KO. B) Soft Agar Colony Formation Assay. Formation of colonies in soft agar is a measure of invasive capabilities. Cells were supplemented with low EGF containing assay media. Neither the TP53 KI or TP53 KO were capable of forming colonies in soft agar. All images shown at x20 magnification.

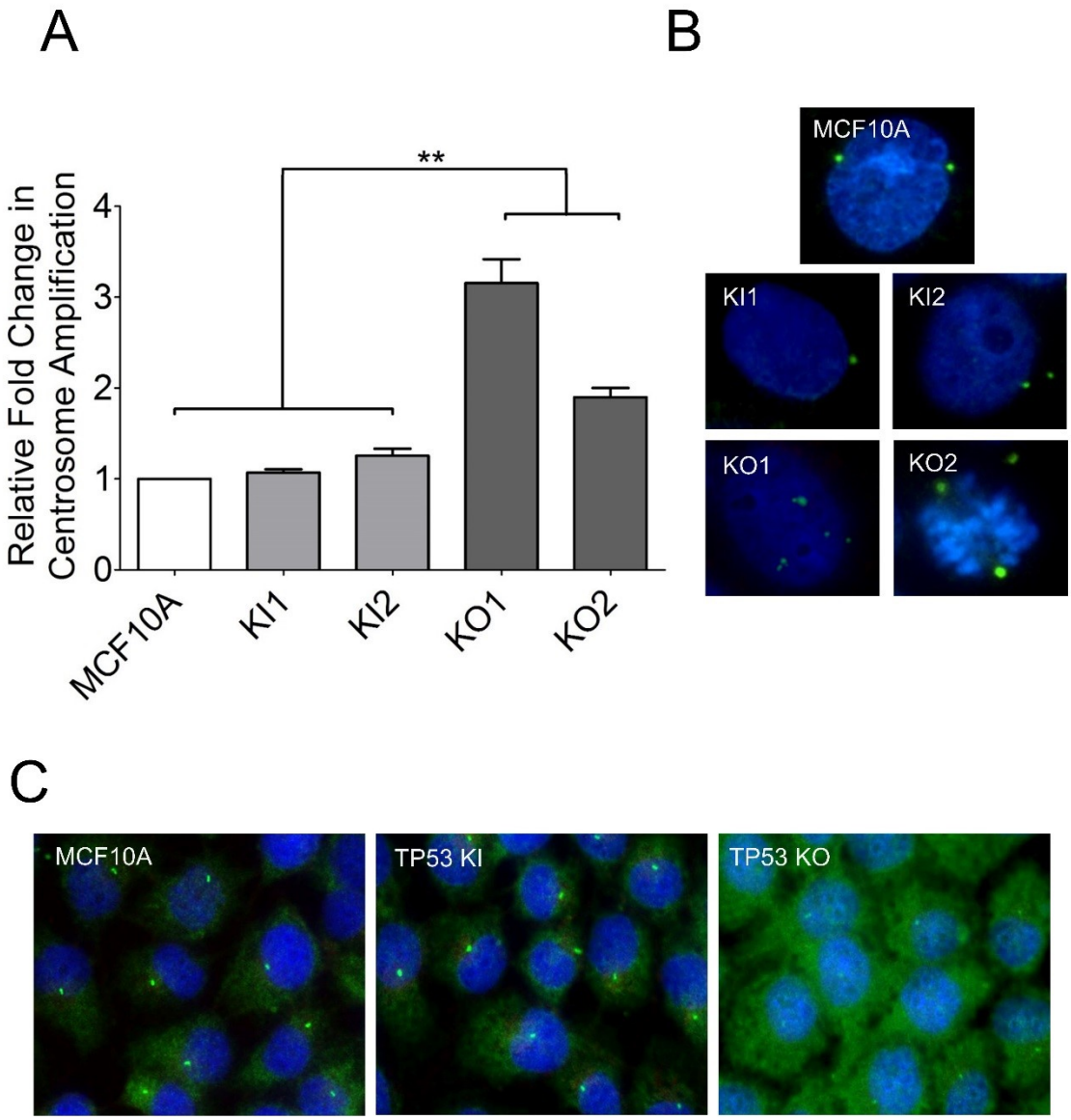

Figure 2.6: Centrosome amplification in the TP53 mutant cell lines. A) Relative fold change of average centrosome amplification normalized to parental MCF10A. TP53 KO cells showed statistically significant (**p<.01) amplification of centrosomes. B) Centrosome amplification was determined by immunofluorescence. Representative images for cells are shown. Green represents immunofluorescent staining of ɣ-tubulin, blue identifies nucleic acids (DAPI). Centrosome counts of one and two are considered normal. C) In high dosages of EGF, TP53 KOs experienced an elevated signal level for the staining of ɣ-tubulin.

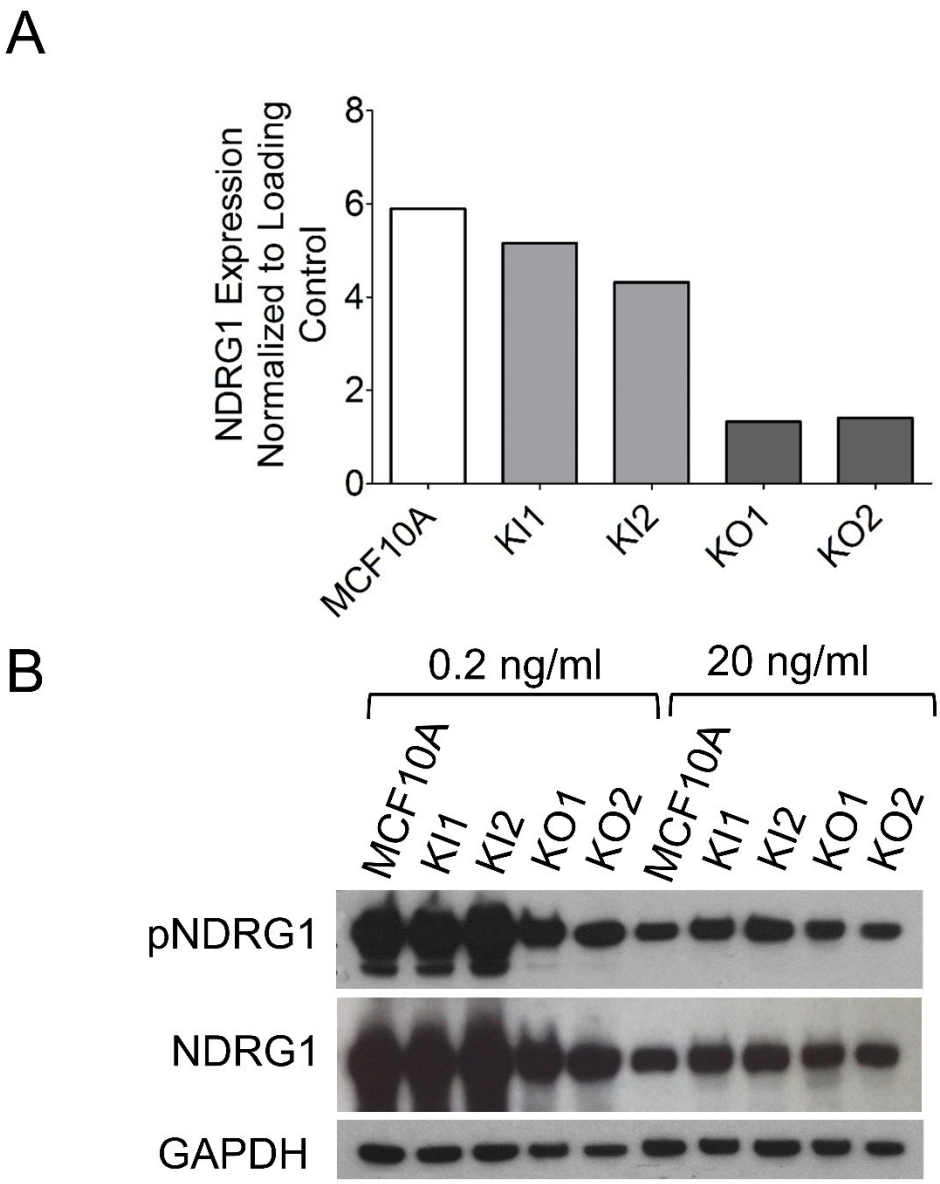

Figure 2.7: NDRG1 expression in TP53 mutant cell lines. A) Relative pNDRG1 expression in cell lines. Reverse Phase Protein Array (RPPA) was carried out on MCF10A and the TP53 mutant cell lines in physiological EGF conditions. pNDRG1 exhibited a 5-fold increase in the presence of at least one WT TP53 allele (MCF10A and TP53 KI). B) Western blot analysis of pNDRG1 and total NDRG1 levels in TP53 mutant cell lines to confirm RPPA expression levels. Elevated levels of pNDRG1 and total NDRG1 were observed in physiological EGF conditions in the presence of at least one WT TP53 allele. At higher levels of EGF, all cell lines exhibited similar levels of pNDRG1 and total NDRG1.

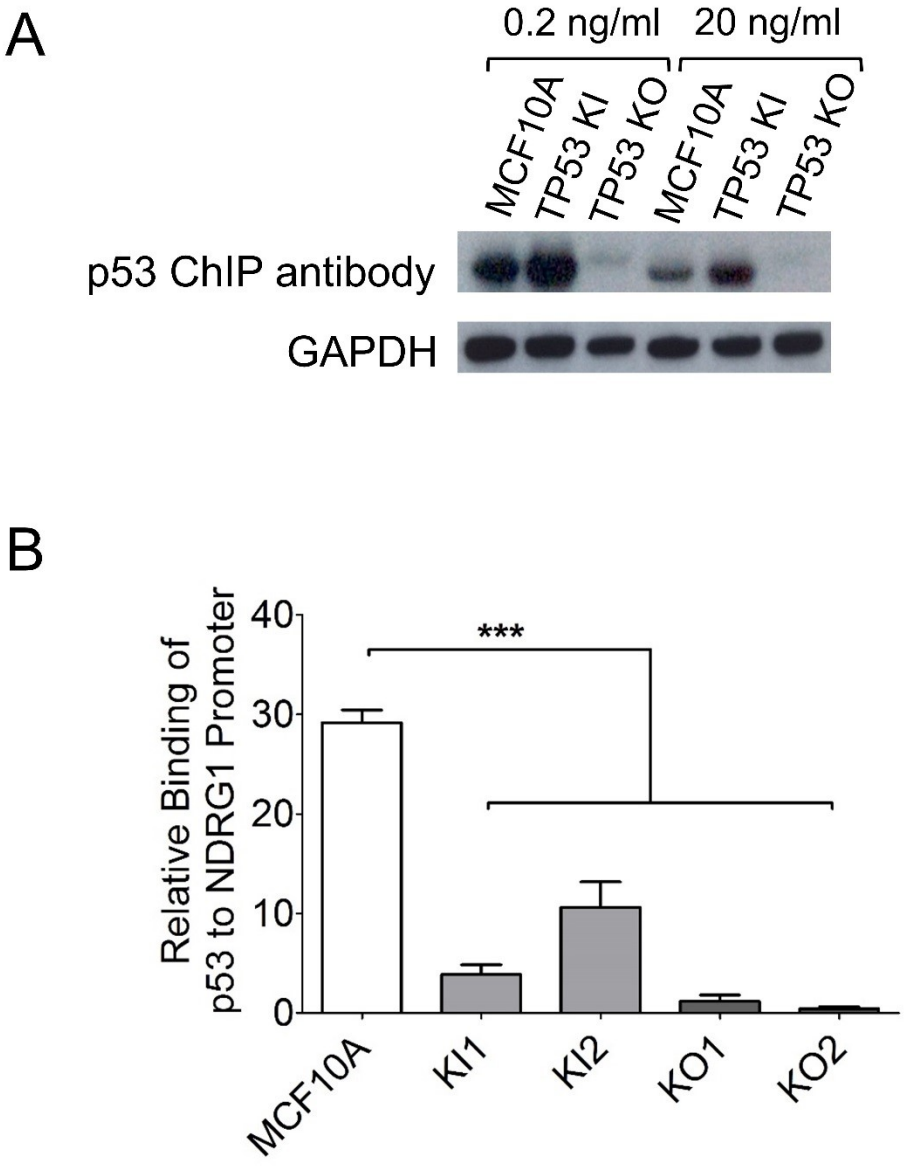

Figure 2.8: NDRG1 is upregulated by p53 and requires one WT TP53 allele in low EGF. A) Western blot of p53 expression in varying doses of EGF. Elevated protein levels were detected for MCF10A and TP53 KI in physiological doses of EGF. p53 bands were not observed for the TP53 KOs in either EGF condition. B) Chromatin Immunoprecipitation of TP53 Derivatives in MCF10A. ChIP analysis of MCF10A and TP53 derivatives in low and high EGF levels revealed a statistically significant (***p<.001) differences in the fold change (low:high). TP53 KIs showed intermediate fold changes in expression which corroborates with the presence of one WT TP53 allele.

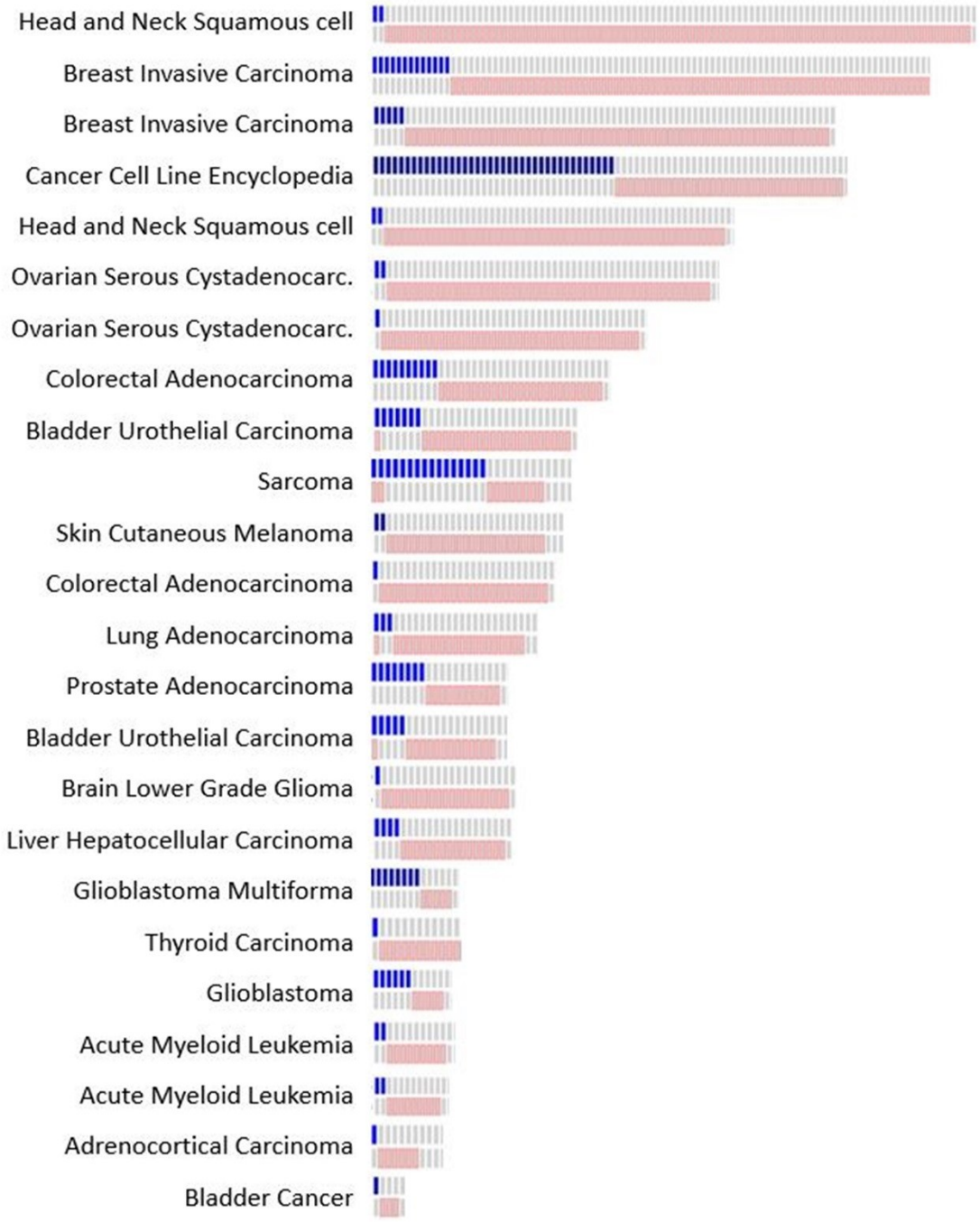

Figure 2.9: CBioPortal Data. Representative data for the 24 cases studies pulled from the cBioPortal Database. Studies were queried for both TP53: HOMDEL and NDRG1: EXP > 2. 3132 tumors harboring a TP53 mutation were analyzed. 3.9% of tumors with HOMDEL mutations exhibited NDRG1 overexpression. Contrastingly, 14.0% of TP53 missense mutations had NDRG1 overexpression (***p <.000957).

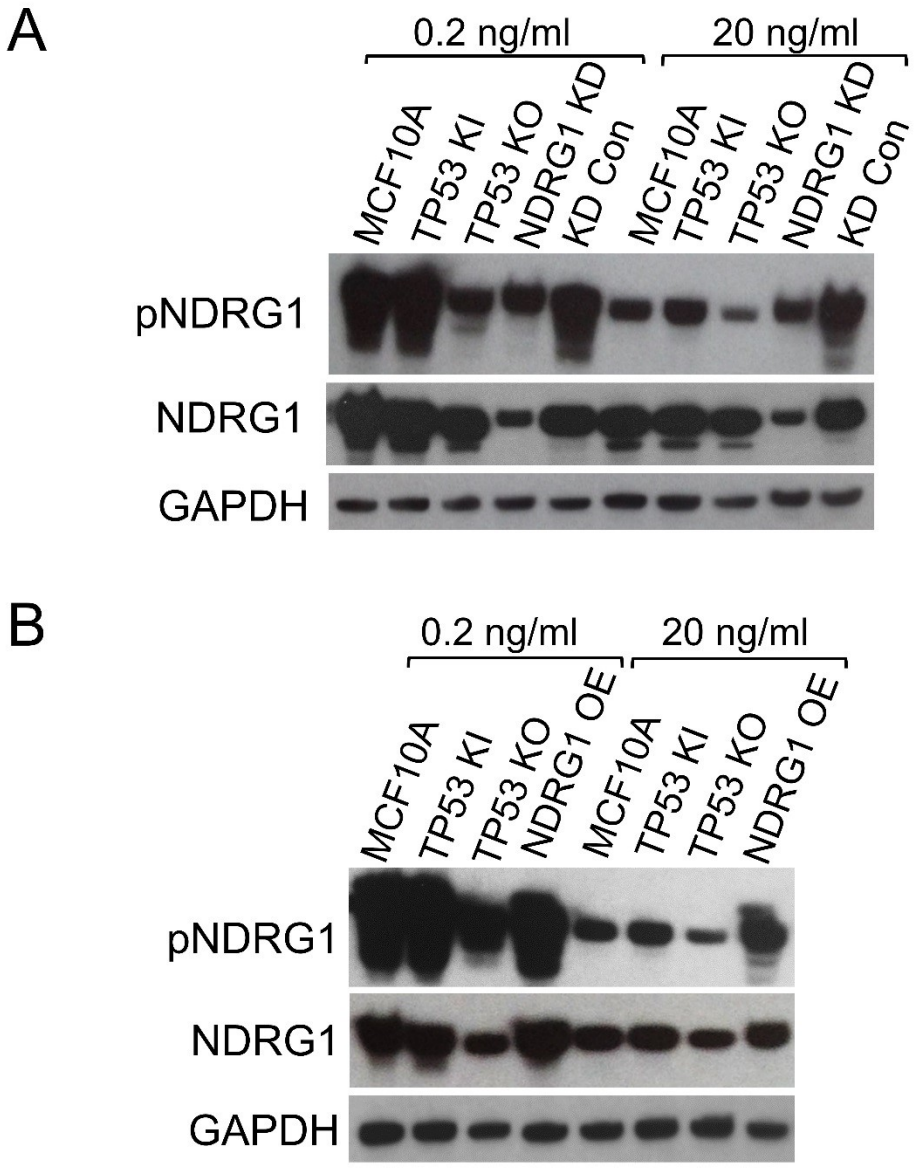

Figure 2.10: Altered NDRG1 Expression in MCF10As and MCF10A Derivatives. A) NDRG1 knockdowns in parental MCF10A (NDRG1 KD) and a vector control in parental MCF10A (KD Con) were created using shRNA, Western blot analysis was used to confirm the decreased expression of pNDRG1 and total NDRG1 in the NDRG1 KD. In physiological levels of EGF, NDRG1 KD showed NDRG1 levels comparable to the TP53 KO clones. B) NDRG1 Overexpression in the TP53 KO cell line was developed using a CMV-Entry Overexpression vector. Western blot analysis was used to confirm increased expression of NDRG1. TP53 KO cell lines with the NDRG1 overexpression vector (NDRG1 OE) showed levels comparable to MCF10A and TP53 KIs.

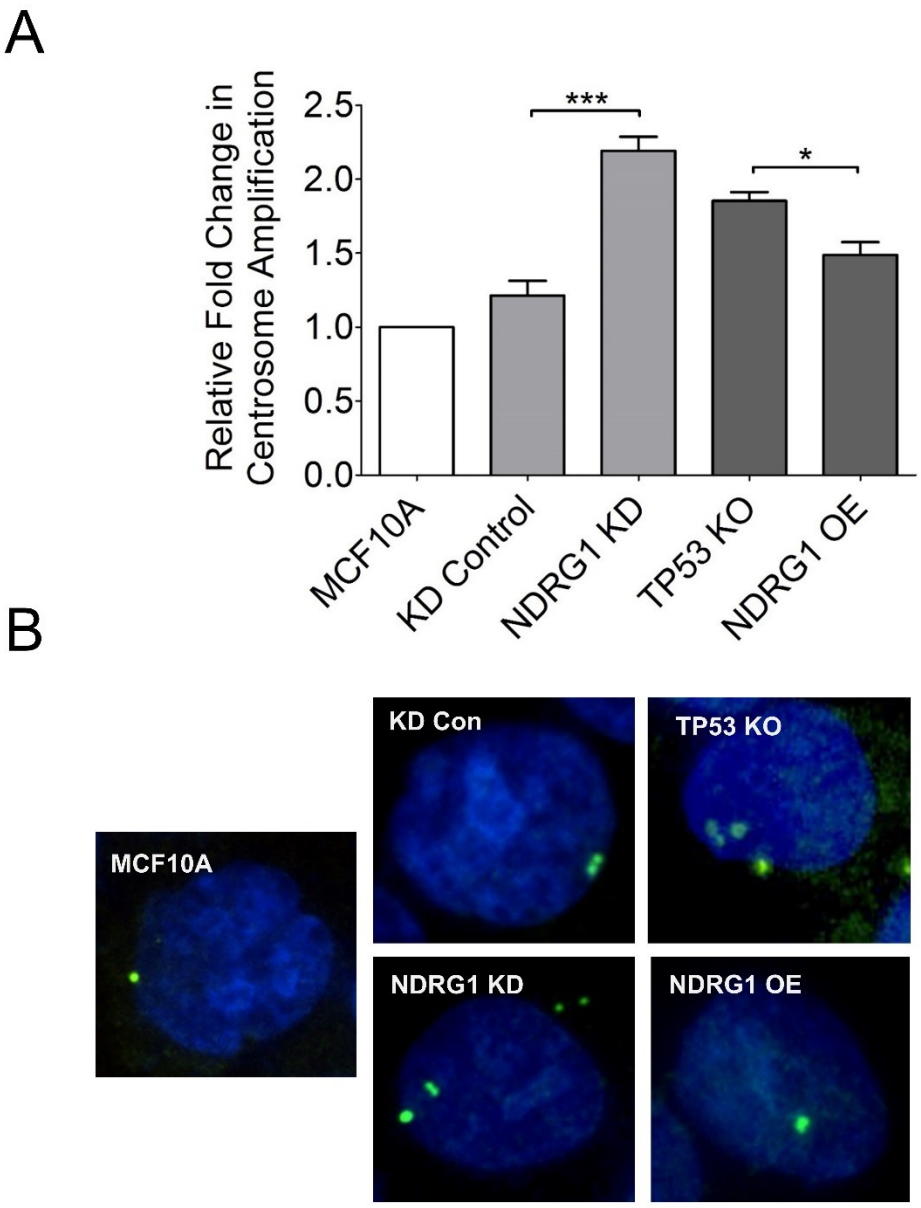

Figure 2.11: Centrosome Amplification is inversely correlated to NDRG1 Expression. A) Relative fold change of average centrosome amplification normalized to parental MCF10A. MCF10As with shRNA knockdown of NDRG1 (NDRG1 KD) showed statistically significant (***p<.001) amplification of centrosomes. When NDRG1 is overexpressed in TP53 KOs centrosome amplification is decreased and showed marginal significance (*p<.05). B) Centrosome amplification was determined by immunofluorescence. Green represents immunofluorescent staining of γ-tubulin, blue identifies nucleic acids (DAPI). Centrosome counts of one and two are considered normal

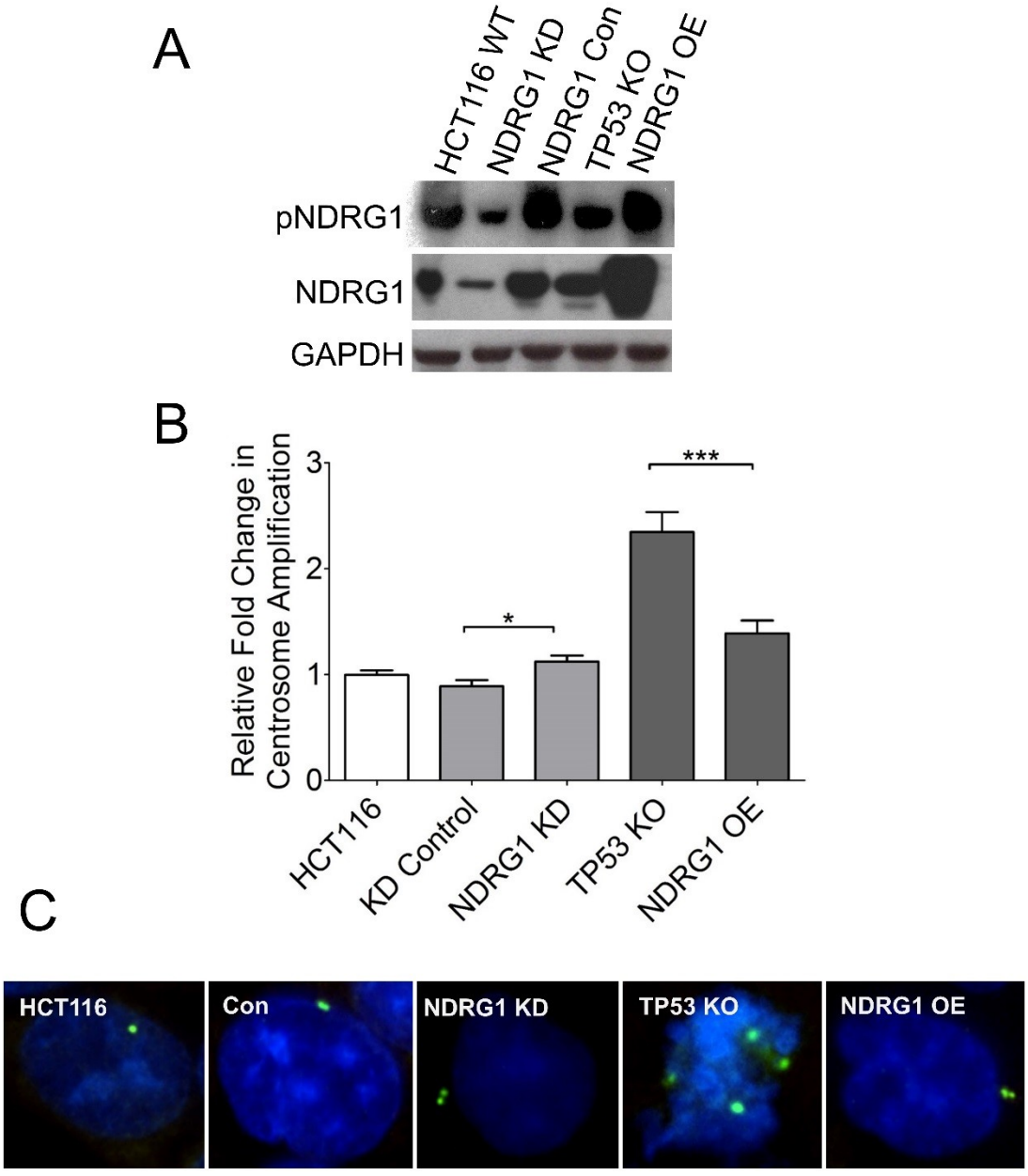

Figure 2.12: Altered NDRG1 Expression in HCT116 cells and Centrosome Assay. A) NDRG1 knockdowns (HCT116 KD) in parental HCT116 and NDRG1 Overexpression (NDRG1 OE) in HCT116 TP53 KO were developed as previously described and confirmed using western blot analysis. B) As with the MCF10A derivatives, centrosome amplification was observed in HCT116 cells with NDRG1 knockdown and the HCT116 TP53 KO cell lines. Furthermore, HCT116 TP53 KO cell lines with NDRG1 Overexpression showed a decrease in centrosome amplification. C) Fluorescent representative images of each cell line.

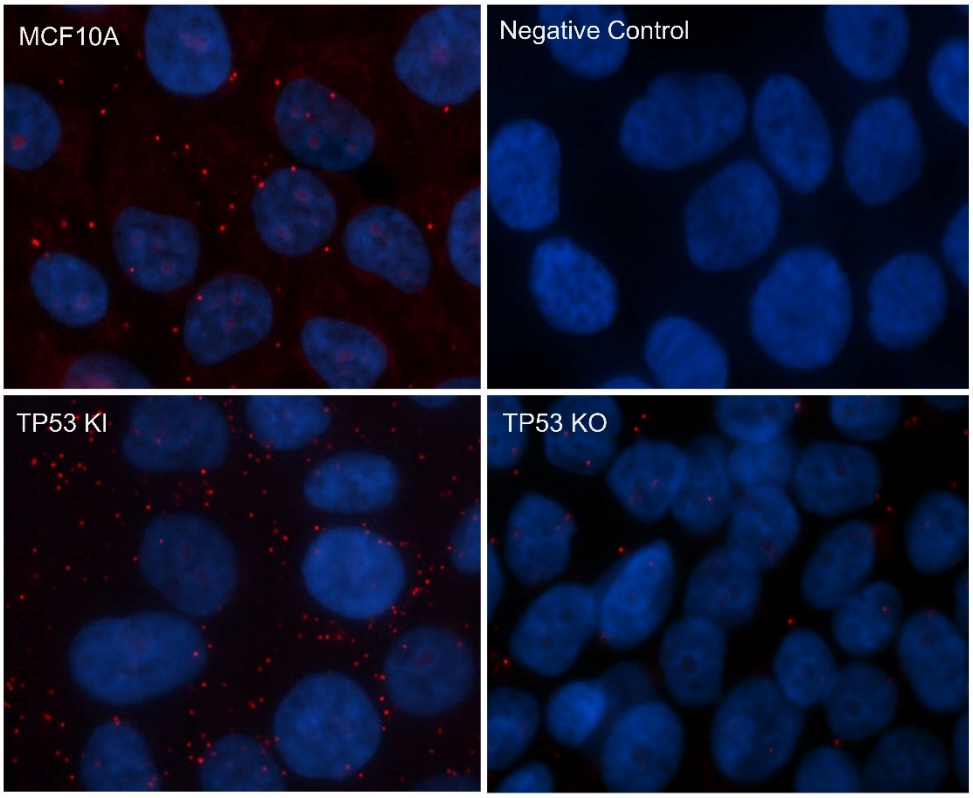

Figure 2.13: NDRG1 colocalizes with γ-Tubulin *in vitro*. Proximity Ligation Assay (PLA) of NDRG1 and γ-tubulin. DuoLink PLA was used to determine if NDRG1 and γ-tubulin colocalize *in vitro*. Red signal represents areas of colocalization between 0-40 nm. Negative controls showed no aberrant signal. DAPI staining of nucleic acids shown in blue.

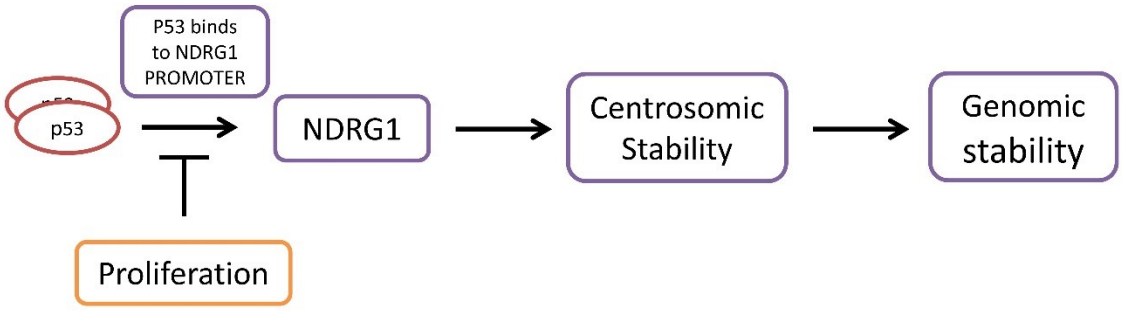

Figure 2.14: Proposed mechanism of NDRG1 expression in TP53 mutant cells. The experiments discussed in Chapter 2 suggest that in low proliferating conditions there is a distinct link between p53 status and NDRG1 expression in the development of genomic instability. In the presence of at least one WT TP53 allele, p53 was shown to bind at a higher affinity to the NDRG1 promoter. The upregulation of NDRG1 in low proliferating conditions leads to an increase in centrosomic stability which leads to genomic stability. However, homozygous deletion of p53 leads to the inability to activate NDRG1. The absence of NDRG1 in low proliferative conditions leads to an increase in centrosomes, abnormal mitotic spindle formation, and an increase in genomic instability.

3 MCF10As harboring both a *TP53* and *PIK3CA* mutation

Introduction

As mentioned in Chapter 1, each year approximately 11,000 new cases of breast cancer will harbor both a *TP53* and *PIK3CA* mutation. *TP53* and *PIK3CA* are the two most frequently mutated genes in primary breast cancer and have the highest rate of co-occurrence among the top five mutated genes in breast cancer (75). While most clinical samples consist of primary tumors, *TP53* is often associated with late stage cancer progression and metastasis. This suggests there is a higher co-occurrence of *TP53* and *PIK3CA* in metastatic disease than the co-occurrence that is presented in primary tumors. The studying of *PIK3CA* and *TP53* in the context of one another will provide invaluable insight into how genetic mutations cooperate to develop breast cancer.

It has previously been shown that the p53 and PI3K pathways intersect and interact at several points. In the early 2000s, a number of studies revealed several points of interaction between p53 and PTEN (phosphatase and tension homolog). PTEN's primary function is a lipid phosphatase that works to reverse the phosphorylation reaction catalyzed by PI3K. The first point of interaction was identified by Stambolic *et al.* in which they showed a functional p53 binding site within the PTEN promoter (101). This interaction suggests that p53 is capable of directly regulating PTEN expression within the PI3K pathway. A second point of interaction was identified at the Mdm2 point on the

p53 pathway and showed that PTEN was able to negatively regulate Mdm2 through its P1 promoter. This implies that PTEN was capable of preventing the degradation of p53 by suppressing the AKT pathway (102, 103). Soon after, a third point of interaction was suggested by Freeman *et al*. which demonstrated a physical association between p53 and PTEN proteins, preventing the degradation of p53 (104). In 2002, Singh *et al.* suggested the two pathways interacted at the transcriptional level and provided evidence that p53 negatively regulates *PIK3CA* transcript and protein levels (105). This observation was reconfirmed in 2007 when Kim *et al* demonstrated that the activation of PI3K signaling by mutations in *PIK3CA* can lead to the activation of p53-mediated growth suppression in human cells. These studies suggested that functional p53 provides a brake on phosphatidylinositol (3,4,5)-triphosphate-induced mitogensis during human carcinogenesis (106). This was confirmed by a study suggesting that *PIK3CA* is regulated by p53 at an alternative promoter site. Furthermore, the study suggests that the loss of p53 function may be one of the mechanisms that contributes to the increased p110α levels in ovarian and other cancers (107).

In 2011, a group of scientists suggested that in the absence of DNA damage the activated AKT pathway induces senescence in human cells via mTORC1 and p53. Through shRNA-mediated knockdown of p53, Astle *et al* identified p53 as an important potential barrier to PI3K/AKT-driven tumorigenesis (108). In the same year, Adams *et al* used a mouse model to imply that *PIK3CA* and *TP53* mutations cooperate in mouse mammary tumor formation. Using a MMTV-Cre system, Adams showed that cooperation between the *PIK3CA* H1047R mutation and a p53 loss-of-function mutation was not on the level of proliferation or apoptosis, the two gene's respective pathways.

Furthermore, the study showed that mutations within the two genes lead to mammary-specific tumor formation with poor differentiation and an increased aggressive phenotype (109). This implied that the two genes interacted synergistically in breast carcinogenesis. All these studies suggest that the accumulation of both a *PIK3CA* and *TP53* mutation play a combined and important role in breast tumor development.

However, despite evidence and a heavy focus on the interplay of oncogene and tumor suppressor genes, two important caveats of current models must be addressed. First, most studies are performed in murine, not human, cells and therefore are not completely representative of human cancers. Second, most human studies utilize ectopic overexpression of oncogenes, which is not representative of biologically expression in cancers, and could lead to the artificial activation of p53 and other important pathways (106, 110). This study addresses these issues through the development of a panel of human cell lines within a relatively isogenic background in a biologically relevant setting. Furthermore, the panel of cell lines provides an accurate representation of tumor heterogeneity and may provide a platform for understanding and overcoming this problem in a clinical setting.

Cancer is a highly complex and multifaceted disease with varying acquired capabilities, hallmarks, and phenotypes due to both inter- and intratumroral heterogeneity. This inherent functional variability is due to both genetic and non-genetic processes. Genetic variations among tumors are the result of genomic instability, secondary mutations, and clonal variation and selection. However, tumor heterogeneity in the absence of genetic differences remains incompletely understood. Mechanisms of nongenetic tumor heterogeneity consist of, but are not limited to, bidirectional interaction

between tumor cells and microenvironment, the inter-convertible activation of GTPases, metastable configurations of intracellular networks, and altered epigenetic states (111). The most prominent genetic mechanism of heterogeneity is genomic instability which generates a pool of somatic mutations that can result in the potential selection given microenvironment context and development of varying hallmark capabilities (112). In this study we demonstrate that the incorporation of both a *TP53* and *PIK3CA* mutation into a panel of closely related cell lines results in the development of genomic instability in a controlled, relatively stable background. The panel also provides an invaluable tool in comparing and attributing phenotypic differences to primary and/or acquired secondary mutations.

A panel of isogenic cell lines harboring both a *TP53* and *PIK3CA* mutation will provide a biologically relevant model to investigate the proposed synergistic relationship between the two mutations. Furthermore, the panel will provide an environment in which the mutations are expressed at physiological levels within a controlled background. Through the incorporation of these mutations and the onset of genomic instability in a stable cell line provides an important tool in understanding how different mutated pathways behave in cancer. Furthermore, the inherent tumor heterogeneity observed between clones within the panel provides a model for associated primary and secondary mutations to observed phenotypes. Understanding how multiple pathogenic mutations and pathways interact and the ability to take advantage of these alterations will provide the basis and rationale for future targeted therapies and a better understanding of breast carcinogenesis.

Results

Cells harboring both a PIK3CA and TP53 mutation exhibit a distinct growth advantage. In order to study *TP53* and *PIK3CA* mutations in the context of one another, an isogenic panel of cell lines harboring both a *PIK3CA* mutation and *TP53* mutation was developed using genome editing with recombinant adeno-associated virus (rAAV) (83). A schematic representation of the panel is shown in Figure 3.1. Two vectors previously developed in the lab were utilized to knock in the oncogenic hotspot *PIK3CA* mutations, E545K and H1047R into MCF10A cells already containing either the *TP53* R248W mutation or a homozygous deletion (Fig. 3.2) (59, 113). Sanger sequencing was used to confirm the incorporation of both the *PIK3CA* and *TP53* mutation in their respective genes, a 50:50 biallelic ratio, and cDNA expression (Fig 3.3-3.6). Clones for each set of mutations were developed separately using independently derived parental clones.

To assess growth phenotype, proliferation assays were carried out in 6 well plates in the absence of EGF. As previously mentioned, parental MCF10As require the presence of EGF to maintain normal growth and avoid growth arrest. It was previously shown by the lab that incorporation of a *PIK3CA* hotspot mutation lead to EGF-independent growth (59). In the absence of EGF, all cell lines harboring a *PIK3CA* mutation exhibited increased growth (Fig 3.7A). Furthermore, cell lines harboring both the R248W hotspot mutation and a *PIK3CA* mutation showed a significant growth advantage (***$p<.001$) to the *TP53* KO/*PIK3CA* counterpart. In physiological doses of EGF, initially the double mutant cell lines experienced similar growth to the parental cell lines. However, as the parental and single mutant cells become confluent they experience cell-cell contact inhibition to suppress further cell proliferation. Conversely, cells

harboring two mutations exhibited continued proliferation after reaching confluency (Fig. 3.7B. The loss of contact inhibition is a transformative property often leading to the development of cancer (6). The loss of contact inhibition in cell lines harboring both mutations suggests that *PIK3CA* and *TP53* cooperate in cancer-like properties. To investigate this synergistic relationship between *PIK3CA* and *TP53*, other transformative properties were further investigated.

Double mutant cell lines exhibit morphological changes and anchorage-independent growth in 3D culture. The panel of isogenic double mutant cell lines and parental cell lines were cultured in Matrigel, a three-dimensional basement membrane culture which supports acini formation of mammary epithelial cells *in vitro*. Matrigel provides a culture environment similar to the natural interstitial space and provides a better medium for observing morphological changes. Normal morphology is a round acinar with well-defined borders and central clearing for the formation of the lumen. It has been previously shown that the parental MCF10As and single mutant cell lines form regular acini in physiological doses of EGF (59). Cell lines harboring both a *TP53* and *PIK3CA* mutation showed significant morphological changes, including protrusions at the borders of acini, bridging between neighboring acini, and loss of structural integrity (Fig. 3.8). It was previously shown that these features resembled the invasive process of cancers and are often seen in cells with increased MAP Kinase and PI3 Kinase activation as a result of high supplemental doses of EGF (114). The observed phenotype for the double mutant cell lines suggests an increase in MAP Kinase activation and cooperation of *TP53* and *PIK3CA* in breast carcinogenesis.

In order to assess the double mutant panel's capacity for anchorage-independent growth and invasive capabilities, cells were grown in a semi-solid soft agar. Growth in soft agar allows for early microscopic examination of transformation, and allows for the observation of morphological changes. A liquid layer of media on top of the semi-solid medium allows for the replenishment of nutrients at frequent intervals. As with the Matrigel acini formation assay, all cells were cultured in physiological doses of EGF. In agreement with previously published studies, parental and single mutant cells did not exhibit transformative or invasive properties. However, the double mutant cell lines were capable of extensive colony formation (Fig. 3.9). This confirmed that the double mutant cell lines, in physiological doses of EGF, exhibit transformative properties that cause an increased capacity for anchorage independent growth and invasive capabilities.

Double mutant cell lines show increased AKT phosphorylation and pathway activation. In order to determine if the increased transformative properties observed in the three dimensional tissue culture was due to *PIK3CA-TP53* cooperative activation, the AKT and ERK pathways were examined using western blot analysis. It was previously shown that the incorporation of a *PIK3CA* mutation into MCF10A led to increased phosphorylation and therefore, activation, of the AKT pathway (59). Using RPPA and western blot analysis it was observed that in the absence of EGF, cell lines harboring both a *PIK3CA* and *TP53* mutation showed increased AKT phosphorylation when compared to both the single mutant cell lines and parental MCF10A (Fig 10A). This suggests that mutations within the *PIK3CA* and *TP53* gene show a synergistic relationship within the AKT pathway. All double mutant cell lines showed increased phosphorylation within the AKT

pathway when compared to the single *PIK3CA* mutant cell lines. Similarly, the double mutant cell lines showed elevated phosphorylation of ERK and p90RSK in the absence of EGF when compared to both the parental and single mutant cell lines (Fig. 3.10B). It was previously demonstrated that in the absence of EGF, single *PIK3CA* mutations were not sufficient for mTOR activation but showed a reduced activation threshold in low levels of EGF. However, unlike the single mutant *PIK3CA* KIs, in the absence of EGF the double mutant cell lines showed varying levels of phosphorylation of p70RSK (Fig. 3.10B). This suggests that mutations in both *TP53* and *PIK3CA* are required to accomplish complete mTOR activation.

Double mutant cell lines exhibit a higher rate of centrosome amplification and genomic instability which may lead to increased copy number variation (CNV). As previously mentioned in Chapter 2, another known mechanism of genomic instability is supernumerary centrosome numbers leading to abnormal chromosomal segregation and aneuploidy (24, 115). To determine whether altered centrosome homeostasis was present in the double mutant panel of cell lines, we stained for γ-tubulin as previously described in Chapter 2. In physiological EGF conditions, it was observed that all double mutant cell lines experienced a significant (* $p<.05$) increase in centrosome amplification when compared to the parental and single mutant cell lines (Fig. 3.11A). Additionally, cell lines harboring both a mutation in *PIK3CA* and *TP53* exhibited irregular mitotic bodies due to centrosome amplification (Fig. 3.11B). This has been shown to lead to chromosomal misseggregation and aneuploidy, and is an underlying contributor to loss of cell cycle fidelity, genomic instability, and loss of tissue structure in human cancers

(116). In order to determine if double mutants experienced a higher rate of genomic instability, Fluoresence *In Situ* Hybridization (FISH) was performed on the panel of cell lines. FISH provides information for changes in both the genomic state, aneuploidy, and the genomic rate, change from the modal population. Double mutants showed varying degrees of increased genomic instability when compared to the parental, single mutant cell lines (Fig. 3.12). The variability may be due to the randomized selection of a limited number of genes. The successful incorporation of genomic instability into a panel of cell lines with a relatively isogenic background provides a novel and invaluable resource for understanding and exploiting characteristics of cancer for individualized therapy. Furthermore, the variability observed among the panel suggests that any observed CIN would be an indirect effect of the mutation of the two pathways. Through additional analysis, the identification of clone specific modifications and secondary mutations could potentially be attributed to variations in phenotypes and provide a better understanding of carcinogenesis.

Preliminary genomic analysis was carried out using Illumina's OmniExpress ChIP Array in order to do a genome wide SNP and CNV analysis within the panel. Within the double mutant panel, cell lines harboring both a *PIK3CA* and a *TP53* mutation showed a higher number of genomic alterations (Fig. 3.13). Although some genomic alterations were shared among the different clones, varying degrees of loss and gain suggest that in the presence of two mutations there is a considerable increase in genomic instability leading to changes in SNP and CNV. Furthermore, as expected based on chapter 2's studies, cell lines with a *TP53* homozygous deletion exhibited the highest

level of CNV. This coincides with the increased levels of genomic instability observed in Figure 3.12.

Double mutant cell lines show an increase in cell cycle progression and aneuploidy. In order to determine if the loss of *PIK3CA* and *TP53* lead to an increase in cell cycle progression, the panel of cell lines was analyzed using propidium iodide and flow cytometry. In both the absence and low doses of EGF, the double mutants showed a significantly (** $p<.01$) higher population of cells in S and G2/M phase (SI Fig. 3A). It can be theorized that this is due to the loss of the critical p53 cell checkpoint and the increase in proliferation due to the *PIK3CA* mutation. Often the loss of p53 has been found to lead to a G2/M cell cycle arrest, regardless of external growth factors (24). Furthermore, it was observed that the KO_9 experienced a higher population of G2/M phase. This is attributed to the clonal variation and tumor heterogeneity. The loss of p53 leads to the accumulation of many other mutations which in turn can be cause for variations observed between clonal cell lines. As with the *TP53* single mutant cell lines, the ploidic state of the cell line was also observed using flow cytometry. It was found that the double mutant panel, as a whole, exhibited a higher percent population of cells exhibiting > 4n, in both the absence and low doses of EGF (SI Fig. 3B). Similar to the cell cycle analysis, when individual cell lines were analyzed, the KO_9 cell line exhibited almost a 10-fold higher percentage of polyploidal cells (Fig 3.10B). This was again attributed to tumor heterogeneity and the possibility of acquired contributing genetic mutations.

Discussion

Since the discovery of *TP53* and *PIK3CA* mutations in human cancer, ample data has been accumulated describing their involvement in tumorigenesis and demonstrating the dysregulation of these two pathways in cancer. However, studies have only recently begun to focus on the interaction of these two mutated pathways together in cancer. Using a panel of isogenic cell lines harboring both a *PIK3CA* and *TP53* mutation in a nontumorgenic breast epithelial background, our study provides a better understanding for mutational cooperation in breast carcinogenesis and furthermore, helps to elucidate on tumor heterogeneity. The ability to understand the molecular and phenotypic differences within cancer subtypes is critical for understanding and overcoming disease heterogeneity.

With only rare exceptions, all spontaneous tumors theoretically originate from a single cell, yet the majority of human tumors display a high degree of heterogeneity in many morphological and physiological features (117). Due to substantial technical challenges, definitive publications on clonal heterogeneity are scarce. This study provides a platform for understanding clonal differences between a set of closely related cell lines harboring the two most common mutations in breast cancer. As demonstrated by our study, certain phenotypic transformations were the cooperative result of the dysregulation of *PIK3CA* and *TP53*. In both the absence and physiological doses of EGF, the double mutants demonstrated a significant growth advantage. In physiological doses of EGF, the double mutants did not experience cell-cell contact inhibition suggesting the potential for uncontrolled growth, a main characteristic of cancer. Additionally, irregular acini formation and invasive growth in 3D culture were observed

only in the presence of mutations in both *TP53* and *PIK3CA*, regardless of the type of mutation. Similar transformative properties are not observed in the parental MCF10A or single mutant clones. The absence of these transformations in the single mutant cell lines suggests that mutations in both pathways are required to observe transformative properties in 3D culture. This suggests that these observed transformations are the synergistic result of dysregulation of the two pathways. While the dysregulation of both the *TP53* and *PIK3CA* pathway was enough to confer increased proliferation and irregular growth in 3D culture, it was not sufficient for tumor development *in vivo*. Therefore we can infer that the acquisition of these two mutations may be critical but not sufficient for tumorgenesis.

Conversely, when looking at certain molecular changes, such as phosphorylation within the AKT and ERK pathway, there was significant clonal variation within the panel. It was previously shown that mutations within the PIKCA gene lead to elevated levels of AKT phosphorylation in the absence of EGF, as well as a reduced threshold for ERK pathway phosphorylation in low EGF conditions (59). Cells harboring a mutation in both *PIK3CA* and *TP53* showed varying degrees of elevated phosphorylation in the absence of EGF when compared to the single mutant counterparts. It was concluded that mutations in *TP53* and *PIK3CA* lead to cooperated dysregulation of the AKT and ERK pathways but the varying degrees of phosphorylation were due to secondary mutations resulting from genomic instability. Genomic instability was confirmed in the double mutants using fluorescent *in situ* hybridization (FISH). Genomic instability has been implicated as a common result of p53 alterations, regardless of type, however, no systematic analysis of several p53 mutant clones has not been conducted (118, 119). Our

studies show that while genomic instability was the direct result of the two mutations, CIN was not. The significant level of variability suggests that observations of CIN would be the result of secondary mutations and not the direct result of alterations in *TP53* and *PIK3CA*. Furthermore it was observed that there was significant variability in the genomic stability among the different p53 clones. This proposes that tumor heterogeneity and secondary, acquired mutations, play a significant role in the development of genomic instability as a result, p53 mutants have significant variability. The successful incorporation of genomic instability into a panel of related cell lines more accurately mimics the clinical manifestations of a tumor and allows observed transformative properties to be conclusively associated with either primary mutations, which were intentionally incorporated, or secondary mutations, which were acquired through genomic instability.

A noteworthy contribution of the panel is that it provides a solution to a significant flaw in previously models, which focused on a single clonal population. By providing two separately derived clones with the same set of mutations, and furthermore, looking at two different mutations per gene, we gain the ability to attribute observed transformative phenotypes to the dysregulation of both genes or a single, a specific mutation, a clonal subset of the population, or any potential combination. Furthermore, due to relatively isogenic nature of MCF10A derivatives, clones expressing unique transformative properties can be compared to their sister cell line, which contains the same primary mutations. SNP and CNV variations observed within the varying clone could potentially be linked to the observed unique transformative property and provide a stronger understanding for how cancer develops.

The panel demonstrates and provides a strong model for observing and understanding tumor heterogeneity and resulting phenotypic differences. The development of a panel of independently derived mutations in the same parental background provides a relatively controlled model for observing clonal variation. A significant obstacle in tumor resistance is tumor heterogeneity and acquisition of secondary mutations.

Table 3.1: *PIK3CA* E545K Cloning and Screening Primers

Locus	Homology Arm	Forward/Reverse
PIK3CA E545K (Ex.9) Homology Arm Cloning Primers	5’	5’-ATCTCTTTCCTGGACTACTGG
		5’-GATTGGTTCTTTCCTGTCTC
	3’	5’-TGAAAATAAAGTCTTGCAATG
		5’-GCCATTATAACTGTGCCTA
PIK3CA E545K (Ex. 9) Pre-Cre	5’	5’-ATCTCTTTCCTGGACTACTGG
		5’-GCAGACAGCGAATTAATTCC
	3’	5’-TTAAGGTACCACTGTGCATATG
		5’-TAAAATTCAAAAGACATCAGTG
PIK3CA E545K (Ex. 9) Post Cre	-	5’-ATCTCTTTCCTGGACTACTGG
		5’-CATATGCACAGTGGTACCTTAA

Table 3.2: *PIK3CA* H1047R Cloning and Screening Primers

Locus	Homology Arm	Forward/Reverse
PIK3CA H1047R (Ex.20) Homology Arm Cloning Primers	5’	5’-AAGTCAGTCAACCATAATCACC
		5’-GCTTTAGAATAATGCGCAAT
	3’	5’-TTCATGTTATGCCTTAAGTCC
		5’-CTCAGGCACTATCCCATTTA
PIK3CA H1047R (Ex.20) Pre-Cre	5’	5’-TTTTGGTCATACACTTTGAGG
		5’-GCAGACAGCGAATTAATTCC
	3’	5’-TTAAGGTACCACTGTGCATATG
		5’-TAAATGGGATAGTGCCTGAG
PIK3CA H1047R (Ex.20) Post-Cre	-	5’-TTTTGGTCATACACTTTGAGG
		5’CATATGCACAGTGGTACCTTAA

Table 3.3: *PIK3CA* E545K Ex. 9 Sequencing Primers

Screen	Primer Direction	Sequence
Targeted Allele Sequencing Primers	FWD	5'-TTAAGGTACCACTGTGCATATG
	REV	5'-TAAAATTCAAAAGACATCAGTG
	SEQ	5'-AGTAACAGACTAGCTAGAGA
Bi-Allelic Sequencing	FWD	5'-TGAAAATAAAGTCTTGCAATG
	REV	5'-TTAGGCACAGTTATAATGGC
	SEQ	5'-AGTAACAGACTAGCTAGAGA
cDNA Sequencing	FWD	5'-CGACTTTGCCTTTCCATTTG
	REV	5'-GGGTAATTACAGTCCAGAAG
	SEQ	5'-CAGGATTTAGCTATTCCCAC

Table 3.4: *PIK3CA* H1047R Ex. 20 Sequencing Primers

Screen	Primer Direction	Sequence
Targeted Allele Sequencing Primers	FWD	5'-TTTTGGTCATACACTTTGAGG
	REV	5'CATATGCACAGTGGTACCTTAA
	SEQ	5'-GAAAGCCTCTCTAATTTTGT
Bi-Allelic Sequencing	FWD	5'-AAGTCAGTCAACCATAATCACC
	REV	5'-ATTGCGCATTATTCTAAAGC
	SEQ	5'-GAAAGCCTCTCTAATTTTGT
cDNA Sequencing	FWD	5'-TAACATCATGGTGAAAGACG
	REV	5'-TCAGTTCAATGCATGCTGT
	SEQ	5'-TGTTACAAGGCTTATCTAGC

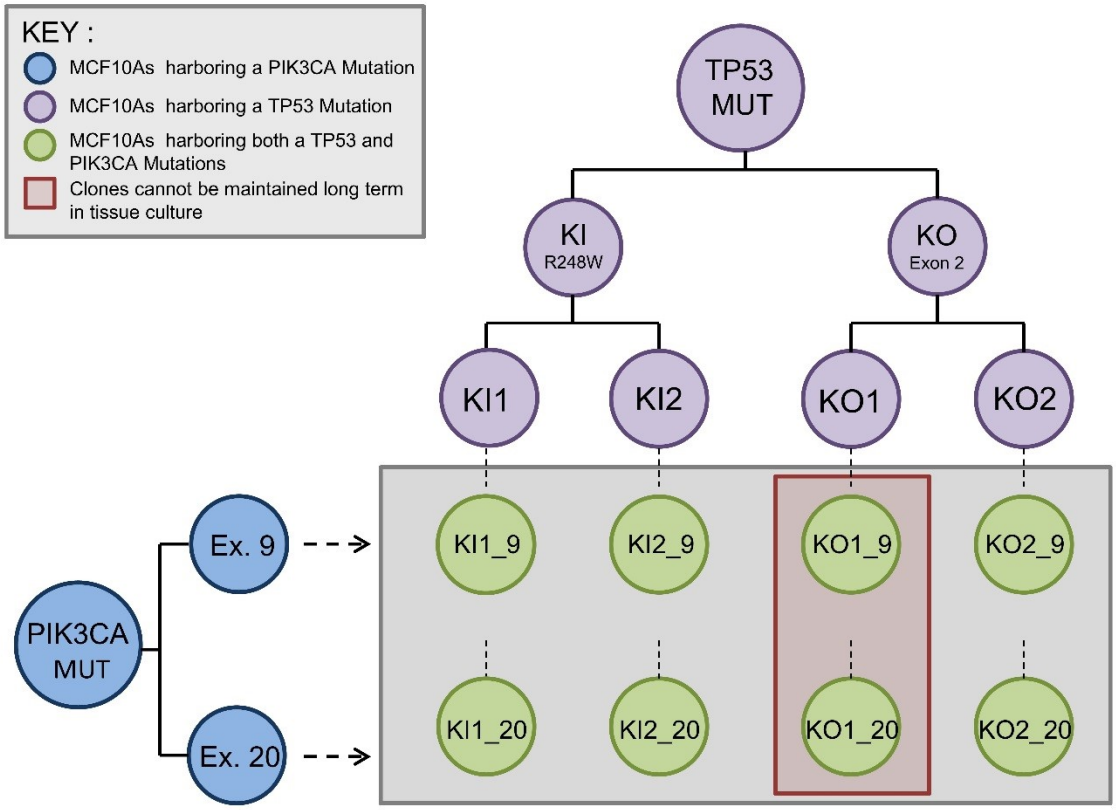

Figure 3.1: Schematic of developed isogenic panel. A panel of isogenic cell lines were developed that contained both a PIK3CA and TP53 mutation. Parental cell lines harboring a TP53 mutations (purple) included previously developed homozygous deletion (KO) and the previously discussed R248W hotspot mutation (KI). TP53 mutant cell lines acted as the parental cell line and were infected with AAV viral vectors containing either the E545K mutation (Ex. 9) and H1047R (Ex. 20) PIK3CA mutation (blue). Double mutant cell lines were developed (green) from independently derived parental clones. Nomenclature for the developed cell lines indicates the TP53 status, clone number followed by a hyphen and the PIK3CA mutation. Ie. KI1_9 : TP53 KI, clone 1, PIK3CA Ex. 9

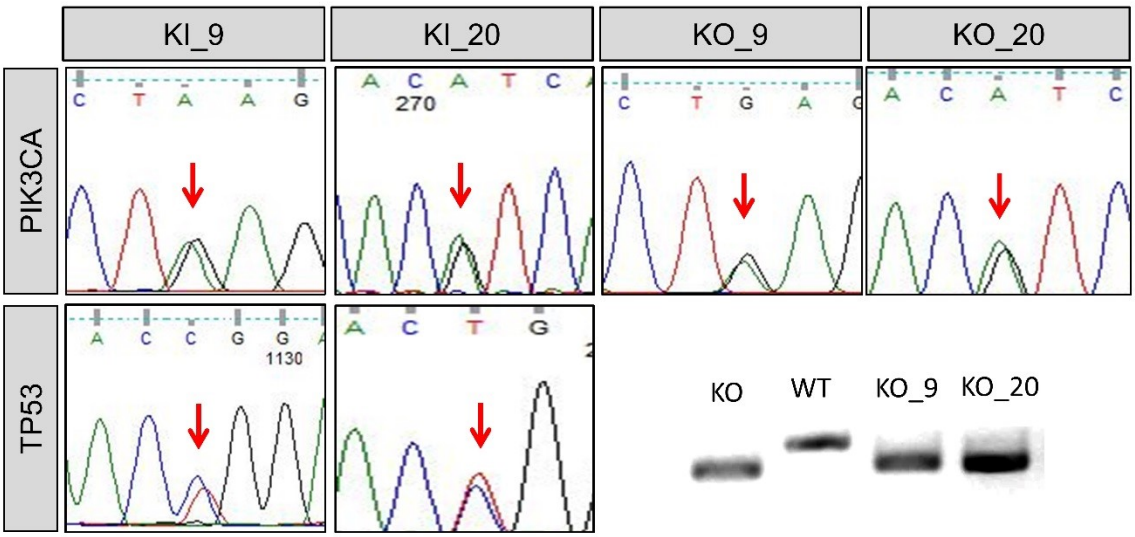

Figure 3.3: Representative Sanger sequencing traces for the isogenic panel. Traces for the PIK3CA and TP53 mutation status for representative clones (Termed Double Mutant). Equal peaks (indicated by the red arrows) indicate 50:50 allelic ratios suggesting that the mutation incorporated into one of the 2 alleles. TP53 homozygous deletion is detected through excision of a small portion of gDNA in exon 2 (bottom right). The lower bands indicate a smaller DNA fragment due to the loss of the excised DNA.

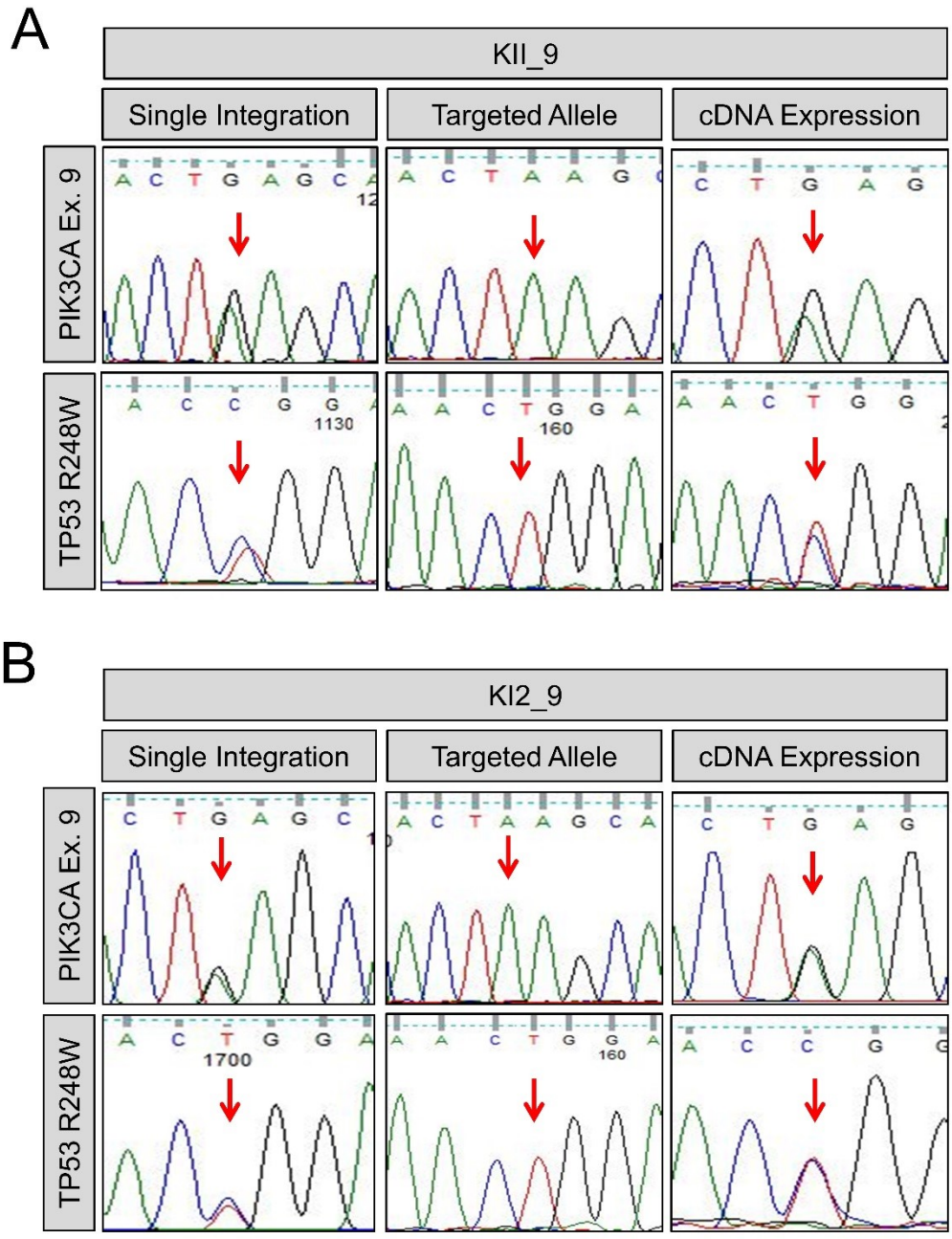

Figure 3.4: Sanger sequencing of double mutant cells with TP53 KI and PIK3CA Ex. 9 mutations. Sequence traces for double mutant cell lines harboring a *TP53* R248W KI mutation and *PIK3CA* E545K KI mutation Clone 1 (A) and Clone 2 (B). To confirm single integration, primers were selected within the homology arms that were not vector specific. Single integration is confirmed by a 1:1 ratio of MUT:WT. Confirmation of the targeted region was carried by selecting primers outside of the homology arm and within the vector. Expression of the mutation was confirmed through cDNA sequencing. A 1:1 ratio of MUT:WT should be observed

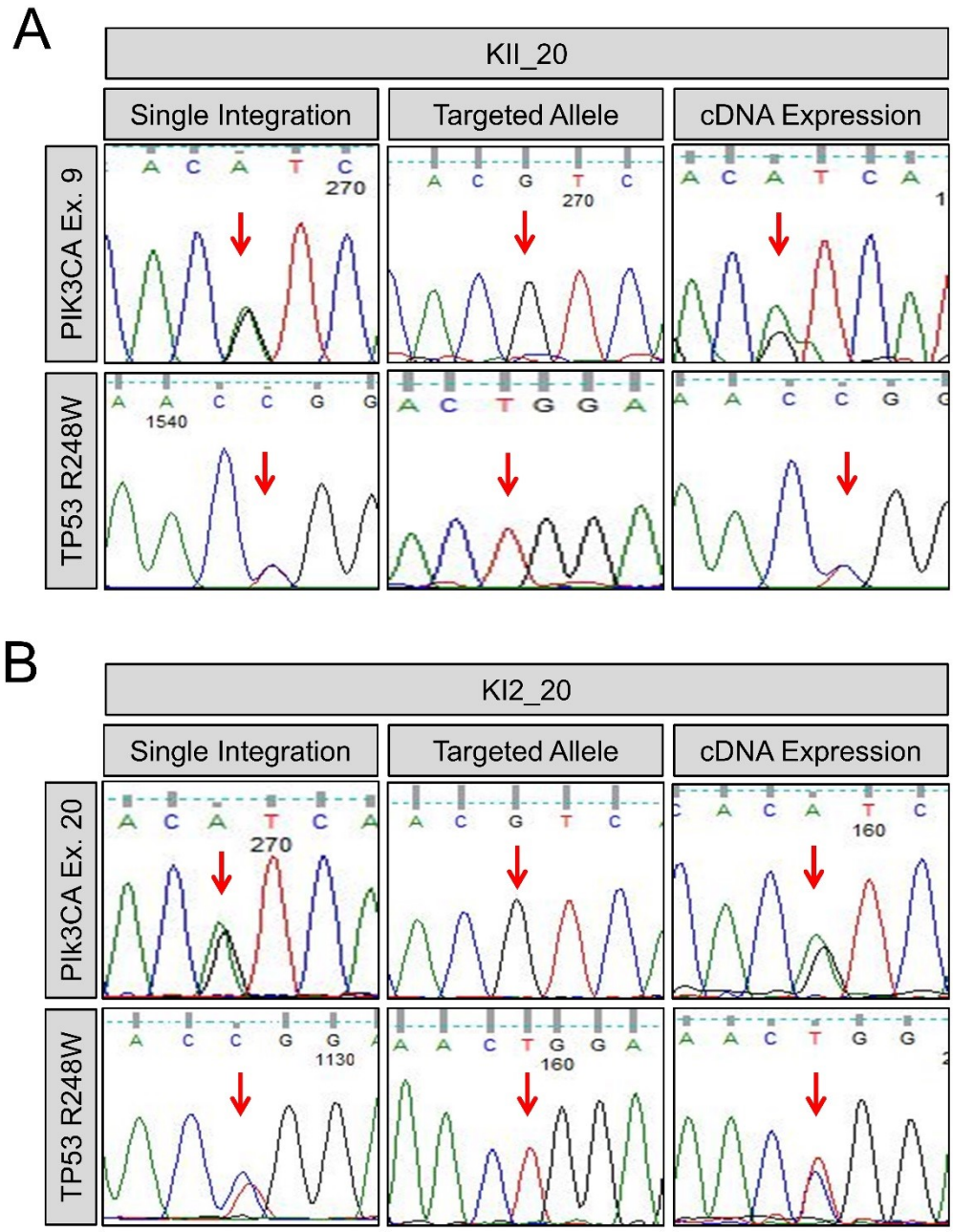

Figure 3.5: Sanger sequencing of double mutant cells with TP53 KI and PIK3CA Ex. 20 mutations. Sequence traces for double mutant cell lines harboring a TP53 R248W KI mutation and *PIK3CA* H1047R KI mutation Clone 1 (A) and Clone 2 (B). To confirm single integration, primers were selected within the homology arms that were not vector specific. Single integration is confirmed by a 1:1 ratio of MUT:WT. Confirmation of the targeted region was carried out by selecting primers outside of the homology arm and within the vector. Expression of the mutation was confirmed through cDNA sequencing. A 1:1 ratio of MUT:WT should be observed

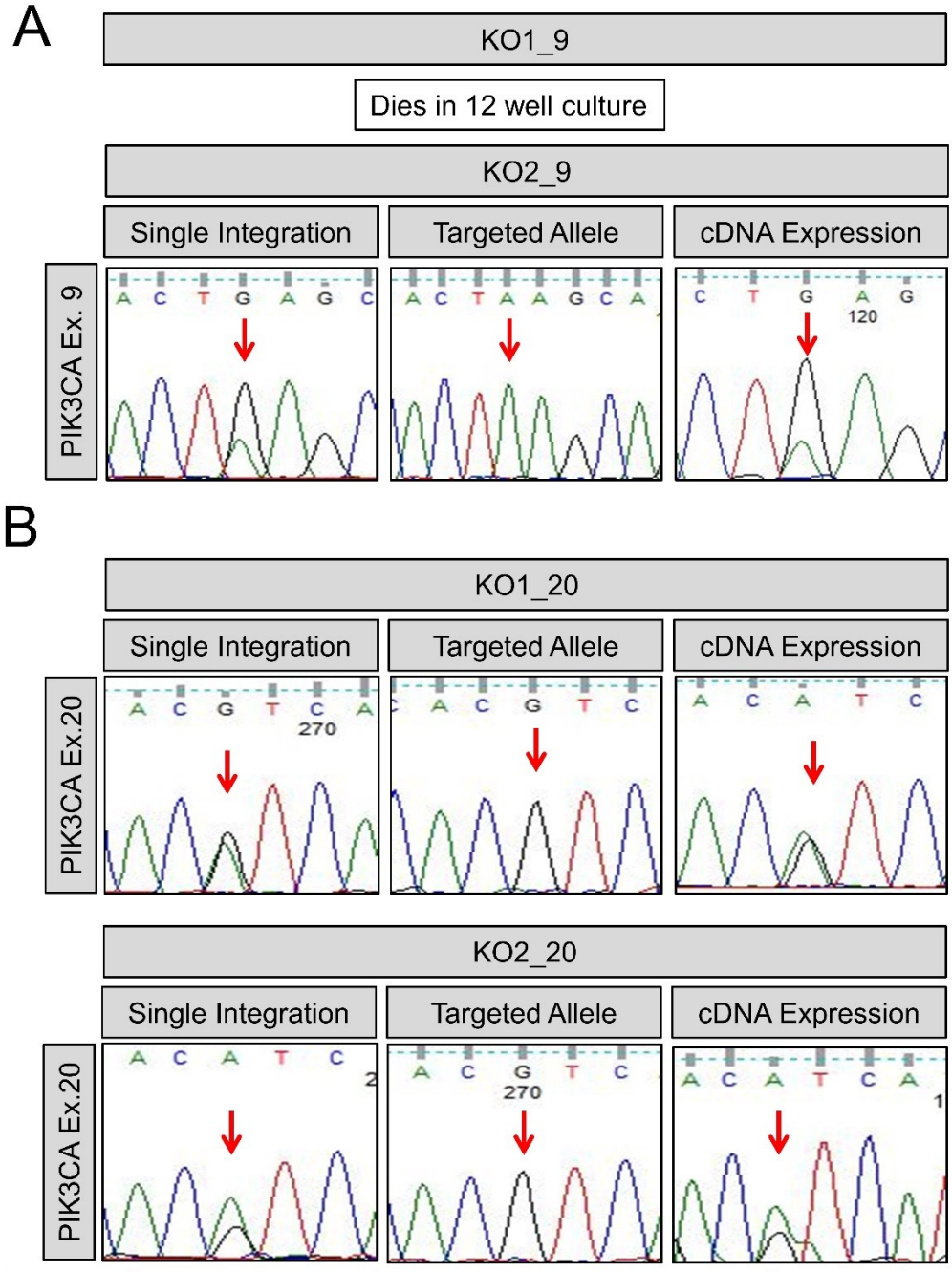

Figure 3.6: Sanger sequencing of double mutant cells with TP53 KO and PIK3CA Mutations. Sequence traces for double mutant cell lines harboring a TP53 KO mutation and either a *PIK3CA* E545K (A) or H1047R KI mutation (B). Confirmation of the targeted region was carried out by selecting primers outside of the homology arm and within the vector. Expression of the mutation was confirmed through cDNA sequencing. KO status was confirmed using a PCR screen shown in Fig 3.3

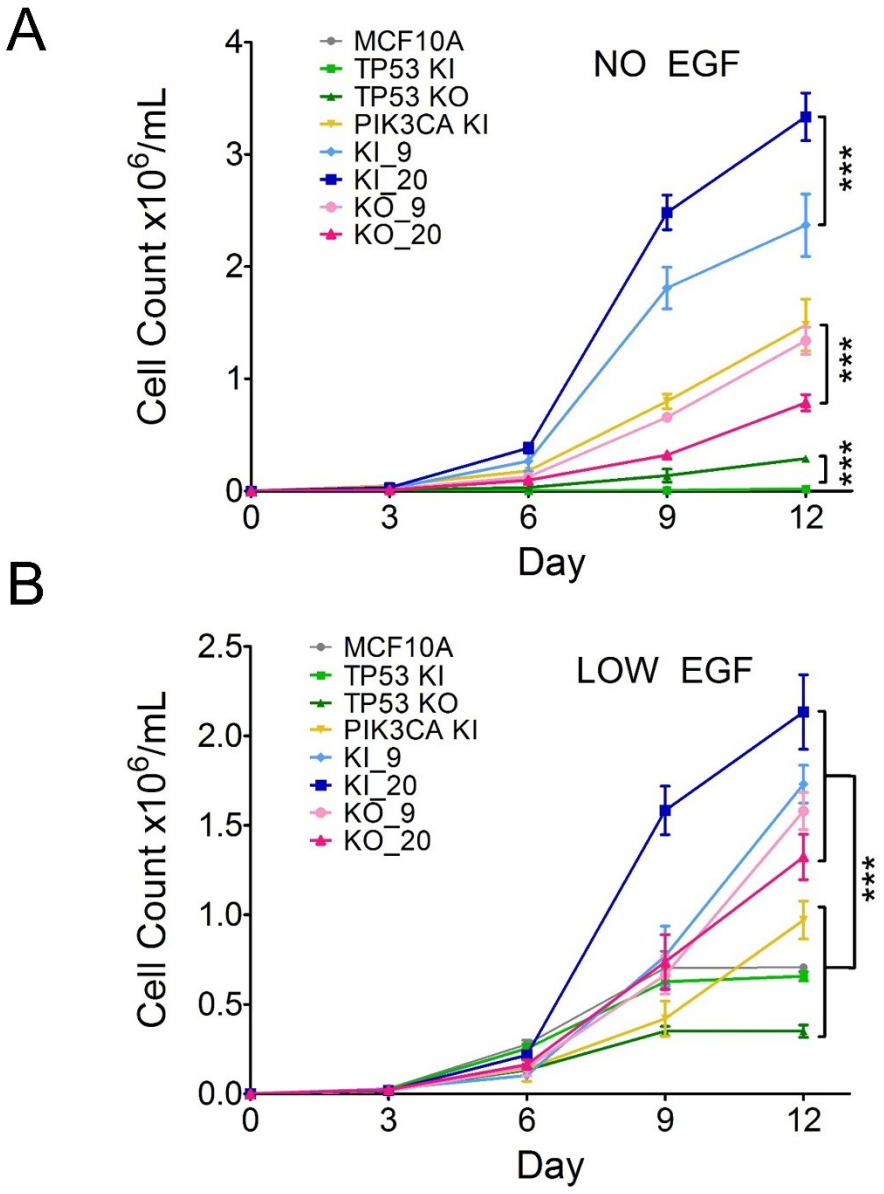

Figure 3.7: Proliferation assay of double mutant panel. A) Double mutant cells showed an increase in proliferation in no EGF conditions. Double mutants with TP53 KI mutations showed a growth advantage over double mutants harboring a TP53 KO mutation (***p value <.001). B) In physiological (low) doses of EGF, the double mutant cells showed a growth advantage and no contact inhibition after day 9 when compared to the parental, single mutant cell lines (***p value <.001). Assays were performed in triplicate within each proliferation assay and each assay was performed at least 4 times.

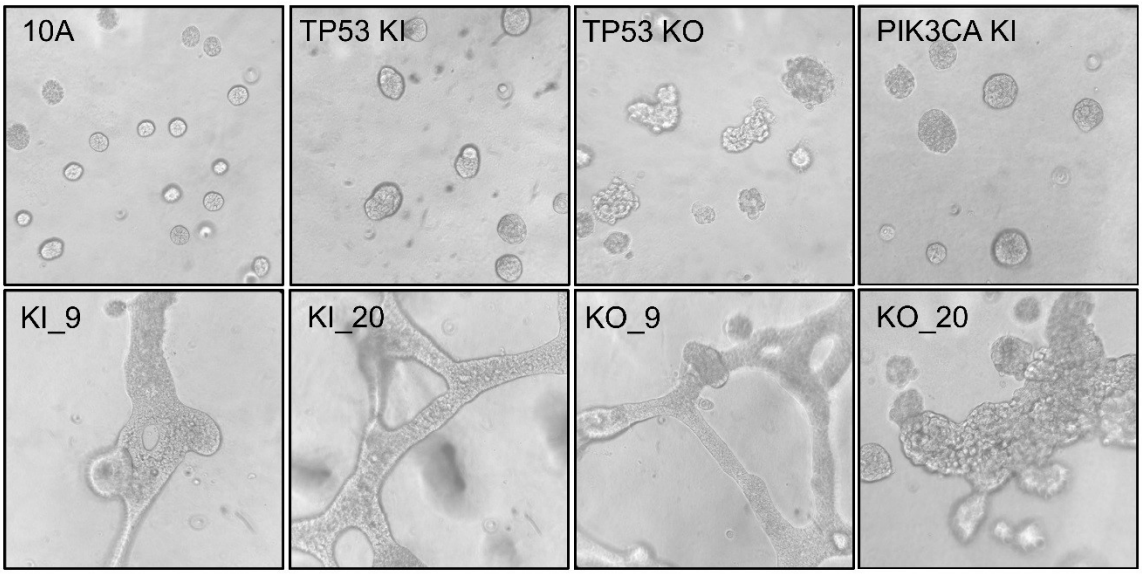

Figure 3.8: Matrigel acini formation assay of double mutant panel. Cells were seeded at equal densities in Matrigel in physiological doses of EGF. Matrigel provides a three-dimensional basement membrane culture that allows for acini formation of mammary epithelial cells. All double mutant cells showed extensive protrusions and irregular morphological transformations. All parental, single mutant cell lines show normal, spherical acini formation. All images shown at x20 magnification.

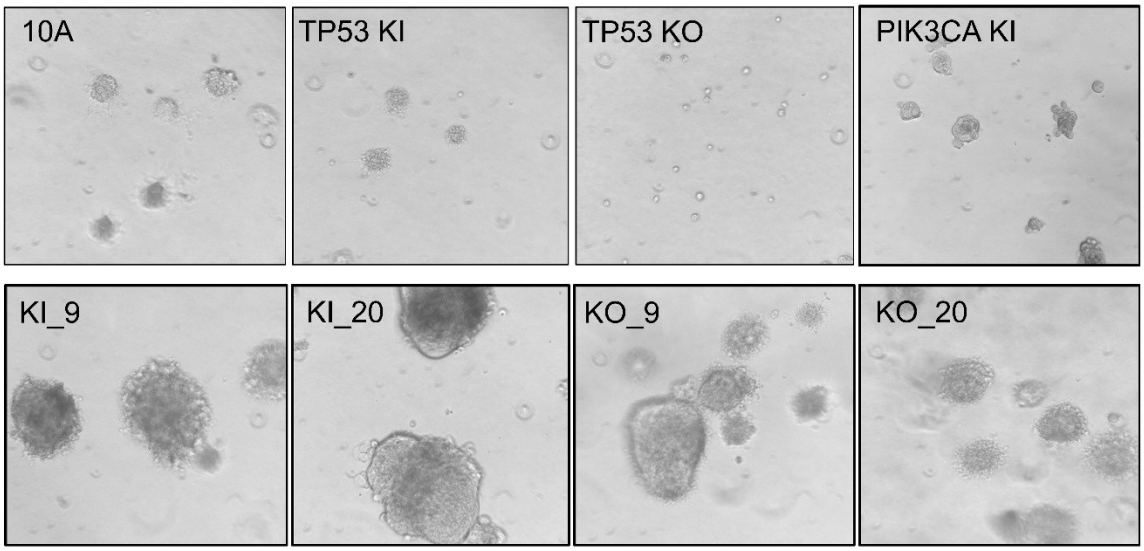

Figure 3.9: Soft agar invasive assay of double mutant panel. Formation of colonies in soft agar is a measure of anchorage independent growth and the potential for invasive capabilities. All cell lines were grown in physiological doses of EGF. All double mutants showed an increased capacity for anchorage independent growth and invasive capabilities. Parental and single mutant cell lines did not show soft agar growth. All images shown at x20 magnification.

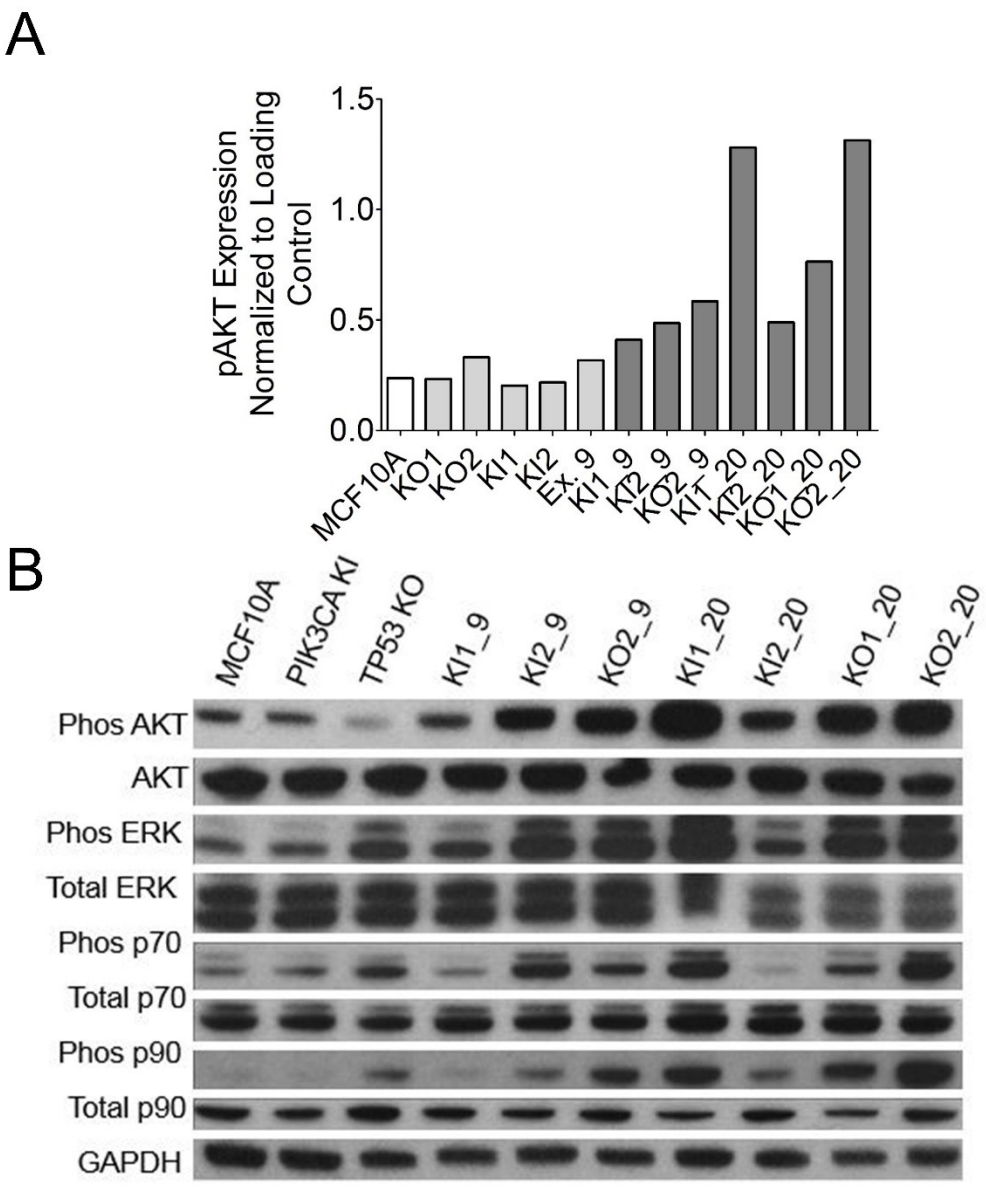

Figure 3.10: Double mutant cell lines show increased AKT phosphorylation and pathway activation. A) Relative pAKT expression in cell lines in physiological EGF determined by RPPA. B) Western blot analysis of AKT and ERK pathway activation. RPPA expression levels were confirmed with Western blot analysis and determined to be quantitatively accurate for validated RPPA antibodies. Western blot analysis of components of the AKT pathway in the parental MCF10As, representative single mutants, and the double mutant panels. The double mutant cell lines showed varying degrees of increased phosphorylation when compared to the parental MCF10As and single KI cell lines.

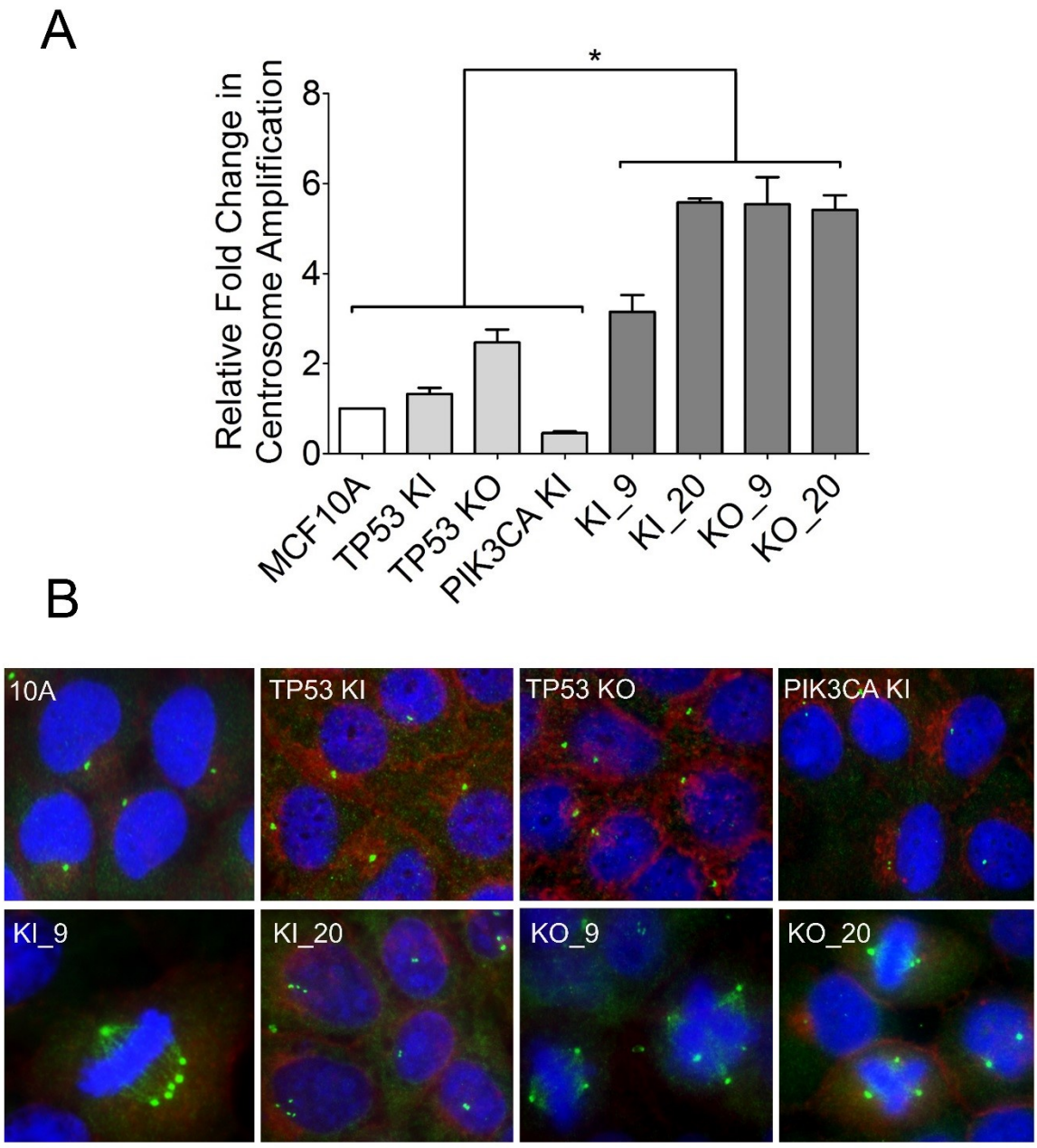

Figure 3.11: Centrosome amplification assay in double mutant panel. A) Relative fold change of average centrosome amplification normalized to parental MCF10A. Double mutants showed statistically significant (*p<.05) amplification of centrosomes. B) Centrosome amplification was determined by immunofluorescence. Representative images for cells are shown. Green represents immunofluorescent staining of γ-tubulin, blue identifies nucleic acids (DAPI). Centrosome counts of one and two are considered normal

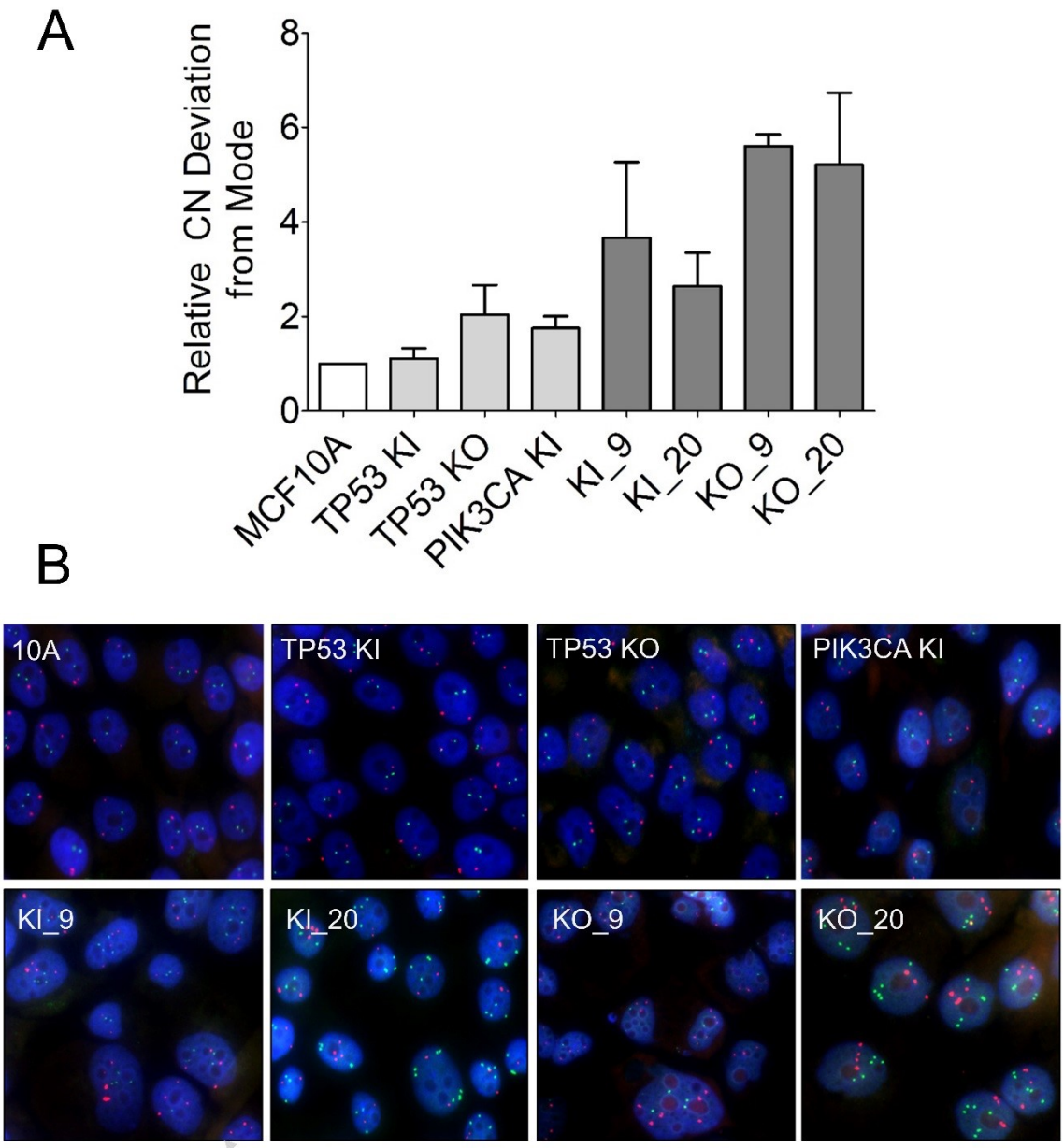

Figure 3.12: Genomic instability of DM panel measured by Fluorescent *In Situ* Hybridization. A) Relative copy number (CN) deviation from the modal population was determined using Fluorescent *In Situ* Hybridization (FISH). The relative change from the modal population is equivalent to the amount of genomic instability experienced by the cell. Three genes were objectively selected and probed (c-MYC, EGFR, BCR). Double mutants showed a marginal increase in genomic instability B) Representative FISH Images for each cell line. EGFR probe (red) and BCR probe (green) with DAPI staining for nucleic acids shown in blue. White arrows indicate irregular cells.

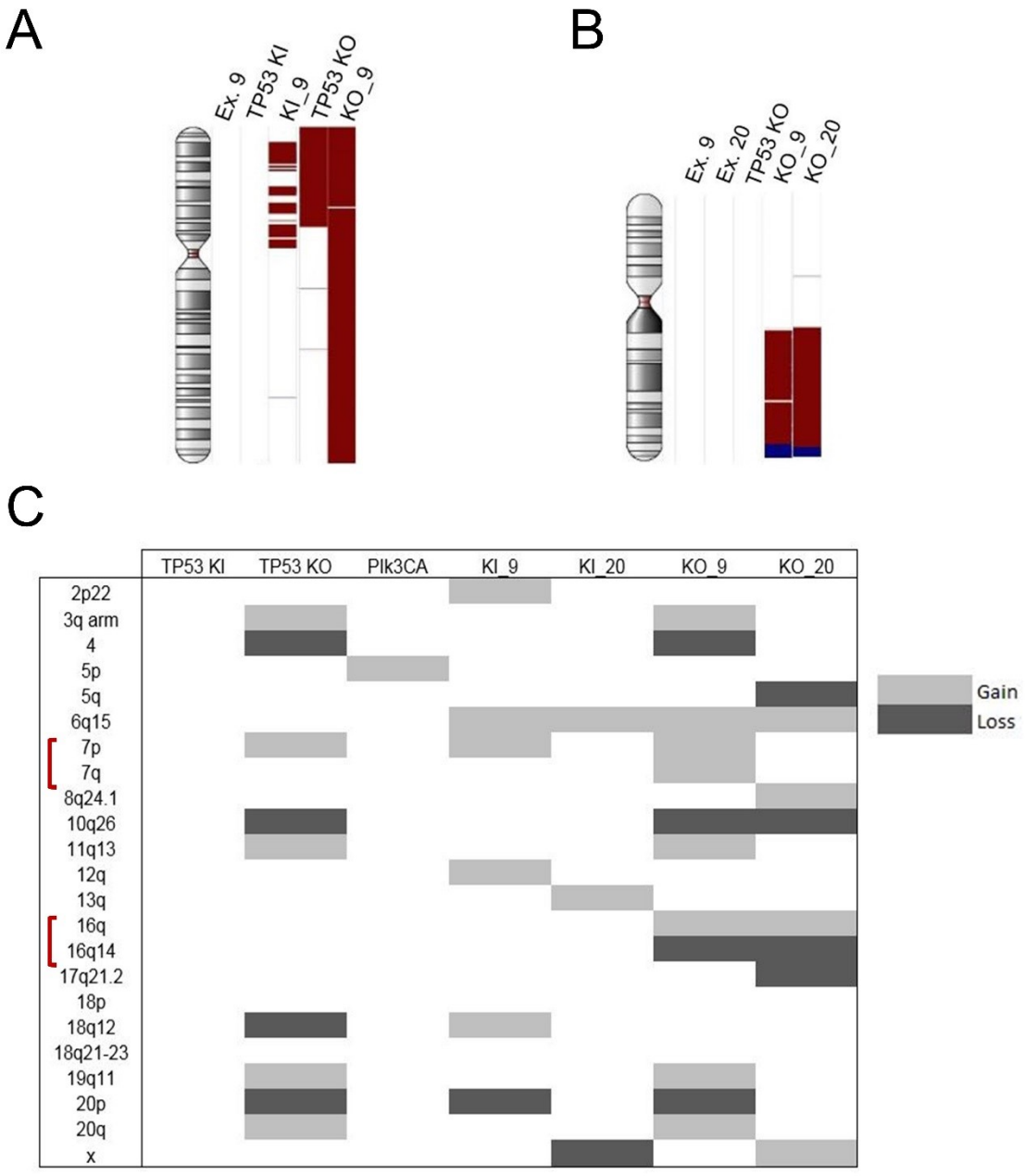

Figure 3.13: SNP and CNV analysis of double mutant panel. Illumina's OmniExpress ChIP genome wide association studies. CNV analysis was performed on the parental, single and double mutant cell lines. Representative alterations shown in A) chromosome 7 and B) Chromsome 16 exhibit gains (red) and losses (blue) found in the double mutant cell lines. All cells were normalized to parental MCF10As. C) CNV data was summarized in the table with representative clones for each set of mutations.

4 Clinical Applications of the Double Mutant Panel

Introduction

Drug resistance is a significant obstacle in cancer treatment and severely limits the effectiveness of chemotherapies. In 2005, 90% of treatment failure in patients with metastatic cancer was attributed to both intrinsic and acquired drug resistance (120). Often times, acquired resistance to one chemotherapy has also been shown to lead to cross-resistance to other drugs with different mechanisms of action. The ability to further understand the molecular mechanisms of drug resistance and to characterize pathways involved in regulating tumor cell response to therapy will significantly aid in the development of new targeted therapies. Furthermore, the ability to develop a regime of combined chemotherapies utilizing both new targeted therapies and cytotoxic drugs to enhance chemotherapy activity will provide increased success in battling drug resistance. This study proposes the utilization of a double mutant panel to identify effective regimes based on a cell's genetic composition. A panel of closely related cell lines harboring variations of the two most commonly mutated genes in breast cancer may provide new insight for both novel and current chemotherapies.

In recent years the rise of genome-scale gene expression profiling and continued advances in genetics and genomics have revealed new genes and pathways that are somatically altered and coexist in human cancers. These technologies have been used to emphasize that mechanisms of carcinogenesis rely on the interaction of

genes/proteins/molecules rather than individual mutations (121). As previously mentioned, Di Nicolantonio and colleagues demonstrated that *PIK3CA* mutations, while sensitive to rapamycin individually, became resistant in the presence KRAS or BRAF mutations demonstrating the importance of studying molecular markers in the context of one another (76, 122). Therefore, it is becoming increasingly apparent that the successful understanding and treatment of breast cancer will rely on understanding multiple targets and utilizing combined therapies.

While combination therapies and the targeting of multiple biomarkers will increase the effectiveness of current and new chemotherapeutics, a continued obstacle in the effective treatment of cancer is genomic instability and continued tumor heterogeneity. Often, genetically unstable tumor cells can harbor pre-existing primary mutations or acquire secondary mutations which lead to the development of drug-resistance. The successful incorporation of genomic instability and the resulting tumor heterogeneity into a panel of closely related cell lines allows for the understanding and identification of effective targeted therapeutics across a clonally diverse population. In addition to understanding and combating mechanisms of drug resistance, it is imperative to increase the ability to better predict therapy response. Currently, no valid practical biomarkers exist for many commonly used cytotoxic drugs, including but not limited to doxorubicin, paclitaxel, and docetaxel. In this study we demonstrate through an extensive panel of relatively isogenic cell lines, that in the presence of a *PIK3CA* mutation, regardless of *TP53*'s mutational status, cell lines have an increased sensitivity to Paclitaxel. The identification of multiple biomarkers would provide the opportunity

for individualized combination therapies that would potentially lead to an increase in successful treatment of cancer.

The characterization and potential variations in drug response of the proposed *PIK3CA-TP53* double mutant model may provide essential insight in the mechanism of common chemotherapeutic drug resistance. Recently, it has been demonstrated that combination therapies that target multiple molecular markers offer a highly specific method for eradicating cancer and may provide an effective strategy for eliminating potential drug resistance (123). Targeting *PIK3CA* and *TP53* hotspot mutations in a single model provides better insight on drug effects in the context of multiple mutations and offer a more accurate molecular model for treating cancer. The successful incorporation of genomic instability and modeling of tumor heterogeneity provides a biologically relevant platform for modeling cancer *in vitro* and providing a platform for the development and testing of personalized therapy. Furthermore it may provide the basis for the development of multi-biomarker systems.

Results

Double mutant cells show drug-specific susceptibility and resistance when compared to single mutation and parental cell lines. In order to determine the appropriate drug concentrations specific for the panel of cells in the specified conditions (see Materials and Methods), IC50 curves were performed for each drug (Fig 4.1). Concentrations which indicated potential selective toxicity were selected and pharmacokinetic studies were performed. A table of the drugs involved in this study are listed in Table 4.1. Initially, pharmacokinetic studies in which the double mutants experienced an obvious

decrease or increase in viability were examined and two drugs were identified. The first drug, MK2206, is an AKT inhibitor which binds to and inhibits AKT in a non-ATP competitive manner (124). The expected result is a decrease in PI3K/AKT signaling and the induction of cell apoptosis. The panel of cell lines was exposed to 1.5 μM for 1 week in 6 well plates. Parental MCF10As and cell lines harboring only a *TP53* mutation experienced insignificant changes in growth. However, as predicted, cell lines harboring a *PIK3CA* mutation experienced a marginally significant (*p<.05) decrease in viability (Fig 4.2). Additionally, cell lines harboring both a *PIK3CA* and *TP53* mutation exhibited a slightly larger decrease in viability. The increased susceptibility of cells harboring both a *PIK3CA* and *TP53* mutation suggests that MK2206 may be the ideal drug for tumors harboring both these mutations and that the mTOR activation in the absence of EGF previously shown suggests that these two pathways may be exploited for increased specificity and toxicity.

The second drug with an observable difference between cell sets was Lapatinib. Lapatinib is an EGFR/Her2 inhibitor that reversibly blocks phosphorylation of the epidermal growth factor (EGFR), ErbB2, Erk-1/2, and AKT kinases (124). As with MK2206, the expected result is a decrease in phosphorylation and activity of the AKT pathway in cells harboring a *PIK3CA* mutation. The panel of cell lines was exposed to .26 μM for 1 week in 6 well plates. However, unlike MK2206, there was a significant increase (*p<.05) in resistance in cells harboring both a *PIK3CA* Ex. 20 and *TP53* mutation (Fig 4.3). The same resistance was not observed for cells harboring a *PIK3CA* Ex. 9 mutation. Similar to Nicolantonio *et al*'s findings, the Lapatinib pharmacokinetic study provides another example of how cells react to drugs very differently depending on

the presence or absence of certain mutations and may help to provide a stronger understanding to drug resistance.

Double mutant cells exhibit drug-specific tumor heterogeneity. Within the double mutant panel, many drugs did not perform as expected. PRIMA-1 (p53-Reactivation and Induction of Massive Apoptosis), is a small molecule that was previously shown to restore p53 function in cells harboring mutant p53 (125). The panel was exposed to 6 μM for 1 week in 6 well plates. There was no observable difference between the parental MCF10A, *TP53* KOs and *TP53* R248W KIs (Fig. 4.4). However, when *TP53* KI mutations were in the presence of a second, *PIK3CA* there was a marginal but observable decrease in cell viability (indicated by the red arrows). Previous studies have shown that a variety of other factors have been shown to effect the toxicity of PRIMA-1, including but not limited to, cell type, cell density, gain-of-function properties, and presence of siRNAs (126, 127). This suggests that in MCF10As (and potentially other breast cells) in order for PRIMA-1 to effectively restore p53 function, a second mutation may be required. These secondary mutations may impart varying degrees of sensitivity or resistance that result in drug-specific tumor heterogeneity.

Another example of drug-specific tumor heterogeneity was observed when the panel was exposed to 15 nM of Doxorubicin in 6 wells for one week. Doxorubicin is an anthracyclin antibiotic and is classified as a topoisomerase II inhibitor (124). Doxorubicin is also capable of other cellular effects such as DNA intercalation, inhibition of DNA ligases, helicases, and other DNA dependent proteins, radical generation, and DNA damage (128). Although doxorubicin is a commonly used chemotherapy, the

mechanisms of selectivity and/or resistance are still not well understood. Within the panel, varying degrees of cell viability were observed. However, most notable were two clones that seemed to exhibit increased resistance, the single mutant *TP53* KO and the double mutant KO_9 (Fig 4.5) Interestingly, the same level of resistance was not observed for KO_20. Again, the panel allows the observation of a set of closely related cell lines with different mutations and different degrees of genomic instability. Further analysis of clones exhibiting increased resistance or susceptibility may identify secondary mutations and provide a better understanding behind drug sensitivity and resistance.

MCF10As harboring a PIK3CA mutation, regardless of TP53 status exhibit a Paclitaxel-specific susceptibility. The double mutant panel was further utilized in the drug studies to identify potential predictive markers. Ideal drug candidates would be effective, FDA approved chemotherapies which have limited known predictive markers. In this assay we utilized a class of widely-used chemotherapies known as Taxanes. Taxanes are a group of drugs that disrupt microtubule function and inhibit mitosis. Along with anthracyclines, taxanes are the most active and widely used chemotherapeutic agents either alone or in combination (129). However, due to their increase use, often recurrent disease is resistant and currently no valid predictive biomarkers exist. The panel was exposed to a high concentration, bolus dose for 24 hrs as well as a low concentration, steady dose for 1 week in order to mimic the two different clinical dosing methods. Within the panel, it was demonstrated that breast epithelial cells with *TP53* mutations showed varying degrees of unaffected viability, indicating a potential for resistance. However, in the presence of a *PIK3CA* mutation, regardless of *TP53*'s

mutational status, there was a significant (**p<.01) decrease in viability (Fig 4.6). This was observed for both the continuous and bolus dosages.

In order to determine if this was paclitaxel specific or observable within the entire class of taxanes, a second taxane, Docetaxel was administered to the panel. Again both a high bolus dose for 24 hrs, as well as a low, continuous dose for 1 week was applied to the cells. However, unlike the paclitaxel, there was no significant differences observed within the panel of single and double mutant cell lines (Fig 4.7). This suggests that the presence of a *PIK3CA* mutation, regardless of *TP53* status, may provide a predictive biomarker for increased response specifically for paclitaxel. Contrary to this finding, previous studies have proposed a potential link between increased AKT activity and paclitaxel resistance (130). However, most of these studies are retrospective analysis of multidrug clinical samples and therefore, adequate controls are not provided.

MCF7s with a wild type corrected PIK3CA mutation exhibit Paclitaxel-specific resistance. In order to determine if the relationship of paclitaxel-susceptibility and the presence of a *PIK3CA* mutation could be observed in a cancer background, MCF7s harboring a somatic *PIK3CA* Ex. 9 mutation (MCF7s) and an isogenically modified *PIK3CA* WT (Corrected) (131) were analyzed. As with the MCF10A derivatives, IC50 curves for both paclitaxel and docetaxel were carried out on the MCF7 and Corrected cell lines. As seen with the MCF10A derivatives in the double mutant panel, MCF7s harboring a *PIK3CA* mutation showed an overall decrease in viability in the presence of paclitaxel across a 10-fold change in concentration (Fig 4.8A). However, in the presence of another taxane, docetaxel, the same susceptibility was not observed (Fig 4.8B).

Similar to the MCF10A derivatives, an ideal concentration was selected for both a high bolus dose for 24 hrs, as well as a low, continuous dose for 1 week. In the presence of Paclitaxel, both dose administration models exhibited a significant (**$p < .01$) decrease in viability in the presence of a *PIK3CA* Ex.9 mutation (Fig 4.9). This coincides with the results observed with the double mutant panel. Similarly, there was no significant difference in viability among the MCF7s and Corrected cell lines when exposed to docetaxel, regardless of dosing model (Fig. 4.10).

Discussion

Drug resistance continues to be a major problem in the successful treatment of human cancers. Due to the inherent genetic instability and heterogeneity of human cancers, virtually all therapies have exhibited drug resistance. A significant mechanism of drug resistance is due to the clonal selection of somatic genetic alterations which lead to increasingly severe phenotypes in the presence of drugs (132). In this study, we utilized a panel of relatively isogenic cell lines in which we successfully incorporated genomic instability and modeled heterogeneity to provide a preliminary system for understanding and predicting drug response. The developed panel provides a biologically relevant model of tumor heterogeneity and clonal variability among a closely related set of cell lines.

Using the panel of cell lines a small cohort of chemo- and targeted therapies were explored. Within the cohort some drugs (Table 4.1) showed little to no difference between the different mutations within the panel. Drugs such as cisplatin, a platinum based drug which binds DNA bases and leads to apoptosis, were designed as nonselective

chemotherapies and showed no differences among the panel. These drugs were quickly eliminated from the study. Surprisingly, some previously developed and approved targeted therapies did not behave as expected. BYL719, a PI3K inhibitor involved in phase 1 clinical trials, was expected to specifically target cells harboring a *PIK3CA* mutation and lead to decrease viability (SI Fig. 5). However, within the panel only two clones containing a *PIK3CA* mutation showed increase viability suggesting that the BYL719 targeted therapy is significantly affected by clonal variability and secondary mutations. This would further suggest that BYL719 is not a reliable targeted therapy and may lead to increased rates of therapy failure due to the high variability exhibited within the panel. The use of several closely related but separately derived clones for the screening of novel, targeted therapies helps to eliminate the potential for misinterpreting drug functionality. Similarly, Everolimus, an mTOR inhibitor, showed no selective toxicity despite the panel containing several cells with upregulated mTOR activity. These drugs were not discussed in the results section and can be found in the Appendices (SI Figure 5).

The expected utility of the panel is the identification and confirmation of novel viable targeted therapies. In order to demonstrate this utility, the panel was exposed to a set of drugs that were previously developed and expected to target and exploit the incorporated mutations. As anticipated, when the panel was exposed to MK2206, an AKT inhibitor, all cell lines harboring a *PIK3CA* mutation experienced a significant decrease in viability. In concordance with the developed panel, it was previously reported that breast cancers with PI3K mutations were sensitive to AKT inhibition (133). The increased efficacy of MK2206 for tumors harboring a *PIK3CA* mutation both *in vitro*

and *in vivo* implicates that trends observed within the panel may be directly applicable to the clinical setting (134). Furthermore, the success of MK2206 *in vivo* suggests that the panel may be able to accurately identify drugs affecting specific biomarkers, such as *PIK3CA* mutations.

Another important factor in determining molecular biomarkers for drug response is tissue type and genetic variants. When the panel was exposed to PRIMA-1, a *TP53* R248W targeting drug, results revealed that in a relatively normal background, PRIMA-1 had no effect on viability of cells harboring the *TP53* R248W hotspot. However, in the context of a *PIK3CA* mutation, cells showed a marginal decrease in viability. Previous studies with PRIMA-1 were performed using two cancer cell lines, MCF7 and T47Ds which harbor thousands of SNPs when compared to a 'normal' genome. Among these differences, the two cell lines harbor a *PIK3CA* Ex.9 and Ex.20 mutation, respectfully (135). It is tempting to speculate that PRIMA-1's function is dependent on the presence of a *PIK3CA* mutation, based on the panel of cell lines and previous studies. By providing a relatively isogenic background within the panel, this potential relationship was easily observed. However, this cannot be concluded without further extensive studies. It does provide convincing evidence that the panel of cell lines is capable of identifying additional biomarkers of resistance and susceptibility for targeted therapies, and provides a greater opportunity for developing more individualized therapies based on how a drug will respond to variations in the genetic composition of a tumor.

A novel application of the panel is the ability to identify potential biomarkers of current nonselective chemotherapies. Paclitaxel, a nonselective chemotaxane, continues to be one of the most commonly used drugs for treating breast cancer and metastatic

disesase (130). However, to date, there are not predictive biomarkers and a significant portion of patients eventually show increased resistance. The ability to successfully identify a potential biomarker of paclitaxel would help predict response and potentially prevent increased resistance and metastatic recurrence. Furthermore, identifying a predictive marker for paclitaxel would provide a better ability for selecting personalized therapeutic options based on the genetic components of the primary disease. Using the panel of cell lines we were able to determine that the presence of *PIK3CA*, regardless of *TP53* status, may provide a predictive biomarker for increased susceptibility to paclitaxel. Furthermore, in the absence of *PIK3CA*, it could be hypothesized based on observed trends, that there was an increase in resistance in the *TP53* KOs. This would suggest that tumors harboring a *TP53* homozygous deletion may respond better to other chemotherapies, while tumors harboring a second mutation in *PIK3CA* would be a candidate for paclitaxel. Additionally, this relationship was not observed with docetaxel, another chemotaxane, suggesting that the observed relationship is specific to paclitaxel. The relationship between the presence of *PIK3CA* and paclitaxel susceptibility was further validated in cancer cell line model, MCF7. MCF7s inherently contain four *PIK3CA* alleles, two of which harbor an E545K mutation. Both mutations were genetically targeted and corrected back to WT. In the presence of four WT *PIK3CA* alleles, corrected MCF7s showed an increase in paclitaxel resistance. As a cancer cell line, MCF7 is considerably less stable than MCF10A and contains a higher number of SNPs, CNV, and secondary mutations. Observing the same relationship between *PIK3CA* and paclitaxel susceptibility within a less stable, cancer model suggests that the relationship is unaffected by the presence of other mutations.

Previous studies have contradicted our observations and suggested that inhibition of the *PIK3CA* pathway lead to an increase to paclitaxel response. However these studies, both *in vivo* and *in vitro*, were flawed in several ways (130, 136). Within the *in vitro* study, the overexpression of the PI3K pathway, rather than the incorporation of a biologically relevant mutation makes it difficult to apply *in vivo*. As previously discussed, overexpression models produce protein levels significantly higher than those observed *in vivo* and therefore are not accurate for modeling clinical outcomes. Secondly, the study was performed in ovarian cell lines which may elicit a tissue-specific response. Lastly, the study was performed in the presence of multiple drugs, making it difficult to attribute observed outcomes to a single component. Similarly, in the clinical setting, paclitaxel is often combined with doxorubicin or other common chemotherapies during treatment. Therefore, it is difficult to assess the effect of paclitaxel as an individual component in a clinical setting.

This study presents the panel of developed cell lines as an invaluable tool in the development and screening of effective therapies. It provides an accurate model of tumor heterogeneity, a significant problem in drug resistance, and allows us to predict, with increased certainty, the response to current and novel drugs. Furthermore, the utility of this panel suggests that current drug development and screening should adopt panels modeling several different mutations and permutations, with each combination modeling two or more individually derived clones. This would allow for increased opportunities for individualized medicine and account for the genetic components of a tumor when determining the appropriate combination of therapeutics.

Table 4.1: Drug Concentrations

Drug	Target	IC50
BYL719	*PIK3CA* inhibitor	1.5 uM
Docetaxel	Chemo Taxane	60 pM
Doxorubicin	Chemo	15 nM
Everolimus	mTOR inhibitor	0.25 uM
Gefitinib	EGFR Inhibitor	0.25 uM
Lapatinib	EGFR/Her2 inhibitor	0.25 uM
MK2206	AKT inhibitor	1.5 uM
Paclitaxel	Chemo Taxane	2.5 nM
Prima-1	*TP53* R248W inhibitor	5 uM

Table 4.2: Taxane Concentrations

Drug	Low Dosage, 1 week	High Dosage, 24hr
MCF10A Derivatives		
Paclitaxel	2.5 nM	10 nM
Docetaxel	60 pM	350 pM
MCF7 Derivatives		
Paclitaxel	1.2 nM	7 nM
Docetaxel	25 pM	125 pM

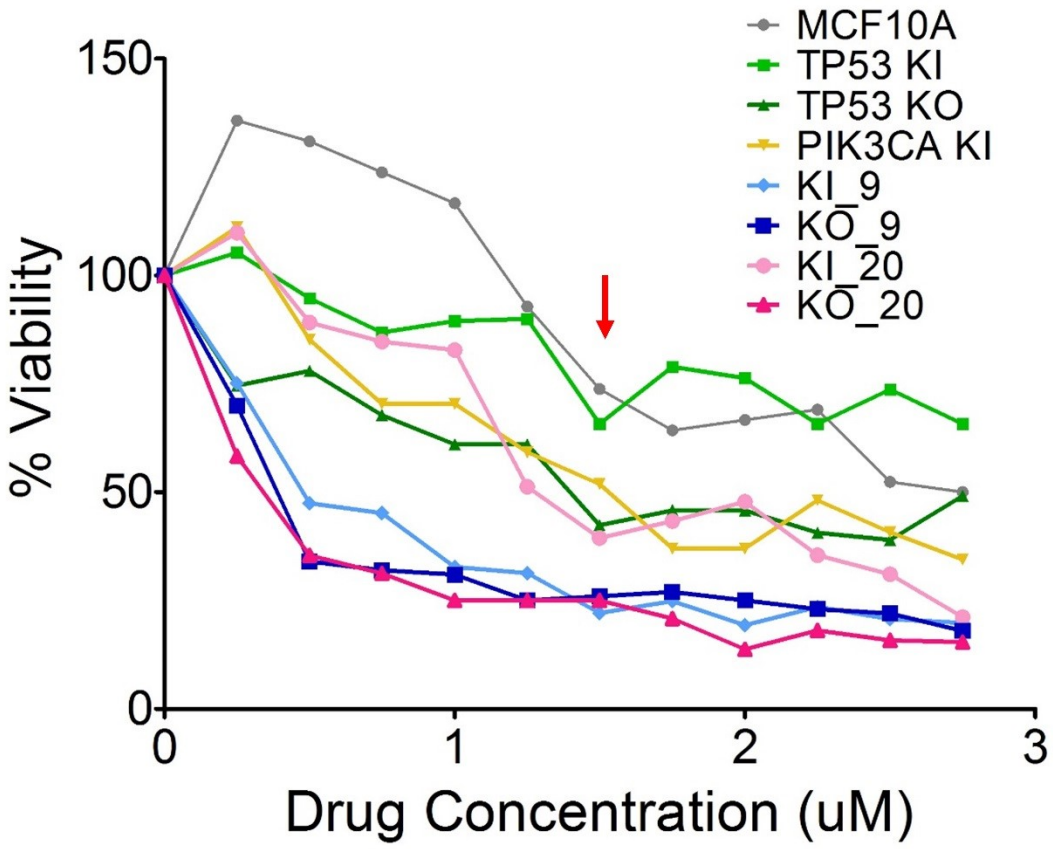

Figure 4.1: Representative IC50 curve for pharmacokinetic study on DM panel. IC50 curves were initially performed to determine the optimal concentration for pharmacokinetic studies in the double mutant cell lines. The curve above is representative of a IC50 curve. Shown is the % viability of cells in varying concentrations of MK2206. The red arrow represents the selected IC50 .

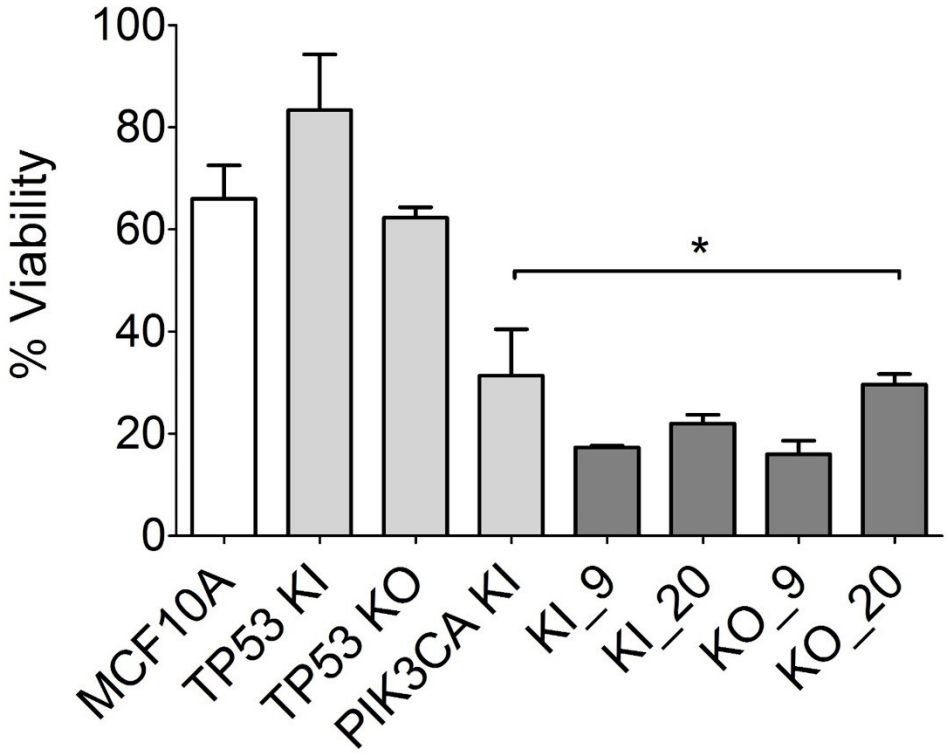

Figure 4.2: MK2206 pharmacokinetic study on DM panel. The panel was exposed to 1.5 μM of MK2206 (AKT Inhibitor) for one week in 6 well plates. Cell counts were done in triplicate and normalized to DMSO vehicle controls. Cell lines harboring a PIK3CA mutation showed a marginally significant (*p<.05) decrease in viability when compared to the parental and single mutant cell lines.

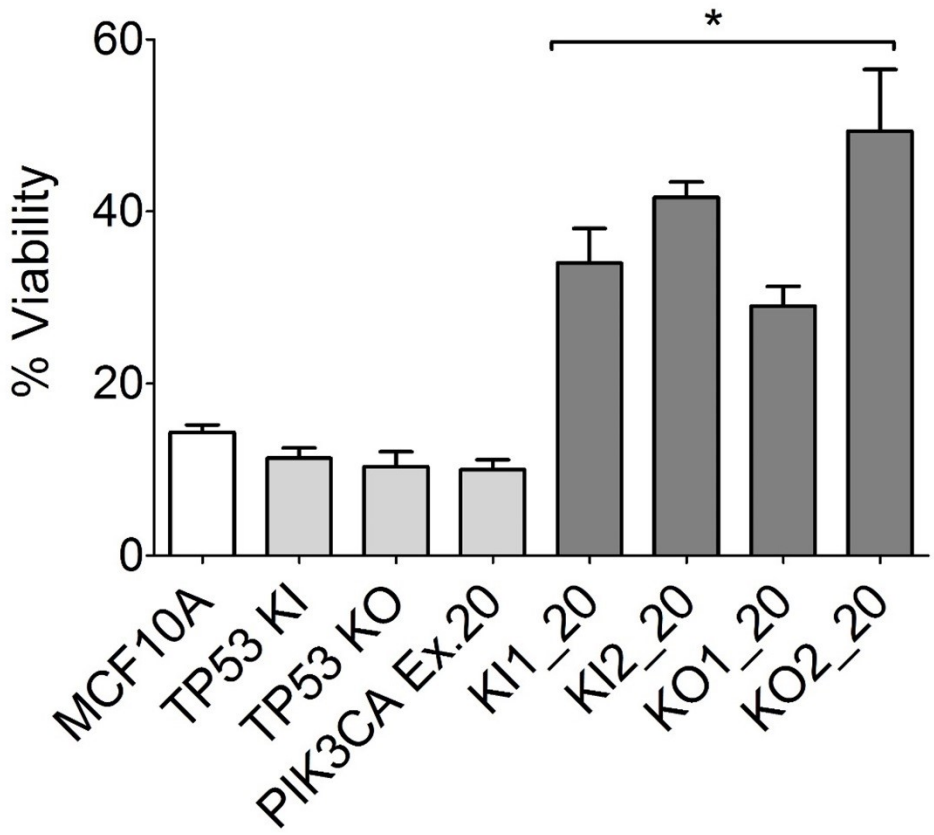

Figure 4.3: Lapatinib pharmacokinetic study on DM panel. The panel was exposed to .25 μM of Lapatinib (EGFR/Her2 Inhibitor) for one week in 6 well plates. Cell counts were done in triplicate and normalized to DMSO vehicle controls. Within the panel it was found that the PIK3CA H1047R single mutation cell line was susceptible to Lapatinib. However, cell lines harboring a second mutation in TP53 exhibited an increase in viability suggesting a potential synergistic mechanism of drug resistance. The same relationship was not observed for the PIK3CA E545K mutation.

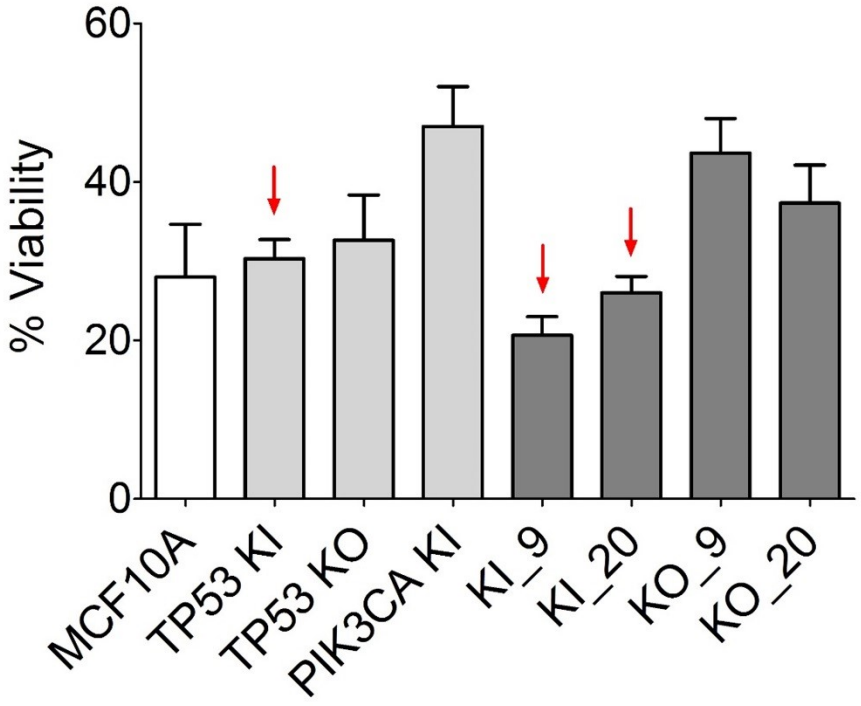

Figure 4.4: Prima-1 pharmacokinetic study on DM panel. The panel was exposed to 6 μM of Prima-1 (R248W small molecule inhibitor) for one week in 6 well plates. Cell counts were done in triplicate and normalized to DMSO vehicle controls. Contrary to the expected pharmacokinetics, Prima-1 did not target and induce apoptosis in the TP53 KI. However, double mutant cells harboring both the TP53 KI mutation and PIK3CA mutation showed a decrease in viability when compared to both single mutant cell lines.

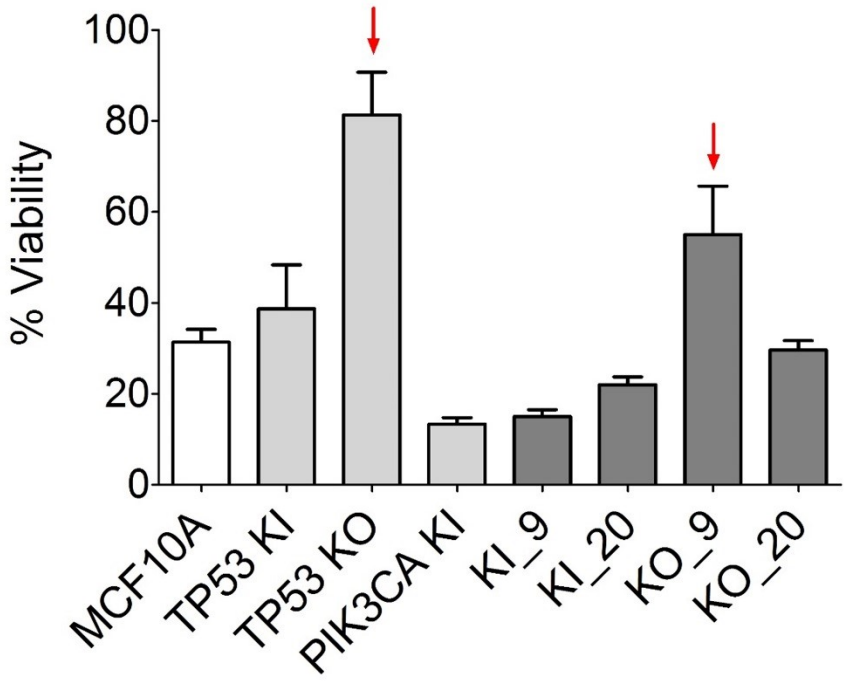

Figure 4.5: Doxorubicin pharmacokinetic study on DM panel. The panel of cell lines was exposed to 15 nM of Doxorubicin for one week in 6 well plates. Cell counts were done in triplicate and normalized to DMSO vehicle controls. Two cell lines within the panel exhibited increased viability in the presence of Doxorubicin (red arrows). This is most likely due to tumor heterogeneity and the acquisition of secondary mutations resulting from the previously observed increased in genomic instability.

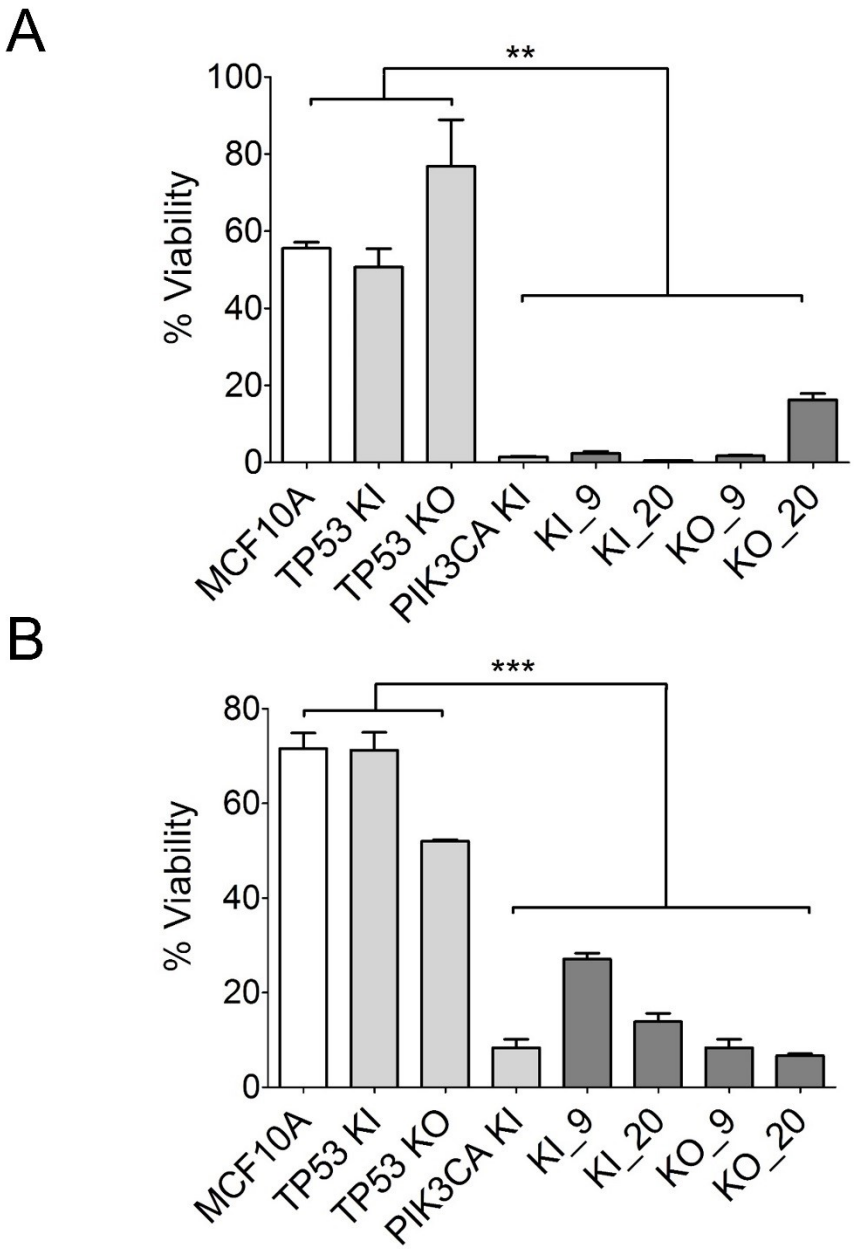

Figure 4.6: Paclitaxel pharmacokinetic study on DM panel. A) 10 nM of paclitaxel was administered for 24 hours and then removed. This was used to mimic a intermittent bolus dosing system. Cells were allowed to recover in normal media for 1 week before cell counting. B) Cells were maintained in 2.5 nM paclitaxel supplemented media for 1 week. This was used to mimic a continuous dosing system. In both administration models, the presence of a PIK3CA mutation, regardless of TP53 status resulted in a significant decrease (**p<.01 and ***p<.001) in cell viability.

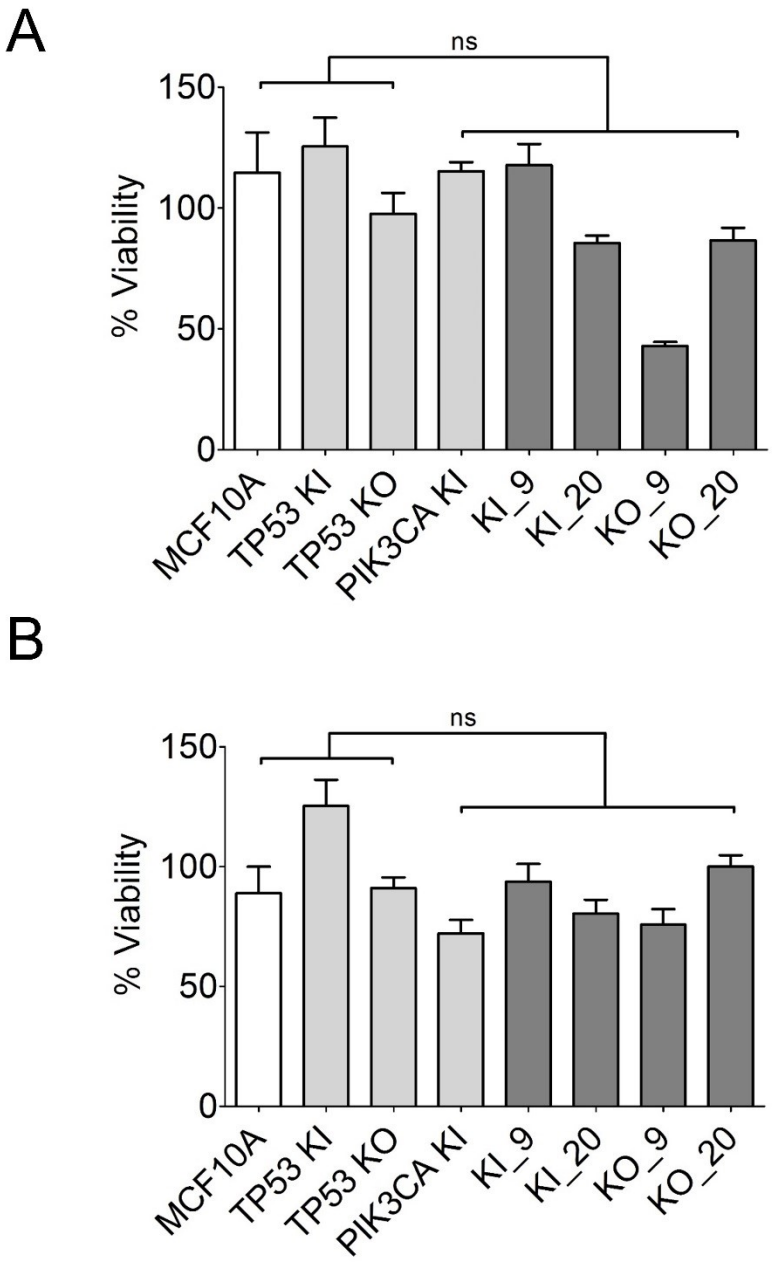

Figure 4.7: Docetaxel pharmacokinetic study on DM panel A) 350 pM of docetaxel was administered for 24 hours and then removed. This was used to mimic a intermittent bolus dosing system. Cells were allowed to recover in normal media for 1 week before cell counting. B) Cells were maintained in 60 pM of docetaxel supplemented media for 1 week. This was used to mimic a continuous dosing system. In both administration models, there was no significant difference between cells indicating that the observed paclitaxel response is taxane-specific

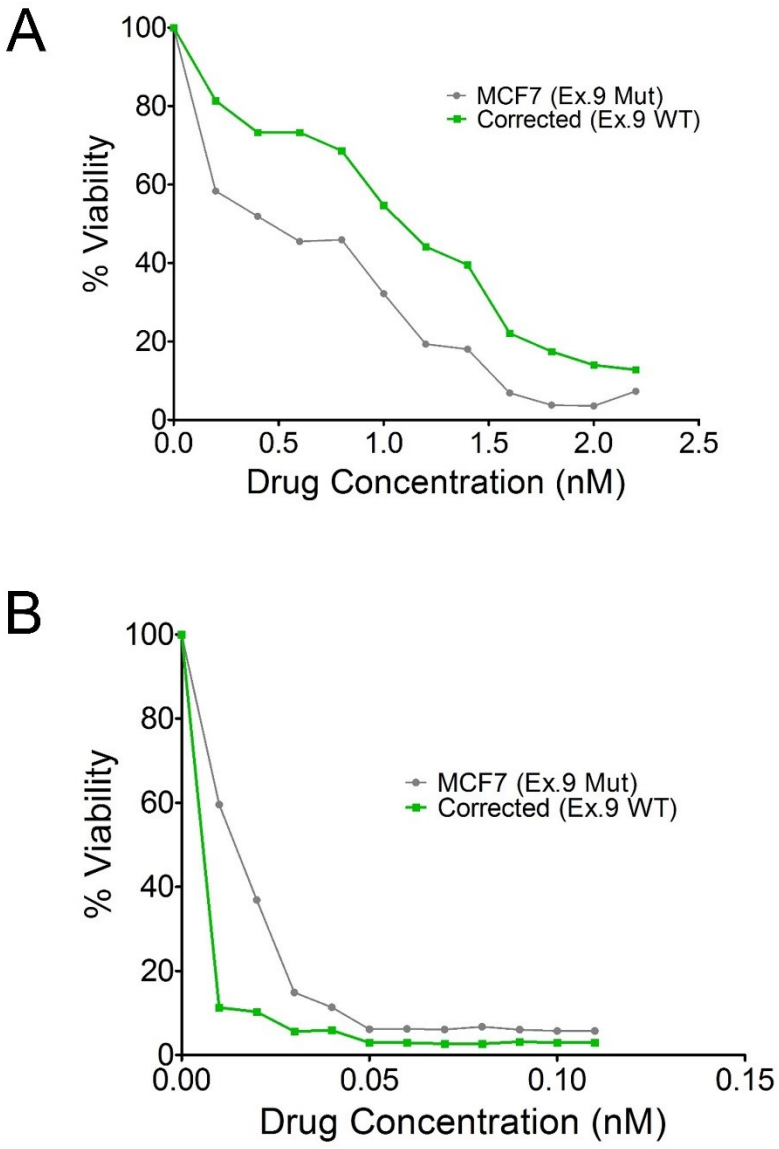

Figure 4.8: Representative IC50 curve for pharmacokinetic study on MCF7s and Derivatives. IC50 curves were initial performed to determine the optimal concentration for taxane pharmacokinetic studies on MCF7s. MCF7s harbor two PIK3CA E545K (Ex.9) mutations out of four PIK3CA alleles. Corrected MCF7 were genetically modified to contain 4 WT PIK3CA alleles (Corrected). A) Paclitaxel IC50 curve exhibits MCF7s with the PIK3CA Ex.9 mutation show decreased viability when compared to the Corrected PIK3CA WT counterpart. B) Docetaxel IC50 curve does not exhibit the same relationship between PIK3CA mutations and decreased viability.

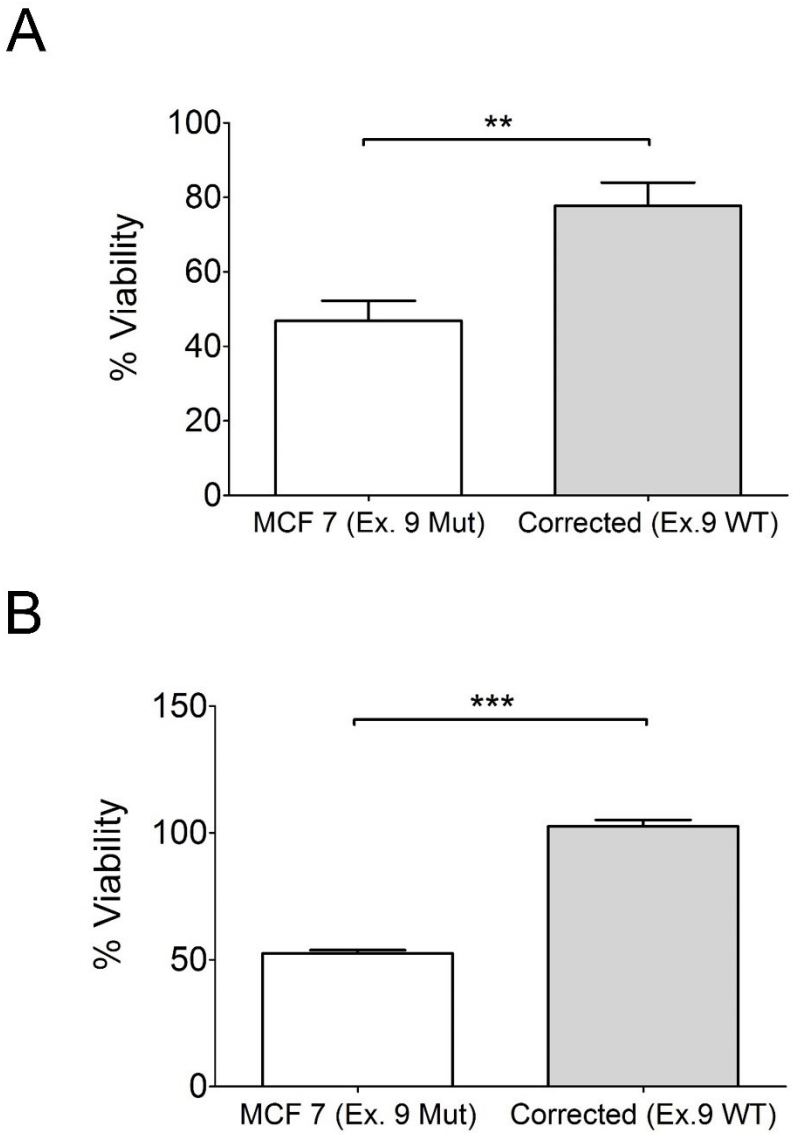

Figure 4.9: Paclitaxel pharmacokinetic study on MCF7. A) 125 nM of paclitaxel was administered for 24 hours and then removed. This was used to mimic a intermittent bolus dosing system. Cells were allowed to recover in normal media for 1 week before cell counting. B) Cells were maintained in 1.2 nM paclitaxel supplemented media for 1 week. This was used to mimic a continuous dosing system. In both administration models, the presence of a PIK3CA mutation resulted in a significant decrease (**p<.01 and ***p<.001) in cell viability and confirms the observations seen with the DM panel.

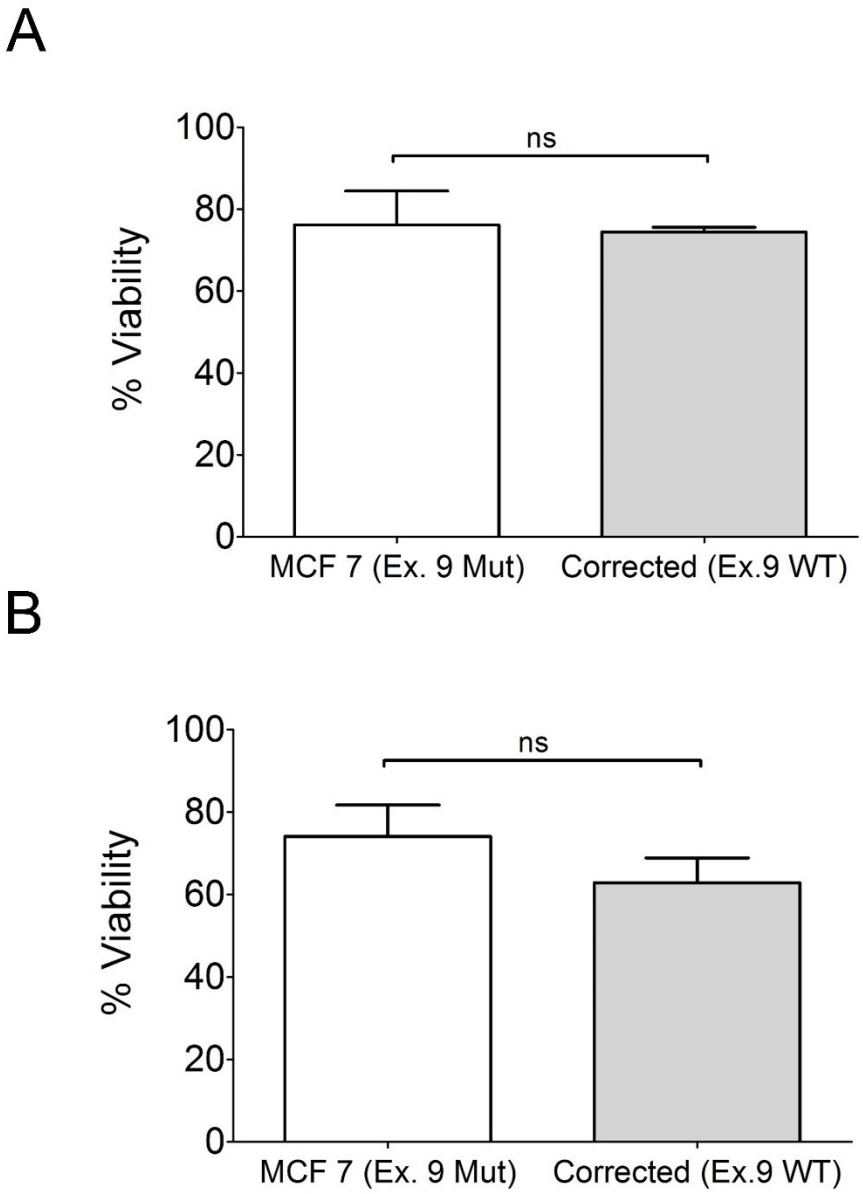

Figure 4.10: Docetaxel pharmacokinetic study on MCF7. A) 125 pM of docetaxel was administered for 24 hours and then removed. This was used to mimic a intermittent bolus dosing system. Cells were allowed to recover in normal media for 1 week before cell counting. B) Cells were maintained in 25 pM of docetaxel supplemented media for 1 week. This was used to mimic a continuous dosing system. In both administration models, there was no significant difference between cells reconfirming that the observed paclitaxel response is taxane-specific

5 Materials and Methods

Cell Culture. Cell lines were grown in 5% CO_2 at 37 ºC The non-transformed human breast epithelial cell line MCF-10A (84) and its derivatives were grown in DMEM/F12 (1:1) supplemented with 5% horse serum (Hyclone), EGF at 20 ng/ml, insulin at 10 μg/ml, hydrocortisone at 0.5 μg/ml, and cholera toxin at 0.1 μg/ml (hereafter denoted as ‘‘supplemented DMEM/F12’’). Cell lines with gene targeted *PIK3CA* mutations were grown in supplemented DMEM/F12 media without EGF due to the observation that when chronically grown in media supplemented with EGF, these cell lines become paradoxically growth-dependent on EGF. Retroviral infected cells were grown in supplemented DMEM/F12 media with 120ng/ml G418. All assays were performed in Supplemented DMEM/F12 containing 1% charcoal dextran-treated fetal bovine serum instead of 5% horse serum. “Supplemented Assay media” contained varying EGF conditions of .02ug/ml, .0002ug/ml and 0ug/ml as indicated. All supplements were purchased from Sigma-Aldrich unless otherwise noted. Cell lines and their corresponding media conditions are listed in Table 5.1.

Targeted knock in of oncogenic TP53 hotspot mutation. A promoterless gene targeting vector was previously designed and generously provided by Bert Vogelstein. Targeted knock in of the *TP53* R248W point mutation into MCF-10As was conducted as previously described (137). Briefly, the targeting vector was transduced into cells and G418 (Invitrogen) antibiotic selection was performed at 120 ug/mL in 96-well plates. Transduced colonies expressing Neomycin resistance were expanded, replicated, and then pooled as previously described (59). Targeted cells

were identified using PCR and infected with adenovirus-encoding Cre recombinase to remove the Neomycin selection cassette. Selected cells were single cell diluted and screened for successful Cre recombination. Knock in clones were determined to be single targeted homologous integrants with equal expression of mutant and wild type *TP53* through PCR and direct sequencing of both the gDNA and cDNA. Single stranded cDNA was generated using First Strand cDNA Synthesis Kit (Amersham Biosciences) following the manufacturer's directions. Primer sequences for PCR amplification and sequencing are shown in Table 2.1 and 2.2

Targeted knock in of oncogenic PIK3CA mutations. Promoterless gene targeting vectors were previously designed in the lab such that homologous recombination would introduce a single oncogenic mutation within *PIK3CA* [3]. Targeted knock in of *PIK3CA* exon 9 (E545K) and exon 20 (H1047R) mutations into MCF-10A cells already carrying a heterozygous *TP53* R248W knock in mutation or MCF-10A cells carrying a homozygous *TP53* deletion in exon 2 were conducted as described in the previous section. Primer sequences for PCR amplification and sequencing are shown in Table 3.1 and 3.2

Cell Proliferation Assay. For cell proliferation assays, exponentially growing cells were washed with HBSS and seeded at a density of $1x10^3$ cells/mL in 6 well plates. Cells were assayed in supplemented DMEM/F12 medium with 1% charcoal dextran-treated fetal bovine serum with varying EGF conditions of .02ug/ml, .0002ug/ml and 0ug/ml. At days 0, 3, 6, 9, and 12 cells were counted using a Beckman Coulter Vi-Cell XR counter. All cell lines were counted in triplicate.

Matrigel Aaar Formation Assay. 5,000 cells were seeded into 8-well chamber slides containing a solid-form base layer of Growth Factor Reduced Matrigel (BD Biosciences). Cells were cultured in a 2% matrigel in supplemented DMEM/F12 assay medium with 1% charcoal dextran-treated fetal bovine serum with varying EGF conditions of .02ug/ml, .0002ug/ml and 0ug/ml. The 2% matrigel in supplemented assay media was changed every 4 days for two weeks.

Ancorage Independent Growth in Semisolid Medium. $2x10^4$ exponentially growing cells were cast in 3 ml of top-layer medium comprised of supplemented assay media of varying EGF conditions of .02ug/ml, .0002ug/ml and 0ug/ml and 0.4% UltraPure Agarose (Invitrogen). This mixture was poured on top of a 2 ml bottom layer containing 0.6% agarose in 6-well tissue culture plates. Supplemented DMEM/F12 was added to the wells once a week.

Clonogenic Assay. Cells were seeded in triplicate at densities of .5, 1, 2, and 3 cells/well into 96-well plates with supplemented DMEM/F12 assay medium with 1% charcoal dextran-treated fetal bovine serum with varying EGF conditions of .02ug/ml and .0002ug/ml. Media was changed weekly and plates were monitored on days 7, 14, 21, and 28 for colony formation.

Centrosome Immunofluorescence. Cells were seeded at $1 x10^5$ density into 8-well chamber slides and allowed to grow for two days. Slides were washed with ice cold PBS and fixed in cold methanol for 15 min at -20 ^oC. Slides were then incubated in ice cold acetone for 1 min at room temperature. Following several washes with ice cold PBS, slides were treated with a blocking buffer (5% goat serum in .3% Triton X-100) for 2 hr at room temperature. Slides were then treated with a 1:1000 dilution of rabbit anti-ɣ-tubulin primary antibody (Sigma, T5192) in an antibody dilution buffer (.3% Triton X-100 in PBS supplemented with 1% BSA) for 1 hr at room

temperature. Slides were washed several times in a PBS supplemented with 1% BSA wash buffer. A 1:100 dilution of goat anti-rabbit IgG-Alexa488 secondary body (Life, A11034) in antibody dilution buffer was added to the slides for 25 min at room temperature. The slides were then washed several times with wash buffer, followed by a single wash with HBSS. Slides were stained with a 1:200 dilution of Texas Red-X-Conjugate Wheat Germ Agglutinin (Life, W21405) for 5min, followed by several washes with wash buffer. A 1x DAPI stain (Sigma, D9542-SMG) was added for 1 min. Slides were mounted with Prolong Gold and imaged using a Nikon fluorescence microscope and NIS-Elements BR 2.30 imaging program.

Fluorescence In Situ Hybridization (FISH). Cells were seeded at 3 x10^4 density into 8-well chamber slides and allowed to grow to 90% confluency. Cells were fixed overnight in a 10% buffered formalin solution and allowed to dry at bench top the following day. Slides were then treated with 2N HCl for 20 mins and treated with the Vysis Pretreatment Kit I. Briefly, slides are washed with a 2x SSC buffer and incubated in the provided pretreatment buffer at 80 ^oC for 30 min. Slides were rinsed in diH_2O and washed with 2x SSC buffer. The slides were then placed in a Protease Buffer (NaCl pH 2.0 with 25 mg Protease provided in the kit) at 37 ^oC for 8 min. Pretreated slides were then washed with 2x SSC buffer and fixed in 10% buffered formalin for 10 min. Proceeding the pretreatment slides were dehydrated through a series of ethanol baths and allowed to age at bench top for two weeks. Slides were then hybridized with various vysis probes at 95 ^oC for 5 min and incubated at 37 ^oC for 48 hrs. Slides were then treated with a .3% NP-40 (IGEPAl) at 75 ^oC, counter stained with DAPI (1:10,000) and sealed with Prolong Gold (Invitrogen, P36930). Slides were imaged using a Nikon fluorescence microscope and NIS-Elements BR 2.30 imaging program.

Reverse Phase Protein Array (RPPA). Cells were prepared and submitted to MD Anderson Cancer Center RPPA Core Facility for RPPA analysis. RPPA analyzes cellular protein activity in

signaling networks and can be applid to both tissue and cultured cells. Briefly, cells were seeded at $2x10^5$ cells in 6 well plates using EGF-free supplemented DMEM/F12 assay medium with 1% charcoal dextran-treated fetal bovine serum. Cells were harvested after 48 hours for protein lysates. Whole cell protein extracts were lysed using lysis buffer and prepared in provided 4X SDS sample buffer. Cellular proteins were denatured by 1% SDS with beta-mercaptoethanoland diluted in five 2-fold serial dilutions in dilution buffer (lysis buffer containing 1% SDS). Serial diluted lysates were arrayed on nitrocellulose-coated slides (Grace Biolab) by Aushon 2470 Arrayer (Aushon BioSystems). A total of 5808 array spots were arranged on each slide including the spots corresponding to positive and negative controls prepared from mixed cell lysates or dilution buffer, respectively. Each slide was probed with a validated primary antibody plus a biotin-conjugated secondary antibody. Only antibodies with a Pearson correlation coefficient between RPPA and western blotting of greater than 0.7 were used in reverse phase protein array study. The signal obtained was amplified using a Dako Cytomation–catalyzed system (Dako) and visualized by DAB colorimetric reaction. The slides were scanned, analyzed, and quantified using a customized-software Microvigene (VigeneTech Inc.) to generate spot intensities. Each dilution curve was fitted with a logistic model ("Supercurve Fitting" developed by the Department of Bioinformatics and Computational Biology at MD Anderson Cancer Center, "http://bioinformatics.mdanderson.org/OOMPA"). The protein concentrations of each set of slides were then normalized by median polish.

Immunoblotting. Cells were seeded in 6 well plates using EGF-free supplemented DMEM/F12 assay medium with 1% charcoal dextran-treated fetal bovine serum. Cells were harvested after 48 hours for protein lysates. Immunoblotting was performed as previously described (138). Briefly, whole cell protein extracts prepared in Laemmli sample buffer were resolved by SDS-PAGE using NuPAGE gels (Invitrogen), transferred to Invitrolon PVDF membranes (Invitrogen),

and probed with primary antibody followed by incubation with horseradish peroxidase-conjugated secondary antibodies. The primary antibodies can be found in Table 5.2

Cell Cycle Analysis. Previously plated cells were washed and resuspended in ice cold PBS and added dropwise to 70% ethanol. Cells were incubated at -20C overnight for ethanol fixation. The following day, cells were pelleted and washed with cold PBS and resuspended in Propidium Iodide (500 μ/ml) in .1% Triton in PBS. Cells were analyzed by a flow cytometer in the Hopkins FACS Core.

Knockdown of NDRG1 in human cell lines. NDRG1 Knockdown cell lines were a generous gift from the Sushant Kachhap Lab. Briefly, ShRNA vectors were generated using a U6 promoter based vector and used to target the NDRG1 region 304-331 bases to give maximum knockdown. shRNA constructs were transfected into MCF10As using Lipofectamine2000 Reagent (Invitrogen) and knock down of expression was confirmed 24, 48 and 72 h post-transfection using western blotting.

Overexpression of NDRG1 in human cell lines. Cells were grown to 30-40% confluency in antibiotic free medium. A pCMV6-Entry vector expressing Human NDRG1 (Origene RC225609) was used with the Fugene 6 system to transfect cell lines according to the provided protocol. For transient transfections in the HCT116 *TP53* KO cell line cells were plated for assays 24-48 hrs after transfection. Stable transfections in the MCF10A *TP53* KOs were placed on selection 24-48 hours after transfection and

maintained for 2-3 weeks until stable overexpression was established. All overexpressing transfections were confirmed using Western blots.

Clinical Analysis of NDRG1 expression in tumors with TP53 homozygous deletion. Data from the TCGA study was accessed through the cBio Cancer Genomics Portal (http://www.cbioportal.org/public-portal/). Only studies with both mRNA and mutational data were included in the analysis. Studies were queried for both *TP53*: HOMDEL and NDRG1: EXP > 2. Oncoprints and case information for each study were collected, analyzed and compiled.

Proximity Ligation Assay. Cells were seeded in chamber slides and allowed to grow for 24 hours. Slides were fixed the same as in the previously discussed centrosome assay. The proximity Ligation Assay was carried out using the Sigma DuoLink PLA reagents and provided protocol. Total NDRG1 in Rabbit (Cell Signaling XP 9485) at 1:200 and γ-Tubulin in Mouse (Sigma, GTU-88) 1:1000 were incubated overnight. Antibodies are listed in Table 5.2

Chromatin Immunoprecipitation (ChIP). Chromatin Immunopreciptiation was carried out using the EZ-ChIP Millipore Kit and protocol. The Santa Cruz p53 (DO-1): sc126 antibody (listed in Table 5.2) was used for protein pulldown. Primers for the putative p53 binding sites on the NDRG1 promoter were adapted from previously published sequence (95). Sequences in Table 2.3.

In Vivo Assay. *In vivo* assays were performed using 10-week-old athymic nude female mice (Taconic), which were randomly distributed into equal groups (6 mice per group) for each experiment. Mice were injected subcutaneously in the right flank with $2x10^6$ cells of all developed double mutant clones. Cells were prepared in a mixture of 80% growth factor reduced Matrigel and 20% 1X PBS. Mice were not supplemented with estrogen pellets. The National Institutes of Health Guide for the Care and Use of Laboratory Animals was followed in all experiments.

Copy Number Variance and Loss of Heterozygosity. Using the Illumina Human OmniExpress Bead Chip kit (Illumina, WG-312-3001), single and double mutant cell lines were analyzed for global chromosomal changes, including copy number variance (CNV) and loss of heterozygosity (LOH), when compared to the parental MCF10A cell line.

Drug Sensitivity Assay. Initially, Cells were seeded at a density of $1x10^3$ cells/mL in 96 well plates with supplemented assay media containing no EGF. After 24 hours, cells were exposed to serial dilutions of several different drugs (listed in Table 4.1 and 4.2) and allowed to incubate for one week. Drugs were administered in supplemented assay media containing $1/100^{th}$ EGF. Equivalent concentrations of DMSO were used as vehicle controls. Plates were then analyzed on day 7 using the SRB assay. Briefly, cells were fixed with 50% Trichloroacetic Acid (TCA) and incubated at 4 ^oC for 1 hour. Per standard protocol, TCA was removed and plates were rinsed with deionized water, dried, and treated with .4% Sulforhodoamine B in 1% glacial acetic acid at 25 ^oC for 15 minutes. Plates were rinsed with 1% glacial acetic acid, dried and resolubilized with 10 mM Tris Base. Plates were read by a microplate reader at a wavelength of 515 nm. Once an IC50 was established, cells were seeded $2x10^3$ cells into 6 well plates and exposed to drugs at a concentration determined from the IC50 curves. Cells were counted on Day 7. Each cell line

was run in triplicate and compared to individual vehicle controls with equivalent concentrations of DMSO.

Statistical Considerations. All statistical analyses were carried out using GraphPad Prism 6 software with *P* value significant level indicated using one or more asterisks: $P \leq 0.05$ (*),$P \leq 0.01$ (**) and $P \leq 0.001$ (***). Relative proliferation rates were analyzed by two-way ANOVA. Results from the clonogenic assay, ChIP, FISH and centrosome immunofluorescence experiments were compared to control samples using unpaired t-tests.

Table 5.1: Tissue Culture Mediums

Cell Line	Full Growth Media Conditions
MCF10A, *TP53* KIs, *TP53* KOs	SUPPLEMENTED DMEM/F12: Duibecco's modified eagle medium-F12 media with 5% heat-inactivated horse serum, .1ug/ml cholera toxin, .5ug/ml hydrocortisone, .02ug/ml EGF, 10ug/ml insulin, 1% penicillin and streptomycin
PIK3CA KIs	EGF FREE MEDIA: Duibecco's modified eagle medium-F12 media with 5% heat-inactivated horse serum, .1ug/ml cholera toxin, .5ug/ml hydrocortisone, 10ug/ml insulin, 1% penicillin and streptomycin
Double Mutant cell lines	After isolation cells were transitioned from Supplemented media to EGF Free media
ASSAY Conditions	Assay medias replace 5% horse serum w/ 1% charcoal-stripped dextran-treated fetal bovine serum

Table 5.2: Protein Antibodies

Protein Target	Supplier	Assay	Dilution
p53	Santa Cruz Sc-126	ChIP	1:100
pNDRG1	Cell Signaling XP 5482S	Western	1:5000
		PLA	1:400
Total NDRG1	Cell Signaling XP 9485S	Western	1:1000
		PLA	1:100
γ-Tubulin	Sigma T5192	Centrosome	1:1000
γ-Tubulin	Sigma T6557	PLA	1:500
p-AKT	Cell Signaling 9271	Western	1:1000
Total AKT	Cell Signaling 9272	Western	1:5000
p-ERK	Cell Signaling XP 4370	Western	1:5000
Total ERK	Cell Signaling 9102	Western	1:10,000
p-p90RSK	Cell Signaling 9341	Western	1:150
Total p90RSK	Cell Signaling 9333	Western	1:1000
p-p70S6K	Cell Signaling 9205	Western	1:1000
Total p70S6k	Cell Signaling 9202	Western	1:1000
GAPDH	Cell Signaling XP 5174	Western	1:1000

REFERENCES

1. Alteri R, Cammie Barnes ABTGSGMGJK, & et al. (2013) Breast Cancer Facts and Figures 2013-2014. *American Cancer Society*.
2. Wood LD*, et al.* (2007) The genomic landscapes of human breast and colorectal cancers. *Science* 318(5853):1108-1113.
3. Bachman KE*, et al.* (2004) The PIK3CA Gene is Mutated with High Frequency Bio sci MATERIALS AND METHODS No t D ist r ibu te. *Therapy* 3(8):772-775.
4. Sjöblom T*, et al.* (2006) The consensus coding sequences of human breast and colorectal cancers. *Science (New York, N.Y.)* 314(5797):268-274.
5. Loeb LA (1991) Mutator Phenotype May Be Required for Multistage Carcinogenesis Perspectivesin CancerResearch Mutator Phenotype May Be Required for Multistage Carcinogenesis1. *Cancer Research*:3075-3079.
6. Hanahan D & Weinberg Ra (2011) Hallmarks of cancer: the next generation. *Cell* 144(5):646-674.
7. Lengauer C, Kinzler KW, & Vogelstein B (1998) Genetic instabilities in human cancers. *Nature* 396(6712):643-649.
8. Yoon D-S*, et al.* (2002) Variable levels of chromosomal instability and mitotic spindle checkpoint defects in breast cancer. *The American journal of pathology* 161(2):391-397.
9. Samuels Y*, et al.* (2004) High frequency of mutations of the PIK3CA gene in human cancers. *Science (New York, N.Y.)* 304(5670):554-554.
10. Oren M & Rotter V (1999) Introduction: p53--the first twenty years. *Cellular and molecular life sciences : CMLS* 55(1):9-11.
11. Linzer DI & Levine AJ (1979) Characterization of a 54K dalton cellular SV40 tumor antigen present in SV40-transformed cells and uninfected embryonal carcinoma cells. *Cell* 17(1):43-52.
12. Linzer DI, Maltzman W, & Levine AJ (1979) The SV40 A gene product is required for the production of a 54,000 MW cellular tumor antigen. *Virology* 98(2):308-318.
13. Eliyahu D, Michalovitz D, & Oren M (1985) Overproduction of p53 antigen makes established cells highly tumorigenic. *Nature* 316(6024):158-160.
14. Eliyahu D, Raz A, Gruss P, Givol D, & Oren M (1984) Participation of p53 cellular tumor antigen in transformation of normal embryonic cells. *Nature* 312(5995):646-649.
15. Oren M (2003) Decision making by p53: life, death and cancer. *Cell Death Differ* 10(4):431-442.
16. Vogelstein B, Lane D, & Levine aJ (2000) Surfing the p53 network. *Nature* 408(6810):307-310.
17. Finlay CA, Hinds PW, & Levine AJ (1989) The p53 proto-oncogene can act as a suppressor of transformation. *Cell* 57(7):1083-1093.
18. Lane D & Levine A (2010) p53 Research: the past thirty years and the next thirty years. *Cold Spring Harbor perspectives in biology* 2(12):a000893.
19. el-Deiry WS, Kern SE, Pietenpol JA, Kinzler KW, & Vogelstein B (1992) Definition of a consensus binding site for p53. *Nature genetics* 1(1):45-49.
20. Shaw P*, et al.* (1992) Induction of apoptosis by wild-type p53 in a human colon tumor-derived cell line. *Proc Natl Acad Sci U S A* 89(10):4495-4499.

21. Kuerbitz SJ, Plunkett BS, Walsh WV, & Kastan MB (1992) Wild-type p53 is a cell cycle checkpoint determinant following irradiation. *Proceedings of the National Academy of Sciences of the United States of America* 89(16):7491-7495.
22. Whibley C, Pharoah PDP, & Hollstein M (2009) P53 Polymorphisms: Cancer Implications. *Nature reviews. Cancer* 9(2):95-107.
23. Bond GL, Hu W, & Levine AJ (2005) MDM2 is a central node in the p53 pathway: 12 years and counting. *Current cancer drug targets* 5(1):3-8.
24. Hollstein M, Sidransky D, Vogelstein B, & Harris CC (1991) p53 mutations in human cancers. *Science* 253(5015):49-53.
25. Walerych D, Napoli M, Collavin L, & Del Sal G (2012) The rebel angel: mutant p53 as the driving oncogene in breast cancer. *Carcinogenesis* 33(11):2007-2017.
26. Forbes Sa*, et al.* (2011) COSMIC: mining complete cancer genomes in the Catalogue of Somatic Mutations in Cancer. *Nucleic acids research* 39(Database issue):D945-950.
27. Petitjean A*, et al.* (2007) Impact of Mutant p53 Functional Properties on TP53 Mutation Patterns and Tumor Phenotype : Lessons from Recent Developments in the IARC TP53 Database. 28(February):622-629.
28. Cadwell C & Zambetti GP (2001) The effects of wild-type p53 tumor suppressor activity and mutant p53 gain-of-function on cell growth. *Gene* 277(1-2):15-30.
29. Olivier M*, et al.* (2006) The clinical value of somatic TP53 gene mutations in 1,794 patients with breast cancer. *Clinical cancer research : an official journal of the American Association for Cancer Research* 12(4):1157-1167.
30. Olive KP*, et al.* (2004) Mutant p53 gain of function in two mouse models of Li-Fraumeni syndrome. *Cell* 119(6):847-860.
31. Wijnhoven SWP*, et al.* (2007) Dominant-negative but not gain-of-function effects of a p53.R270H mutation in mouse epithelium tissue after DNA damage. *Cancer research* 67(10):4648-4656.
32. Koonin EV, Rogozin IB, & Glazko GV (2005) p53 gain-of-function: tumor biology and bioinformatics come together. *Cell Cycle* (May):686-688.
33. Bullock aN & Fersht aR (2001) Rescuing the function of mutant p53. *Nature reviews. Cancer* 1(1):68-76.
34. Sigal A & Rotter V (2000) Oncogenic Mutations of the p53 Tumor Suppressor : The Demons of the Guardian of the Genome Oncogenic Mutations of the p53 Tumor Suppressor : The Demons of the Guardian of the Genome. *Cancer Res*:6788-6793.
35. Wolf D, Harris N, & Rotter V (1984) Reconstitution of p53 expression in a nonproducer Ab-MuLV-transformed cell line by transfection of a functional p53 gene. *Cell* 38(1):119-126.
36. Dittmer D, Pati S, Zambetti G, & Chu S (1993) Gain of function mutations in p53. *Nature* ….
37. Bossi G*, et al.* (2008) Conditional RNA interference in vivo to study mutant p53 oncogenic gain of function on tumor malignancy. *Cell cycle (Georgetown, Tex.)* 7(12):1870-1879.
38. Di Agostino S*, et al.* (2006) Gain of function of mutant p53: the mutant p53/NF-Y protein complex reveals an aberrant transcriptional mechanism of cell cycle regulation. *Cancer cell* 10(3):191-202.
39. Stambolsky P*, et al.* (2010) Modulation of the vitamin D3 response by cancer-associated mutant p53. *Cancer cell* 17(3):273-285.

40. Bristow RG*, et al.* (2003) Resistance to DNA-damaging agents is discordant from experimental metastatic capacity in MEF ras-transformants-expressing gain of function MTp53. *Oncogene* 22(19):2960-2966.
41. Gualberto A (1998) An oncogenic form of p53 confers a dominant, gain-of-function phenotype that disrupts spindle checkpoint control. *Proceedings of the …* 95(April):5166-5171.
42. El-hizawi S, Lagowski JP, & Kulesz-martin M (2002) Induction of Gene Amplification as a Gain-of-Function Phenotype of Mutant p53 Proteins Induction of Gene Amplification as a Gain-of-Function Phenotype of Mutant.3264-3270.
43. Freed-Pastor Wa & Prives C (2012) Mutant p53: one name, many proteins. *Genes & development* 26(12):1268-1286.
44. Engelman JA, Luo J, & Cantley LC (2006) The evolution of phosphatidylinositol 3-kinases as regulators of growth and metabolism. *Nat Rev Genet* 7(8):606-619.
45. Fruman DA, Meyers RE, & Cantley LC (1998) Phosphoinositide kinases. *Annual review of biochemistry* 67:481-507.
46. Cantley LC (2002) The phosphoinositide 3-kinase pathway. *Science* 296(5573):1655-1657.
47. Katso R*, et al.* (2001) Cellular function of phosphoinositide 3-kinases: implications for development, homeostasis, and cancer. *Annual review of cell and developmental biology* 17:615-675.
48. Byfield MP, Murray JT, & Backer JM (2005) hVps34 is a nutrient-regulated lipid kinase required for activation of p70 S6 kinase. *The Journal of biological chemistry* 280(38):33076-33082.
49. Nobukuni T*, et al.* (2005) Amino acids mediate mTOR/raptor signaling through activation of class 3 phosphatidylinositol 3OH-kinase. *Proc Natl Acad Sci U S A* 102(40):14238-14243.
50. Zardavas D, Phillips WA, & Loi S (2014) PIK3CA mutations in breast cancer: reconciling findings from preclinical and clinical data. *Breast Cancer Res* 16(1):201.
51. O'Brien C*, et al.* (2010) Predictive biomarkers of sensitivity to the phosphatidylinositol 3' kinase inhibitor GDC-0941 in breast cancer preclinical models. *Clinical cancer research : an official journal of the American Association for Cancer Research* 16(14):3670-3683.
52. Lee JW*, et al.* (2005) PIK3CA gene is frequently mutated in breast carcinomas and hepatocellular carcinomas. *Oncogene* 24(8):1477-1480.
53. Levine DA*, et al.* (2005) Frequent mutation of the PIK3CA gene in ovarian and breast cancers. *Clinical cancer research : an official journal of the American Association for Cancer Research* 11(8):2875-2878.
54. Velho S*, et al.* (2005) The prevalence of PIK3CA mutations in gastric and colon cancer. *European journal of cancer (Oxford, England : 1990)* 41(11):1649-1654.
55. Li VSW*, et al.* (2005) Mutations of PIK3CA in gastric adenocarcinoma. *BMC cancer* 5:29-29.
56. Dam V, Morgan BT, Mazanek P, & Hogarty MD (2006) Mutations in PIK3CA are infrequent in neuroblastoma. *BMC cancer* 6:177-177.
57. Mueller W*, et al.* (2005) Mutations of the PIK3CA gene are rare in human glioblastoma. *Acta neuropathologica* 109(6):654-655.
58. Pang JC-s*, et al.* (2006) Rare mutation of PIK3CA in meningiomas. *Acta neuropathologica* 111(3):284-285.
59. Gustin JP*, et al.* (2009) Knockin of mutant PIK3CA activates multiple oncogenic pathways. *Proc Natl Acad Sci U S A* 106(8):2835-2840.

60. Isakoff SJ*, et al.* (2005) Breast cancer-associated PIK3CA mutations are oncogenic in mammary epithelial cells. *Cancer research* 65(23):10992-11000.
61. Guo XN*, et al.* (2007) Mutant PIK3CA-bearing colon cancer cells display increased metastasis in an orthotopic model. *Cancer Res* 67(12):5851-5858.
62. Ikenoue T*, et al.* (2005) Functional analysis of PIK3CA gene mutations in human colorectal cancer. *Cancer Res* 65(11):4562-4567.
63. Samuels Y*, et al.* (2005) Mutant PIK3CA promotes cell growth and invasion of human cancer cells. *Cancer Cell* 7(6):561-573.
64. Zhao JJ*, et al.* (2005) The oncogenic properties of mutant p110alpha and p110beta phosphatidylinositol 3-kinases in human mammary epithelial cells. *Proc Natl Acad Sci U S A* 102(51):18443-18448.
65. Kang S, Bader AG, & Vogt PK (2005) Phosphatidylinositol 3-kinase mutations identified in human cancer are oncogenic. *Proc Natl Acad Sci U S A* 102(3):802-807.
66. Bader AG, Kang S, & Vogt PK (2006) Cancer-specific mutations in PIK3CA are oncogenic in vivo. *Proc Natl Acad Sci U S A* 103(5):1475-1479.
67. Miled N*, et al.* (2007) Mechanism of two classes of cancer mutations in the phosphoinositide 3-kinase catalytic subunit. *Science (New York, N.Y.)* 317(5835):239-242.
68. Kang S, Bader AG, Zhao L, & Vogt PK (2005) Mutated PI 3-kinases: cancer targets on a silver platter. *Cell Cycle* 4(4):578-581.
69. Berns K*, et al.* (2007) A functional genetic approach identifies the PI3K pathway as a major determinant of trastuzumab resistance in breast cancer. *Cancer Cell* 12(4):395-402.
70. Maruyama N*, et al.* (2007) Clinicopathologic analysis of breast cancers with PIK3CA mutations in Japanese women. *Clin Cancer Res* 13(2 Pt 1):408-414.
71. Perez-Tenorio G*, et al.* (2007) PIK3CA mutations and PTEN loss correlate with similar prognostic factors and are not mutually exclusive in breast cancer. *Clin Cancer Res* 13(12):3577-3584.
72. Li SY, Rong M, Grieu F, & Iacopetta B (2006) PIK3CA mutations in breast cancer are associated with poor outcome. *Breast Cancer Res Treat* 96(1):91-95.
73. Kato S*, et al.* (2007) PIK3CA mutation is predictive of poor survival in patients with colorectal cancer. *International journal of cancer. Journal international du cancer* 121(8):1771-1778.
74. Barbareschi M*, et al.* (2007) Different prognostic roles of mutations in the helical and kinase domains of the PIK3CA gene in breast carcinomas. *Clin Cancer Res* 13(20):6064-6069.
75. Boyault S*, et al.* (2011) Mutational characterization of individual breast tumors: TP53 and PI3K pathway genes are frequently and distinctively mutated in different subtypes. *Breast cancer research and treatment*:29-39.
76. Di Nicolantonio F*, et al.* (2010) Deregulation of the PI3K and KRAS signaling pathways in human cancer cells determines their response to everolimus. *J Clin Invest* 120(8):2858-2866.
77. Vousden KH & Lane DP (2007) p53 in health and disease. *Nature reviews. Molecular cell biology* 8(4):275-283.
78. Li L*, et al.* (2008) Genomic instability and proliferative activity as risk factors for distant metastases in breast cancer. *British journal of cancer* 99(3):513-519.
79. Muller PA & Vousden KH (2013) p53 mutations in cancer. *Nat Cell Biol* 15(1):2-8.

80. Ganem NJ, Godinho SA, & Pellman D (2009) A mechanism linking extra centrosomes to chromosomal instability. *Nature* 460(7252):278-282.
81. Cerami E*, et al.* (2012) The cBio cancer genomics portal: an open platform for exploring multidimensional cancer genomics data. *Cancer discovery* 2(5):401-404.
82. Gao J*, et al.* (2013) Integrative analysis of complex cancer genomics and clinical profiles using the cBioPortal. *Science signaling* 6(269):pl1.
83. Weiss MB*, et al.* (2010) Deletion of p53 in human mammary epithelial cells causes chromosomal instability and altered therapeutic response. *Oncogene* 29(33):4715-4724.
84. Soule HD*, et al.* (1990) Isolation and Characterization of a Spontaneously Immortalized Isolation and Characterization of a Spontaneously Immortalized Human Breast.6075-6086.
85. Hart JR*, et al.* (2015) The butterfly effect in cancer: A single base mutation can remodel the cell. *Proc Natl Acad Sci U S A* 112(4):1131-1136.
86. Sur S*, et al.* (2009) A panel of isogenic human cancer cells suggests a therapeutic approach for cancers with inactivated p53. *Proc Natl Acad Sci U S A* 106(10):3964-3969.
87. Tang YC & Amon A (2013) Gene copy-number alterations: a cost-benefit analysis. *Cell* 152(3):394-405.
88. Bunz F*, et al.* (2002) Targeted inactivation of p53 in human cells does not result in aneuploidy. *Cancer Res* 62(4):1129-1133.
89. Cahill DP*, et al.* (1998) Mutations of mitotic checkpoint genes in human cancers. *Nature* 392(6673):300-303.
90. Holland AJ & Cleveland DW (2012) Losing balance: the origin and impact of aneuploidy in cancer. *EMBO reports* 13(6):501-514.
91. Sankaran S, Starita LM, Simons AM, & Parvin JD (2006) Identification of domains of BRCA1 critical for the ubiquitin-dependent inhibition of centrosome function. *Cancer Res* 66(8):4100-4107.
92. Kalaydjieva L, Hallmayer J, & Chandler D (1996) Gene mapping in Gypsies identifies a novel demyelinating neuropathy on chromosome 8q24. *Nature …*.
93. van Belzen N*, et al.* (1997) A novel gene which is up-regulated during colon epithelial cell differentiation and down-regulated in colorectal neoplasms. *Laboratory investigation; a journal of technical methods and pathology* 77(1):85-92.
94. Ellen TP, Ke Q, Zhang P, & Costa M (2008) NDRG1, a growth and cancer related gene: regulation of gene expression and function in normal and disease states. *Carcinogenesis* 29(1):2-8.
95. Stein S*, et al.* (2004) NDRG1 is necessary for p53-dependent apoptosis. *The Journal of biological chemistry* 279(47):48930-48940.
96. Kim K-T*, et al.* (2004) Function of Drg1/Rit42 in p53-dependent mitotic spindle checkpoint. *The Journal of biological chemistry* 279(37):38597-38602.
97. Bunz F*, et al.* (1998) Requirement for p53 and p21 to sustain G2 arrest after DNA damage. *Science* 282(5393):1497-1501.
98. Kim KT*, et al.* (2004) Function of Drg1/Rit42 in p53-dependent mitotic spindle checkpoint. *The Journal of biological chemistry* 279(37):38597-38602.
99. Fukasawa K, Choi T, Kuriyama R, Rulong S, & Vande Woude GF (1996) Abnormal centrosome amplification in the absence of p53. *Science* 271(5256):1744-1747.
100. Meraldi P, Honda R, & Nigg EA (2002) Aurora-A overexpression reveals tetraploidization as a major route to centrosome amplification in p53-/- cells. *The EMBO journal* 21(4):483-492.

101. Stambolic V*, et al.* (2001) Regulation of PTEN transcription by p53. *Molecular cell* 8(2):317-325.
102. Mayo LD & Donner DB (2001) A phosphatidylinositol 3-kinase/Akt pathway promotes translocation of Mdm2 from the cytoplasm to the nucleus. *Proc Natl Acad Sci U S A* 98(20):11598-11603.
103. Chang CJ, Freeman DJ, & Wu H (2004) PTEN regulates Mdm2 expression through the P1 promoter. *The Journal of biological chemistry* 279(28):29841-29848.
104. Freeman DJ*, et al.* (2003) PTEN tumor suppressor regulates p53 protein levels and activity through phosphatase-dependent and -independent mechanisms. *Cancer Cell* 3(2):117-130.
105. Singh B*, et al.* (2002) p53 regulates cell survival by inhibiting PIK3CA in squamous cell carcinomas. *Genes & Development*:984-993.
106. Kim JS, Lee C, Bonifant CL, Ressom H, & Waldman T (2007) Activation of p53-dependent growth suppression in human cells by mutations in PTEN or PIK3CA. *Mol Cell Biol* 27(2):662-677.
107. Astanehe A*, et al.* (2008) Mechanisms underlying p53 regulation of PIK3CA transcription in ovarian surface epithelium and in ovarian cancer. *Journal of cell science* 121(Pt 5):664-674.
108. Astle MV*, et al.* (2011) AKT induces senescence in human cells via mTORC1 and p53 in the absence of DNA damage: implications for targeting mTOR during malignancy. *Oncogene* (January):1-14.
109. Adams JR*, et al.* (2011) Cooperation between Pik3ca and p53 mutations in mouse mammary tumor formation. *Cancer research* 71(7):2706-2717.
110. Serrano M, Lin AW, McCurrach ME, Beach D, & Lowe SW (1997) Oncogenic ras provokes premature cell senescence associated with accumulation of p53 and p16INK4a. *Cell* 88(5):593-602.
111. Kreso A*, et al.* (2012) Variable Clonal Repopulation Dynamics Influence Chemotherapy Response in Colorectal Cancer. *Science (New York, N.Y.)* (December):1-7.
112. McGranahan N & Swanton C (2015) Biological and Therapeutic Impact of Intratumor Heterogeneity in Cancer Evolution. *Cancer Cell* 27(1):15-26.
113. Weiss MB (2010) Deletion of p53 in human mammary epithelial cells causes chromosomal instability and altered therapeutic response. *Oncogene* 29(33):4715-4724.
114. Lauring J*, et al.* (2010) Knock in of the AKT1 E17K mutation in human breast epithelial cells does not recapitulate oncogenic PIK3CA mutations. *Oncogene* 29(16):2337-2345.
115. Hartwell L (1992) Defects in a cell cycle checkpoint may be responsible for the genomic instability of cancer cells. *Cell* 71(4):543-546.
116. Chan JY (2011) A clinical overview of centrosome amplification in human cancers. *International journal of biological sciences* 7(8):1122-1144.
117. Marusyk A & Polyak K (2010) Tumor heterogeneity: causes and consequences. *Biochim Biophys Acta* 1805(1):105-117.
118. Song H, Hollstein M, & Xu Y (2007) p53 gain-of-function cancer mutants induce genetic instability by inactivating ATM. *Nature cell biology* 9(5):573-580.
119. Hanel W*, et al.* (2013) Two hot spot mutant p53 mouse models display differential gain of function in tumorigenesis. *Cell death and differentiation* 20(7):898-909.
120. Longley DB & Johnston PG (2005) Molecular mechanisms of drug resistance. *J Pathol* 205(2):275-292.
121. Warsow G*, et al.* (2013) Differential network analysis applied to preoperative breast cancer chemotherapy response. *PloS one* 8(12):e81784-e81784.

122. Mohseni M & Park BH (2010) PIK3CA and KRAS mutations predict for response to everolimus therapy: now that's RAD001. *J Clin Invest* 120(8):2655-2658.
123. Fan QW*, et al.* (2006) A dual PI3 kinase/mTOR inhibitor reveals emergent efficacy in glioma. *Cancer Cell* 9(5):341-349.
124. National Cancer Institute (2015) NCI Drug Dictionary.
125. Bykov VJN*, et al.* (2002) Restoration of the tumor suppressor function to mutant p53 by a low-molecular-weight compound. *Nature medicine* 8(3):282-288.
126. Shi H*, et al.* (2008) In vitro and in vivo cytotoxic effects of PRIMA-1 on hepatocellular carcinoma cells expressing mutant p53ser249. *Carcinogenesis* 29(7):1428-1434.
127. Kobayashi N, Abedini M, Sakuragi N, & Tsang BK (2013) PRIMA-1 increases cisplatin sensitivity in chemoresistant ovarian cancer cells with p53 mutation: a requirement for Akt down-regulation. *Journal of ovarian research* 6:7.
128. Cutts SM, Swift LP, Rephaeli A, Nudelman A, & Phillips DR (2003) Sequence specificity of adriamycin-DNA adducts in human tumor cells. *Mol Cancer Ther* 2(7):661-670.
129. Moreno-Aspitia A & Perez EA (2009) Treatment options for breast cancer resistant to anthracycline and taxane. *Mayo Clinic proceedings* 84(6):533-545.
130. Murray S, Briasoulis E, Linardou H, Bafaloukos D, & Papadimitriou C (2012) Taxane resistance in breast cancer: mechanisms, predictive biomarkers and circumvention strategies. *Cancer treatment reviews* 38(7):890-903.
131. Beaver JA*, et al.* (2013) PIK3CA and AKT1 mutations have distinct effects on sensitivity to targeted pathway inhibitors in an isogenic luminal breast cancer model system. *Clin Cancer Res* 19(19):5413-5422.
132. Beaver JA*, et al.* (2014) Detection of cancer DNA in plasma of patients with early-stage breast cancer. *Clin Cancer Res* 20(10):2643-2650.
133. Will M*, et al.* (2014) Rapid induction of apoptosis by PI3K inhibitors is dependent upon their transient inhibition of RAS-ERK signaling. *Cancer discovery* 4(3):334-347.
134. Sangai T*, et al.* (2012) Biomarkers of response to Akt inhibitor MK-2206 in breast cancer. *Clin Cancer Res* 18(20):5816-5828.
135. Liang Y, Besch-williford C, & Hyder SM (2009) PRIMA-1 inhibits growth of breast cancer cells by re-activating mutant p53 protein.1015-1023.
136. Hu L, Hofmann J, Lu Y, Mills GB, & Jaffe RB (2002) Inhibition of Phosphatidylinositol 3 ' -Kinase Increases Efficacy of Paclitaxel in in Vitro and in Vivo Ovarian Cancer Models Inhibition of Phosphatidylinositol 3 -Kinase Increases Efficacy of Paclitaxel in in Vitro and in Vivo Ovarian Cancer Models 1.1087-1092.
137. Konishi H*, et al.* (2007) Knock-in of mutant K-ras in nontumorigenic human epithelial cells as a new model for studying K-ras mediated transformation. *Cancer research* 67(18):8460-8467.
138. Wang GM*, et al.* (2013) Single copies of mutant KRAS and mutant PIK3CA cooperate in immortalized human epithelial cells to induce tumor formation. *Cancer research* 73(11):3248-3261.

APPENDICES

A

	Tumor samples	Total Cases with a Mutation	TP53 KO and NDRG1	TP53 KO ONLY	TP53 KI and NDRG1	TP53 KI ONLY	NDRG1 Only	TP53 KO Totals	TP53 KI Totals	Total TP53	Total NDRG1
Acute Myeloid Leukemia NEJM 2013	163	22	0	2	0	11	9	2	11	13	9
Acute Myeloid Leukemia TCGA Provisional	163	22	0	2	0	11	9	2	11	13	9
Adrenocortical Carcinoma, TCGA Provisional	76	19	0	1	2	12	4	1	14	15	6
Bladder Cancer, MSKCC, JCO 2013	58	24	0	1	2	17	4	1	19	20	6
Bladder Urothelial Carcinoma, TCGA, Nature 2014	131	56	1	4	8	55	5	5	63	68	14
Bladder Urothelial Carcinoma, TCGA, Provisional	243	82	1	6	10	53	12	7	63	70	23
Brain Lower Grade Glioma, TCGA, Provisional	517	161	0	1	4	141	15	1	145	146	19
Breast Invasive Carcinoma, TCGA, Nature 2012	825	210	0	5	51	135	19	5	186	191	70
Breast IC, TCGA, Provisional	1062	351	0	13	74	219	45	13	293	306	119
Cancer Cell Line Provisional	877	559	0	38	20	484	17	38	504	542	37
Colorectal Adenocarcinoma, TCGA, Nature 2012	195	117	0	1	11	90	15	1	101	102	26
Colorectal ADC, TCGA, Provisional	195	117	0	1	11	90	15	1	101	102	26
Glioblastoma TCGA, Cell 2013	574	69	0	6	0	58	5	6	58	64	5
Glioblastoma, TCGA, Nature 2008	91	33	0	1	1	31	0	1	32	33	1
Glioblastoma Multiforma, TCGA, Provisional	597	90	0	8	1	77	4	8	78	86	5
Head and Neck Squamous Cell Carcinoma, TCGA, Provisional	517	259	0	2	49	162	46	2	211	213	95
Head and NSCC, TCGA, In revision	279	213	0	2	46	156	9	2	202	204	55
Liver Hepatocellular Carcinoma, TCGA, Provisional	206	20	0	4	0	0	16	4	0	4	16
Lung Adenocarcinoma, TCGA, Nature, In Press	230	113	1	2	12	90	8	3	102	105	21
Lung Adenocarcinoma, TCGA, Provisional	555	130	1	2	9	107	11	3	116	119	21
Ovarian Serous Cystadenocarcinoma, TCGA, Nature, 2011	316	301	0	1	39	260	1	1	299	300	40
Ovarian Serous Cysta., TCGA, Provisional	580	298	0	2	29	245	22	2	274	276	51
Pancreatic Adenocarcinoma, TCGA, Provisional	39	26	0	1	1	24	0	1	25	26	1
Prostate Adenocarcinoma, TCGA, Provisional	337	37	0	8	3	18	8	8	21	29	11
Sarcoma, MSKCC/Broad, Nature Genetics 2010	149	21	0	17	1	3	0	17	4	21	1
Sarcoma, TCGA, Provisional	171	24	2	14	0	0	8	16	0	16	10
Skin Cutaneous Melanoma,TCGA, Provisional	375	70	0	2	3	43	22	2	46	48	25
Sum	9521	3444	6	147	387	2592	329	153	2979	3132	722

B

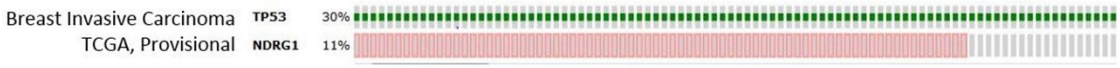

SI Figure 1: CBioPortal Data. A) Data was pooled and organized into a table from cBioPortal database as described in Materials and Methods. B) Representative data of the relatively frequent co-occurrence of TP53 mutations and NDRG1 overexpression

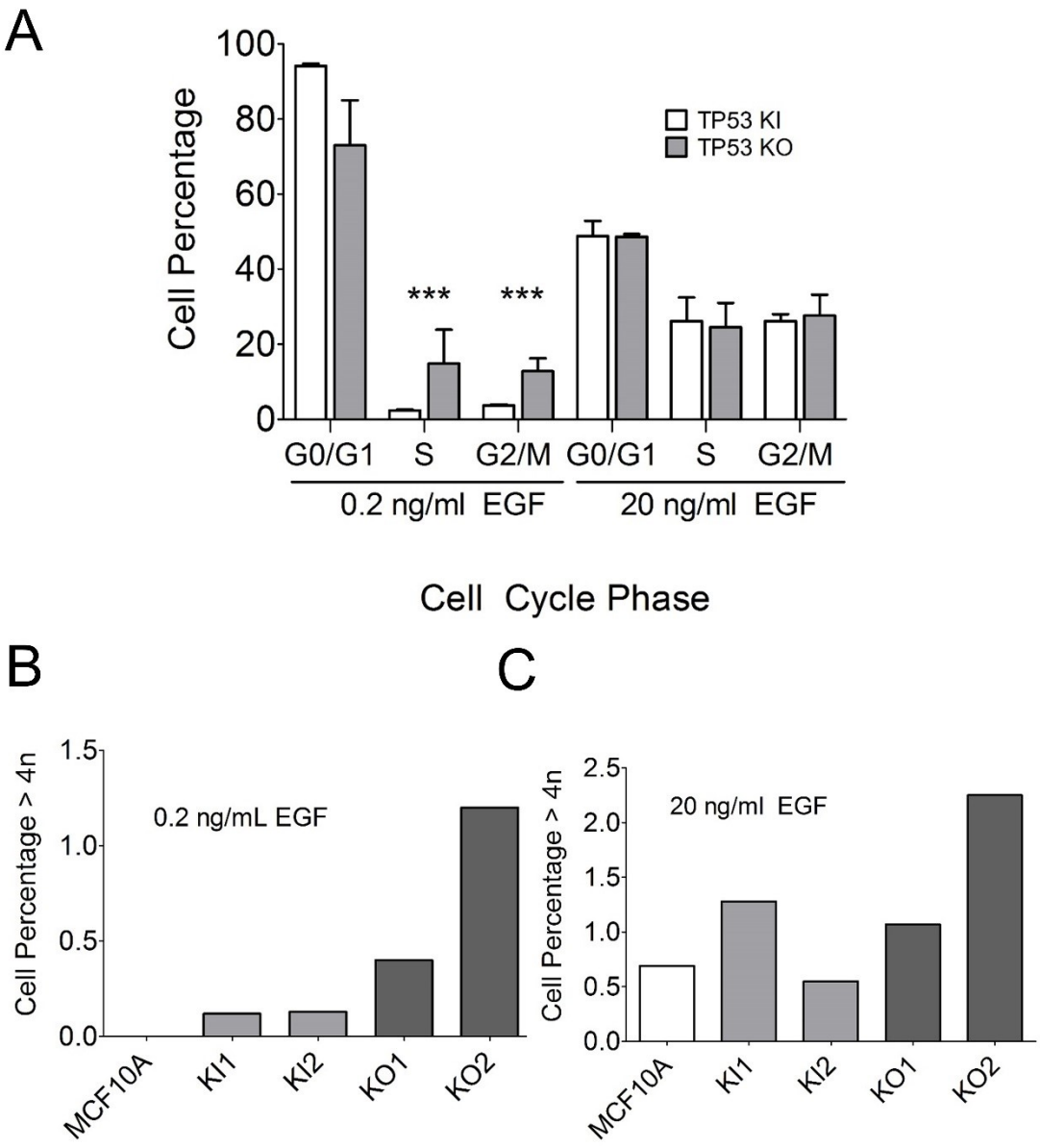

SI Figure 2: Cell cycle analysis of TP53 mutant cell lines. A) Cell cycle analysis using propidium iodide and flow cytometry. In physiological EGF conditions, TP53 KI cells arrest and have the majority of cells in G0/G1 phase. However, TP53 KO cells show a significantly higher percentage of cells in S and G2/M phase (***p<.001). In high doses of EGF, TP53 KI and TP53 KO cells show equivalent levels in all phases of the cell cycle. B) In physiological EGF conditions, TP53 KO cell lines show a higher percentage of polyploidal (>4n) cells than TP53 KI or parental MCF10A cells. C) In high EGF conditions, TP53 KI and MCF10A begin to show an equivalent percentage of polyploidal cells.

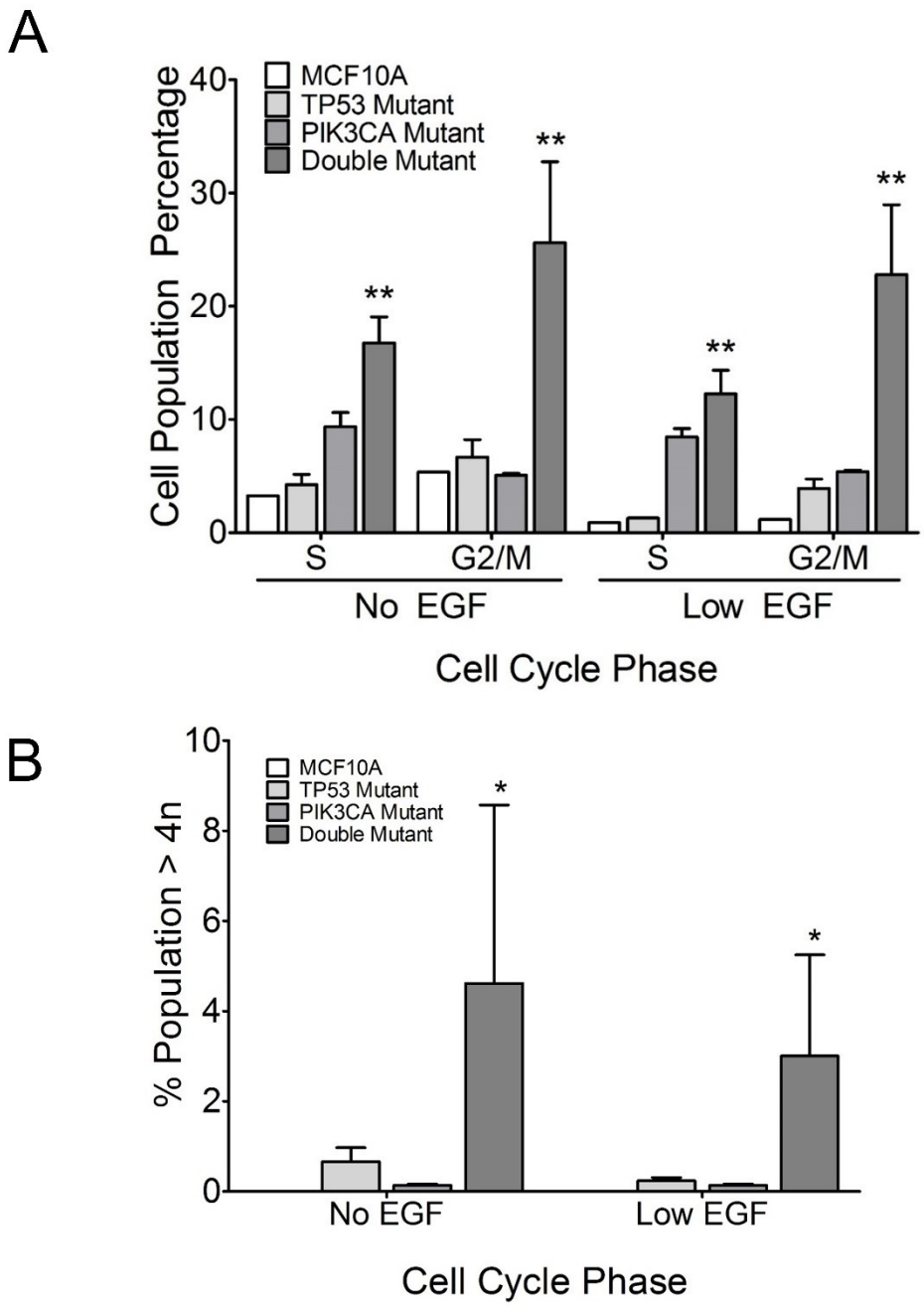

SI Figure 3: Cell cycle analysis of double mutant panel. A) Averaged values of clones in cell cycle analysis using propidium iodide and flow cytometry. In both the absence and low levels of EGF, the double mutants showed a significantly (**p<.01) higher population of cells in S and G2/M phase. B) Averaged values of with polyploidy. Cells with >4n were determined using propidium iodide and flow cytometry. In both the absence and low levels of EGF, the double mutants showed a significantly (*p<.05) higher population of cells exhibiting polyploidy (>4n).

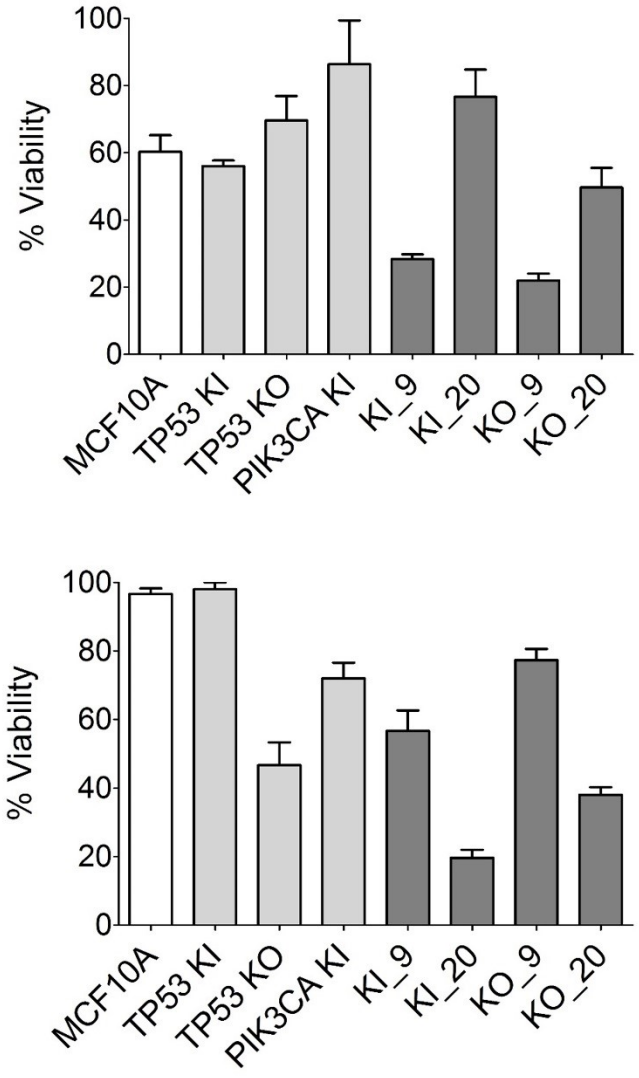

SI Figure 4: Pharmacokinetic studies of BYL719 and Rad001. A) The panel of cell lines was exposed to 1.5 μM of BYL719 for one week in 6 well plates. B) The panel of cell lines was exposed to .25 μM of everoliumus for one week in 6 well plates. Cell counts were done in triplicate and normalized to DMSO vehicle controls. Panels exhibited do discernable trends when exposed to these two drugs

Sarah Croessmann

1650 Orleans Street, CRB1, Rm 128, Baltimore MD 21287
585.507.1891 | scroess1@jhmi.edu

EDUCATION

Johns Hopkins University, School of Medicine, Baltimore, MD 2009-2015
Ph.D. Pathobiology

Thesis: The Role of Mutant *PIK3CA* and *TP53* in Breast Carcinogenesis
Thesis Advisor: Ben Ho Park, MD, PhD

University of Virginia, Charlottesville, VA 2005-2009
B.A. Studio Art
B.S. Chemistry with a specialization in Biochemistry
GPA : 3.70

EXTRAMURAL SUPPORT

National Institute of Health
F31 Research Fellowship Award, National Cancer Institute
Title: Cooperation of Mutant *TP53* and *PIK3CA* in Breast Carcinogenesis
CA167939

AWARDS AND HONORS

B.S. in Chemistry with Distinction 2009
American Chemical Society 2009
Distinguished Majors Program, University of Virginia 2007-2009
Dean's List, University of Virginia 2005-2009
National Scholars Honor Society 2005-2009

WORK AND LEADERSHIP EXPERIENCE

Partnering Towards Discovery Guest Speaker 2013
Conquering Cancer Treatment Resistance through Genetics

Distinguished Majors Thesis Defense 2009
University of Virginia, Charlottesville, VA
Write a thesis, oral dissertation, and oral defense on undergraduate research

Undergraduate Research Assistant, Department of Chemistry 2008-2009
University of Virginia, Charlottesville, VA
Research Goals: Optimization of solid phase extraction in microfluidic devices
Research Advisor: Dr. James P. Landers

Arts and Sciences Council Student Representative 2007-2009
University of Virginia, Charlottesville, VA

TEACHING AND MENTORING EXPERIENCE

Guest Lecturer for Grant Writing 101 2015
Johns Hopkins University, School of Medicine, Baltimore, MD

Pathobiology Graduate Tutor 2010-2011
Johns Hopkins University, School of Medicine, Baltimore, MD

Graduate Student Mentor 2009-2014
Johns Hopkins University, School of Medicine, Baltimore, MD

Chemistry Department Tutor 2008-2009
General Chemistry, Organic Chemistry, Inorganic Chemistry, Physical Chemistry
University of Virginia, Department of Chemistry, Charlottesville, VA
Advisor: Dr. Robert Burnett

Teaching Assistant 2007-2009
Organic Chemistry Lab I and Lab II
University of Virginia, Department of Chemistry, Charlottesville, VA
Course Advisor: Dr. Donald Hunt

PUBLICATIONS

Sarah Croessmann, Hong Yuen Wong, Daniel J. Zabransky, David Chu, Rory L. Cochran,
Heather Parsons, W. Brian Dalton, Bracha Erlanger, Berry Button, Karen Cravero, Kelly Kyker-Snowman, Ben Ho Park. Mutant *PIK3CA* and *TP53* cooperate to increase hallmarks of cancer, manuscript in preparation.

Sarah Croessmann, Hong Yuen Wong, Daniel J. Zabransky, David Chu, Janet Mendonca, Anup Sharma, Morassa Mohseni, D. Marc Rosen, Rob Scharpf, Justin Cidado, Rory L. Cochran, Heather Parsons, W. Brian Dalton, Bracha Erlanger, Berry Button, Karen Cravero, Kelly Kyker-Snowman, Julia A. Beaver, Sushant Kachhap, Paula J. Hurley, Josh Lauring, Ben Ho Park. "NDRG1 links p53 with proliferation mediated centrosome homeostasis and genome stability", submitted.

Rory L. Cochran, Justin Cidado, Minsoo Kim, Daniel J. Zabransky, **Sarah Croessmann**, David Chu, Hong Yuen Wong, Julia A. Beaver, Karen Cravero, Bracha Erlanger, Heather Parsons, Christopher M. Heaphy, Alan K. Meeker, Josh Lauring and Ben Ho Park. "Functional isogenic modeling of BRCA1 alleles reveals distinct carrier phenotypes" *Under review at Oncogene.* (2015)

Patricia Valda Toro; Bracha Erlanger; Julia A Beaver; Rory L Cochran; Dustin VanDenBerg; Elizabeth Yakim; Karen Cravero; David Chu; Daniel J Zabransky; Hong Yuen Wong; **Sarah Croessmann**; Heather Parsons; Paula Hurley; Josh

Lauring; Ben Ho Park. "Comparison of cell stabilizing blood collection tubes for circulating plasma tumor DNA." *Under review at PLOS ONE.* (2015)

Blair, B. G., X. Wu, M. S. Zahari, M. Mohseni, J. Cidado, H. Y. Wong, J. A. Beaver, R. L. Cochran, D. J. Zabransky, **S. Croessmann**, D. Chu, P. V. Toro, K. Cravero, A. Pandey and B. H. Park. "A Phosphoproteomic Screen Demonstrates Differential Dependence on Her3 for Map Kinase Pathway Activation by Distinct *PIK3CA* Mutations." *Proteomics*, (2014).

Beaver, Julia a, Danijela Jelovac, Sasidharan Balukrishna, Rory L. Cochran, **Sarah Croessmann**, Daniel J. Zabransky, Hong Yuen Wong, Patricia Valda Toro, Justin Cidado, Brian G. Blair, David Chu, Timothy Burns, Michaela J. Higgins, Vered Stearns, Lisa Jacobs, Mehran Habibi, Julie Lange, Paula J. Hurley, Josh Lauring, Dustin a VanDenBerg, Jill Kessler, Stacie Jeter, Michael L. Samuels, Dianna Maar, Leslie Cope, Ashley Cimino-Mathews, Pedram Argani, Antonio C. Wolff and Ben Ho Park. "Detection of Cancer DNA in Plasma of Patients with Early-Stage Breast Cancer." *Clinical cancer research : an official journal of the American Association for Cancer Research* 20, no. 10 (2014): 2643-50.

Cochran, R. L., K. Cravero, D. Chu, B. Erlanger, P. V. Toro, J. A. Beaver, D. J. Zabransky, H. Y. Wong, J. Cidado, **S. Croessmann**, H. A. Parsons, M. Kim, S. J. Wheelan, P. Argani and B. H. Park. "Analysis of Brca2 Loss of Heterozygosity in Tumor Tissue Using Droplet Digital Polymerase Chain Reaction." *Hum Pathol* 45, no. 7 (2014): 1546-50.

Mohseni, M., J. Cidado, **S. Croessmann**, K. Cravero, A. Cimino-Mathews, H. Y. Wong, R. Scharpf, D. J. Zabransky, A. M. Abukhdeir, J. P. Garay, G. M. Wang, J. A. Beaver, R. L. Cochran, B. G. Blair, D. M. Rosen, B. Erlanger, P. Argani, P. J. Hurley, J. Lauring and B. H. Park. "Macrod2 Overexpression Mediates Estrogen Independent Growth and Tamoxifen Resistance in Breast Cancers." *Proc Natl Acad Sci U S A* 111, no. 49 (2014): 17606-11.

Croessmann, S., J. Cidado, J. Gustin, D. Cosgrove, B.H.Park. "The *PIK3CA* Gene as a Mutated Target for Cancer Therapy." *Advances in Cancer Drug Targets*, Vol. 1, 2013, 3-21.

Wang, Grace M., Hong Yuen Wong, Hiroyuki Konishi, Brian G. Blair, Abde M. Abukhdeir, John P. Gustin, D. Marc Rosen, Samuel Ray Denmeade, Zeshaan Rasheed, William Matsui, Joseph P. Garay, Morassa Mohseni, Michaela J. Higgins, Justin Cidado, Danijela Jelovac, **Sarah Croessmann**, Rory L. Cochran, Sivasundaram Karnan, Yuko Konishi, Akinobu Ota, Yoshitaka Hosokawa, Pedram Argani, Josh Lauring and Ben Ho Park. "Single Copies of Mutant Kras and Mutant *PIK3CA* Cooperate in Immortalized Human Epithelial Cells to Induce Tumor Formation." *Cancer research* 73, no. 11 (2013): 3248-61.

Konishi, Hiroyuki, Morassa Mohseni, Akina Tamaki, Joseph P. Garay, **Sarah Croessmann**, Sivasundaram Karnan, Akinobu Ota, Hong Yuen Wong, Yuko Konishi, Bedri Karakas, Khola Tahir, Abde M. Abukhdeir, John P. Gustin, Justin Cidado, Grace M. Wang, David Cosgrove, Rory Cochran, Danijela Jelovac, Michaela J. Higgins, Sabrina Arena, Lauren Hawkins, Josh Lauring, Amy L. Gross, Christopher M. Heaphy, Yositaka Hosokawa, Edward Gabrielson, Alan K. Meeker, Kala Visvanathan, Pedram Argani, Kurtis E. Bachman and Ben Ho Park. "Mutation of a Single Allele of the Cancer Susceptibility

Gene Brca1 Leads to Genomic Instability in Human Breast Epithelial Cells."
Proceedings of the National Academy of Sciences of the United States of America 108, no. 43 (2011): 17773-8.